2017-04-30

Cdx4 Regulates the Onset of Spinal Cord Neurogenesis.

Piyush Kumar Joshi
University of Miami, piyushjo@gmail.com

UNIVERSITY OF MIAMI

CDX4 REGULATES THE ONSET OF SPINAL CORD NEUROGENESIS

By

Piyush Kumar Joshi

A DISSERTATION

Submitted to the Faculty
of the University of Miami
in partial fulfillment of the requirements for
the degree of Doctor of Philosophy

Coral Gables, Florida

May 2017

UNIVERSITY OF MIAMI

A dissertation submitted in partial fulfillment of
the requirements for the degree of
Doctor of Philosophy

CDX4 REGULATES THE ONSET OF SPINAL CORD NEUROGENESIS

Piyush Kumar Joshi

Approved:

_____
Isaac Skromne, Ph.D.
Assistant Professor of Biology

_____
Donald L. DeAngelis, Ph.D.
Research Professor of Biology

_____
Julia Dallman, Ph.D.
Associate Professor of Biology

_____
Guillermo Prado, Ph.D.
Dean of the Graduate School

_____
Pantelis Tsoulfas, M.D.
Associate Professor of Neurological Surgery
and Cell Biology and Anatomy

JOSHI, PIYUSH KUMAR (Ph.D., Biology)
Cdx4 Regulates the Onset of Spinal Cord Neurogenesis. (May 2017)

Abstract of a dissertation at the University of Miami.

Dissertation supervised by Assistant Professor Isaac Skromne.
No. of pages in text. (163)

Deciphering the mechanisms involved in regulating cell fate decisions is crucial to understanding the development of living organisms. Cells transition from one cellular state to another during the process of differentiation, ultimately acquiring specialized functions. At each step in the differentiation pathway the next state is prescribed by the regulatory state of the cell, as defined by the totality of the active transcription factors. The activity of these transcription factors determines the response of the cell to the signaling information it may encounter in its immediate surroundings, thus dictating the path taken by the cell in response to the environmental cues. Signaling information in turn regulates the activity of transcription factors that drives differentiation. This cross-regulation between transcription and signaling factors results into a complex network that coordinates developmental events. Hence in order to understand development, it is important to decipher the specific role signaling and transcription factors play in driving differentiation.

The differentiation of neuromesodermal progenitors into neuronal cells provides a striking example of sequential fate transition cued by signals. At the caudal end of the embryo, FGF/Wnt signals antagonize retinoic acid signal to regulate the sequential spatio-temporal maturation of spinal cord cells, from their exit out of the caudal neural progenitor stem zone to their incorporation into the developing neural tube. How the

downstream transcription network, that is active in the cells, responds to the overlying signaling dynamics is not fully understood.

In this dissertation I focused on deciphering the transcription network that interprets the FGF/Wnt and retinoic acid gradient information leading to progressive cell maturation states. Using transient gene manipulation techniques in chicken embryos, this work supports the role of Cdx4 as a core transcription factor that integrate upstream FGF, Wnt and retinoic acid signaling information to regulate the sequential maturation of cells from a biopotent neuromesodermal identity to a neurogenic identity. Based on experimental data, this work proposes a network of gene interactions that regulates the progressive maturation of neuromesodermal progenitors into differentiated spinal cord neural progenitors. Using computational and mathematical simulation of the gene regulatory network, the second part of this work highlights the core function Cdx4 plays in regulating the spatio-temporal pace of maturation events. The study provides evidences for Cdx as a core integrator of signaling information regulating cell fate decision in the embryonic caudal neural tube.

Acknowledgments

I wish to express my sincere gratitude to Dr. Isaac Skromne for providing me the opportunity to pursue my passion in science in his lab. I wish to thank him for his guidance, time and his patience in mentoring me and providing me the means to carry out my research aims. I would also like to thank my committee members Dr. Julia Dallman, Dr. Pantelis Tsoulfas and Dr. Donalnd DeAngelis for their help and guidance throughout the project. I feel fortunate to have these individual in my committee and I am thankful for their effort to enrich my graduate experience.

I would also like to thank all the past and present members of Skromne lab; especially Sapta, Jamie and Tristan for their friendship and support. I also want to extend my thanks to my colleagues and staff in the Department of Biology. Without the happy environment in the Skromne lab and the Biology department, it would have been impossible to sustain the motivation and the energy required in completion of this thesis.

Last, but not the least, I want to thank my family in India and my friends whose unconditional support and belief in me was beyond expectation and helped me pass through tough times. In the end, the most important thanks to all the chicken embryos whose lives were sacrificed in the pursuit of this dissertation.

TABLE OF CONTENTS

LIST OF FIGURES

FIGURES

LIST OF TABLES

TABLES

ABBREVIATIONS

CLE	Caudal lateral epiblast
CNH	Caudal neural hinge
CNS	Central nervous system
DV	Dorso-ventral
FGF	Fibroblast growth factor
GRN	Gene regulatory network
HH	Hamburger and Hamilton
IHC	Immunohistochemistry
ISH	*In situ* hybridization
NMP	Neuromesodermal progenitor
NSB	Node streak border
RA	Retinoic acid
RC	Rostro-caudal

Chapter 1

INTRODUCTION

1.1 Cellular states and their regulation

A cell's identity or state is determined by its developmental ancestry and functional role, and is defined collectively by its transcriptome and epigenome (Trapnell, 2015). Current models emphasize signaling information as determining the dynamic regulation of a cell's transcriptome and epigenome, highlighting the importance of extracellular signals for cell's identity. A cell's state is metastable and can change under the influence of local environmental conditions. Changes in the local environment can drive cells to transition from one state to another through combination of cell-cell, short and long range signals (Harvey Lodish, 2000; Muller and Schier, 2011). A signaling factor involved in cell-cell signaling, on its own or in combination with other signaling factors, determines the stability of a particular cellular state by maintaining it or by driving transition between states (Andersson et al., 2011; Balasubramanian and Zhang, 2015; De Luca et al., 2015; Diez del Corral et al., 2003; Green et al., 2015; Le Dreau and Marti, 2012; Pera et al., 2014; Ruiz-Villalba et al., 2015; Turner and Grose, 2010). However, the question remains how is the extracellular information being read, interpreted and executed by the intracellular machinery?

While signaling factors are known to act as cues to as cell determining the stability of cellular state, it is the downstream transcription factors that are actual effectors (Egli et al., 2008; Holmberg and Perlmann, 2012; Lassar et al., 1986; Nutt et al., 1999). The sum

totality of active transcription factors present in a cell can be termed as its regulatory state (Davidson et al., 2003b). Regulatory state of the cell restricts the path taken by the cell in response to the environmental cue. However, the regulatory state can, and often does change, as the cellular state changes in response to signaling cues. Normally this change is not random but directional, increasing the stability of the cellular state while reducing the cell's developmental potential (Bertrand and Hobert, 2010; Cooper, 2000; Simoes-Costa and Bronner, 2015). The importance of the regulatory state can be appreciated from the fact that a cell can be exposed to a signaling factor but, if the cell lacks the crucial downstream transcription factors, it may either fail or respond differently to the signaling cue (Arce et al., 2006; Aw Yeang et al., 2012; Lock and Cichowski, 2015; Mills et al., 2013; Nakamura et al., 2000; Song et al., 2009). The state of cells that allows or prevents their response to signals is called competence. Thus while signaling information could either stabilize cellular identity or drive transition between states, it is the regulatory state that determines the competence of the cell and thus the response to the signaling information (Oliveri et al., 2008; Rothenberg, 2010; Yang et al., 2003). Utilizing the characteristic of the regulatory state as an interpreter of signaling information, multiple cell types could be obtained using a similar battery of signals. Hence in order to understand the metastable states that correspond to each cell identity, it is not only important to understand the signals that trigger those states, but also the regulatory state (aka, competence) that allows the cell to respond to signals in the first place in a predictable manner.

Given the importance of the regulatory state in determining cellular states and their transitions, it is important to understand the composition and the dynamics of the

regulatory network itself. Historically, most studies have focused on understanding the activity of factors one transcription or signaling factor at a time, as loss of even a single one of them can lead to major developmental defects (Engelkamp and van Heyningen, 1996; Harradine and Akhurst, 2006; Mullor et al., 2002; Nusse, 2005; Packham and Brook, 2003; Turner and Grose, 2010). However, due to the reiterated use of signaling factors during development, the effect of losing a signaling factor can have more severe pleiotropic consequences than the loss of a single transcription factor. On the other hand, loss of transcription factor can, in certain cases, be well tolerated, due to built-in robustness of the transcription network, leading to significantly less severe developmental defect (Cooper et al., 2013; van Dijk et al., 2012). With the advent of high throughput sequencing technology, the study of signaling and transcription factors networks has exploded, resulting in a diametrically opposite problem; an embarrassment of riches (Frelinger, 2015; Wolfe, 2013). The sheer number of factors involved in complex interactions can obscure the interactions that carry the most weight in the system. Hence, to properly understand the role transcription factors play in regulating a process, we must strike balance between high-throughput and candidate gene approaches, as the understanding of the transcription network is crucial to understand normal development and for the preventive treatment of medical disorders.

1.2 Vertebrate spinal cord as a model system to study neuronal differentiation

The vertebrate central nervous system (CNS) is a highly complex organ, chiefly owing to the sheer volume and variety of neurons arranged in intricate configurations (Adler, 2005). Additionally, nervous system development is continuously being remodeled and

refined by social and behavioral components (Lewis, 2004). One successful approach to study CNS development has been focused on utilizing regions that are relatively less complex and more homogeneous. One such particular region is the early spinal cord, that, compared to the brain, is structurally less complex, and yet, it shares many spatial and functional characteristics (Becker and Diez Del Corral, 2015; Lewis and Eisen, 2003).

Early in development, the CNS develops as an extending neural tube that rostrally gives rise to the brain and caudally develops into the spinal cord. As the vertebrate body extends, the multipotent progenitors at the caudal end progressively generate caudal structures of the CNS in a sequential manner. Owing to this characteristic head to tail development, the temporal events of differentiation are spatially organized in the growing spinal cord, thus providing an appropriate system to investigate and understand the mechanisms involved in driving spatiotemporal cellular state transitions (Diez del Corral et al., 2003; Olivera-Martinez and Storey, 2007).

In mouse and chick, the spinal cord arises via two morphologically distinct mechanisms. Rostral regions of the spinal cord (cervical and rostral thoracic segments) are generated by rolling of the neural plate, a process termed primary neurulation (Gilbert, 2000). In chick, during the primary neurulation, around stage HH6-7, the neural cells are derived from the neuro-ectoderm surrounding the primitive streak. Cells from the dorsal part of the node gives rise to the ventral midline of the neural tube (Charrier et al., 2002; Selleck and Stern, 1991), while the rest of the neural tube originates from the epiblast cells lateral to the primitive streak (Brown and Storey, 2000). As the chicken Organizer or Hensen's node regresses caudally, the surrounding region called either the caudal neural plate or

the caudal later epiblast, gives rise to lateral and dorsal portions of the neural tube (Brown and Storey, 2000; Cambray and Wilson, 2007). Significantly, the pluripotent cells present in the caudal lateral epiblast can also contribute to some somitic tissue (Selleck and Stern, 1991). Cells located caudal to the node in a region known as axial-paraxial hinge or node-streak border also contribute to the neural tube development. Epiblast cells together with the cells in the node-streak border are termed neuro-mesodermal progenitors (NMPs) due to their dual potential in giving rise to neural and mesodermal tissues.

The posterior regions of the spinal cord (lumbar and sacral segments) are generated from a solid medullary cord of neuro-ectodermal cells that then hollows out to form the neural tube, a process termed secondary neurulation (Gilbert, 2000). During secondary neurulation, around stage HH14, the primitive streak and surrounding epiblast cells are converted into a dense tissue called tail bud. In the tail bud the chordo-neural hinge, a derivative of node-streak border and parts of caudal later epiblast, serve as the source of NMPs that give rise to the neural tube (Cambray and Wilson, 2002; McGrew et al., 2008). The spatial structure of progenitor domains in the tail bud remains very similar as in the neural plate region (Fig. 1.1) (Wilson et al., 2009).

The origin of most of the trunk and tail CNS can be traced back to NMPs (Cambray and Wilson, 2002; McGrew et al., 2008; Selleck and Stern, 1991) that exhibit self-renewal characteristics (Mathis et al., 2001; Selleck and Stern, 1991). NMPs are initially located in the caudal lateral epiblast and node-streak border, a region that during development becomes the tail bud's caudal neural hinge. Cell labeling and transplantation experiments in both chicken and mouse agree that the node and the epiblast contribute to the neural

tube (Cambray and Wilson, 2007; Selleck and Stern, 1991): while the node contributes to the floor plate cells, the epiblast contribute to the remaining lateral and dorsal portions of the neural tube. However, the node and epiblast can also contribute to other tissues, including mesoderm derivatives such as somites, suggesting their bipotency. Live imaging in chicken has shown that cells in the caudal lateral epiblast divide and give rise to cells which become part of the growing neural tube, with some daughter cells remain in the stem zone area to keep contributing to the elongating axis (Mathis et al., 2001). Together these studies suggest the idea that NMPs satisfy crucial criteria of stem cell identity however as some NMPs might differentiate completely (Tzouanacou et al., 2009), they are considered as multipotent progenitors rather than as axial stem cells.

Cells that differentiate and migrate out of the caudal stem zone, become part of the region called the transition zone or pre-neural tube. Here the cells have lost their multipotency without acquiring neural progenitor identities (due to lack of expression of associated transcription factors; (Delfino-Machin et al., 2005; Sasai et al., 2014)). The pre-neural cells starts differentiating further when they are exposed to the differentiating signal from the surrounding somites, the ectoderm and the underlying notochord, thus becoming a part of the mature neural tube (Diez del Corral et al., 2003).

Hence, in the caudal spinal cord cells with restricted potency are arranged in a caudal to rostral order that is also representative of their temporal identity. This spatio-temporal arrangement of differentiation events allows investigation of the signaling and transcriptional network involved in progressive maturation of NMPs in neural descendants.

1.3 Signaling factors drive caudal neural tube differentiation

Signaling factors play fundamental roles in maintaining the regional identity and integrity of the developing spinal cord, by either maintaining the pool of undifferentiated cells in the precursor zone or by driving cells out of the precursor zone and promoting their differentiation (Diez del Corral and Storey, 2004). Three signaling factors fibroblast growth factors (FGFs), Wnt and retinoic acid (RA) have been shown to regulate cellular states in the caudal neural tube essential for spinal cord formation (Bertrand et al., 2000; Diez del Corral et al., 2002; Diez del Corral et al., 2003; Olivera-Martinez and Storey, 2007; Pituello et al., 1999). Current models propose cross-repressive interaction between FGF and RA that regulate a cell's decision to stay in a proliferative state or undergo differentiation (Diez del Corral and Storey, 2004). At its core this model proposes that the balance between proliferative (FGF, Wnt) and differentiating (RA) signaling determines the pace of growth and differentiation during development of the extending neural tube.

Fibroblast Growth Factors (FGFs)

FGFs are an important proliferative signaling factor involved in maintaining stem cell identity in the caudal stem zone. The caudal end of the embryo expresses several FGF family ligands, including *Fgf2*, 3, 4, 8, 12, 13 and 18 (Boettger et al., 1999; Crossley and Martin, 1995; Karabagli et al., 2002; Mahmood et al., 1995; Ohuchi et al., 2000; Riese et al., 1995; Shamim and Mason, 1999), with several of them showing tissue specific expression. In particular, *Fgf2* and *Fgf3* are expressed exclusively in the stem zone (Mahmood et al., 1995; Riese et al., 1995); *Fgf10* is expressed exclusively in the paraxial

mesoderm (Karabagli et al., 2002); and *Fgf4*, *Fgf8* and *Fgf18* are expressed both in the stem zone and the paraxial mesoderm tissues (Karabagli et al., 2002; Shamim and Mason, 1999). Of these, *Fgf8* has been most extensively studied for its role in body axis elongation and regulation of the caudal stem zone and the paraxial mesoderm differentiation (Bertrand et al., 2000; Diez del Corral et al., 2002; Olivera-Martinez and Storey, 2007; Stavridis et al., 2010). *Fgf8* is expressed in a caudal to rostral gradient with high levels in the primitive streak and Hensen's node regions (Bertrand et al., 2000; Delfino-Machin et al., 2005; Karabagli et al., 2002; Olivera-Martinez and Storey, 2007). Analysis of *Fgf8* transcription has shown that the *de novo* mRNA synthesis takes place in the stem zone exclusively (Dubrulle and Pourquie, 2004), and that the mature mRNA is long lasting. As cells exit the stem cell zone and become part of the transition zone, the *Fgf8* mRNA is slowly degraded, giving the impression of a gradient of transcription. However, the *Fgf8* mRNA gradient, in reality, is a result of a gradient of transcript degradation (Dubrulle and Pourquie, 2004). The mRNA gradient results in a gradient of FGF8 protein synthesis. Being a secreted molecule with high diffusion rates (Yu et al., 2009), FGF8 diffusion further extends the gradient domain of FGF8 beyond the range of the mRNA expression domain (Lunn et al., 2007).

Analysis of downstream FGF targets such as *Erk1/2, mkp3* (Lunn et al., 2007) and *Sprouty2* (Chambers and Mason, 2000) has revealed FGF8's restricted domain of activity around the primitive streak including the caudal neural plate and surrounding pre-somitic mesoderm. This domain of activity includes the epiblast cells lateral to the primitive streak in the stem cell zone, the neuromesodermal progenitors (NMPs). The NMPs domain in the caudal stem zone is defined by the expression of several marker genes

including *T* (*Bra*), *Sox2* (Henrique et al., 2015), *Cash4* (Akai et al., 2005; Bertrand et al., 2000) and *Sax1* (Bertrand et al., 2000; Delfino-Machin et al., 2005; Diez del Corral et al., 2002). FGF8 has shown to be required for the activation of these NMPs domain markers. Loss of FGF signaling by over-expression of dominant negative FGF receptor (dnFGFR) or addition of FGF antagonist leads to downregulation of *T (Bra*)(Olivera-Martinez et al., 2012), *Cash4* (Akai et al., 2005) and *Sax1* (Delfino-Machin et al., 2005). Conversely, ectopic activation of FGF8 leads to reactivation and maintenance and of T (*Bra), Sox2* (Olivera-Martinez et al., 2012) *Cash4* and/or *Sax1* (Bertrand et al., 2000; Diez del Corral et al., 2002), suggesting direct involvement of FGF signaling in the maintenance of the stem cell zone. Consistent with FGF's function in maintaining NMPs pluripotency, attenuation of FGF signaling initiates cell differentiation (Bertrand et al., 2000; Diez del Corral et al., 2002; Diez del Corral et al., 2003). Inhibition of FGF signaling by over-expressing a dnFGFR in the stem cell zone leads cells to precociously leave the cell cycle (Mathis et al., 2001) and to start expressing the neural patterning markers *Pax6* and *Irx3* (Bertrand et al., 2000; Diez del Corral et al., 2003). Similarly, gain of FGF signaling by treatment with FGF4 (a FGF8 homologue) leads to loss of *Pax6* in the transition zone explant (Diez del Corral et al., 2003). Thus, FGF signaling is required both for maintaining the stem cell zone and repressing neuronal differentiation in the caudal spinal cord. However, FGF signaling is not alone in the caudal zone, but collaborates with Wnt signaling in its pro-stem cell identity function.

Wnt factors

The Wnt family of signaling factors is another important group of signals that are transcribed in the region surrounding the primitive streak and that are essential for maintaining stem cell identity in the caudal stem zone. Out of the 24 family members, only three are expressed in the chicken caudal tissue, *Wnt3a*, *Wnt5a/b* and *Wnt8c* (Olivera-Martinez and Storey, 2007).

Wnt3a has several important functions in the NMPs, including their specification (together with FGF8; (Martin and Kimelman, 2008; Yamaguchi et al., 1999)), and subsequent generation of neural versus mesodermal progenitors (Martin and Kimelman, 2012; Takada et al., 1994; Yoshikawa et al., 1997). *Wnt3a* expression is restricted to the region caudal to the Hensen's node (Olivera-Martinez and Storey, 2007; Takada et al., 1994). In the caudal stem zone, Wnt3a works together with FGF8 to induce the NMP markers *Sox2*, *T (Bra)* and *Sax1* (Rivera-Perez and Magnuson, 2005; Takemoto et al., 2006; Tamashiro et al., 2012). When Wnt3a is eliminated, the expression of *T (Bra)* (Martin and Kimelman, 2008; Yamaguchi et al., 1999) and *Sox2* (Takemoto et al., 2006) is strongly reduced, but not eliminated. In addition, Wnt3a is also involved in maintaining the balance between production of neural and mesodermal progenitors from NMPs, by promoting specification of mesodermal identity (Martin and Kimelman, 2012; Takada et al., 1994; Yoshikawa et al., 1997). *Wnt3a* deficient NMPs generate ectopic neural tissue at the expense of somitic tissue, a tissue transformation that results in early axis truncation. Conversely, over-activation of Wnt signaling leads to down regulation of neural progenitors' population (Gouti et al., 2014). *Wnt3a* is under direct regulation of the FGF pathway (Naiche et al., 2011; Savory et al., 2009). Significantly, however, Wnt3a is

also known to activate *Fgf8*, establishing a positive feedback loop that maintains the expression of these two important stem cell factors in the caudal stem zone (Aulehla et al., 2003). The positive feedback between *Wnt3a* and *Fgf8* results in high levels of FGF and Wnt signaling that is involved in regulating NMPs genes and maintaining the identity of NMPs domain.

Another important Wnt family member involved in maintaining the neural progenitor zone is Wnt8c. Similar to the *Wnt3a*, *Wnt8c* is expressed in the caudal neural plate and primitive streak region and later in the transition zone, where its rostral domain extends almost up to the most recently formed somite (Olivera-Martinez and Storey, 2007). Hence *Wnt8c* expression is maintained in the neural progenitors that arise out of the stem zone, and are now part of the transition zone of the neural tube. In the caudal stem zone, it shares its role in maintaining NMPs domain along with Wnt3a and FGF8 (Tamashiro et al., 2012; Turner et al., 2014). Further, Wnt8c has been shown to inhibit neuronal differentiation by inhibiting expression of *NeuroM* and *Ngn1* in the transition zone (Olivera-Martinez and Storey, 2007), supporting its role in preventing precocious differentiation. In addition to this activity, Wnt8c has been shown to activate *Raldh2* in the differentiating pre-somitic mesoderm (Olivera-Martinez and Storey, 2007), the enzyme that synthesizes RA (Molotkova et al., 2005). This activation is restricted only to the most rostral pre-somitic mesoderm, in an area where FGF is not present (FGF represses *Raldh2;* (Olivera-Martinez et al., 2012)). On activation, RALDH2 synthesizes RA in somites, the signaling cue that promotes further neuronal differentiation.

Wnt5a/b are expressed prominently in the primitive streak region (Olivera-Martinez and Storey, 2007). In the caudal region, *Wnt5a/b* are involved in driving non-canonical Wnt

signaling via planar cell polarity pathway or Ca^{2+} signaling and regulating cell migration and gastrulation (Hardy et al., 2008). Hence, while evidence for *Wnt5a/b* in NMPs specification is lacking, it is involved in the migration of the progenitors during gastrulation.

Due to cross regulation between Wnt and FGF signaling factors, and shared functions in maintaining stem cell identity and preventing differentiation; evidence for specific role of FGF and Wnt family members has been difficult to attain. In all, Wnts act in combination with FGF signaling in maintaining proliferation and inhibiting differentiation. Wnt signaling also provide the link between pro-stem cell FGF signaling to pro-differentiation RA signaling.

Retinoic acid (RA)

While FGF and Wnt provide the appropriate signals to maintain the NMPs niche, RA acts as the pro-differentiation signal in the rostral neural tube. RA is produced in the somites flanking the neural tube rostral to the primitive streak by the RA synthesizing enzyme *Raldh2* (Molotkova et al., 2005; Olivera-Martinez and Storey, 2007) Due to the small size of RA molecules, they diffuse rapidly from their source in the somites to the underlying the pre-somitic mesoderm and caudal neural region (White et al., 2007), where they antagonize the effect of FGF/Wnt signaling (Diez del Corral et al., 2003). As cells leave the stem zone and enter the transition zone, they are exposed to increasing RA signaling which drives the expression of early neurogenic markers *Pax6, Nkx6.1, Ngn1/2* (Diez del Corral et al., 2003; Diez del Corral and Storey, 2004; Maden, 2006) and down

regulate pluripotency markers *T* (*Bra)* (Gouti et al., 2014), and *Sax1* (Cunningham et al., 2016). The only pluripotency marker maintained in maturing cells is *Sox2,* whose expression is maintained under RA signaling (Cunningham et al., 2016). The downregulation of pluripotency markers and upregulation of differentiation genes is partly done by RA's inhibition of FGF signaling (Diez del Corral et al., 2003). Loss of RA signaling such as that seen in vitamin-A deficient (VAD) quail embryos, leads to the failure of initiation of neurogenesis (Diez del Corral et al., 2003) with an expansion of FGF signaling as shown by rostralization of *Fgf8* and *Sprouty2* expression (Diez del Corral et al., 2003). RA deficient embryos show dramatic reduction in expression domain of differentiation markers *Pax6, Irx3, Nkx6.1, Olig2, Ngn1/2* (Diez del Corral et al., 2003; Molotkova et al., 2005; Novitch et al., 2003; Ribes et al., 2009; Wilson et al., 2004) in the neural tube, resulting in a decrease in the total number of neurons generated in the spinal cord. Conversely, precocious activation of RA induces early differentiation of cells located in the stem cell zone as shown by the caudal expansion of *Pax6* expression domain (Pituello et al., 1999). In summary, RA signals the initiation of the neurogenesis and differentiation of progenitors into mature neurons by opposing FGF/Wnt signaling.

Signaling integration and differentiation

Prevailing models describe the onset of spinal cord neurogenesis as the crosstalk between FGF, Wnt and RA signaling. FGF and Wnt act in combination to induce and sustain the expression *T (Bra), Cash4* and *Sax1* that are responsible for maintaining the NMPs identity, while inhibiting transcription of differentiation markers *Pax6*, *Irx3*, *Ngn1/2*. These differentiation markers in turn are activated by RA signaling, which represses

NMPs markers' expression. Thus, the switch from NMPs identity to pre-neural to neurogenic identity is the response of cells to change in extracellular signaling, from high FGF/no RA in the caudal to no FGF/high RA in the rostral (Diez del Corral et al., 2003). While the juxtaposition of gradients is primarily driven by the previously described sequential activation of factors, refinement of the gradients is enhanced by cross-repressive interaction between FGF and RA. FGF actively causes the exclusion of RA from the NMPs zone by repressing *Raldh2* (Olivera-Martinez et al., 2012) and activating *Cyp26*, an enzyme that degrades RA (Boulet and Capecchi, 2012; Sakai et al., 2001; White et al., 2007). On the other hand, RA actively inhibits *Fgf8* transcription creating a zone where cell can exit proliferation and differentiate (Diez del Corral et al., 2003; Kumar and Duester, 2014). The cross-repressive and balanced activities of FGF and RA create a rostral to caudal gradient of pro-differentiation signaling and caudal to rostral gradient of anti-differentiation signaling that allows the gradual maturation of spinal cord cells (Fig.1.2).

1.4 Transcription factors involved in onset of neurogenesis

The signaling factor dynamics provide the cues to cells to differentiate; however, the decision and pace of cell differentiation is under the control of a poorly understood transcription network transducing the overlying signaling information. Several transcription factors have been used as markers for different cellular states, particularly for their role in maintaining the identity of cells in the domain where they are transcribed. Key transcription factors include *T (Bra), Sox2, Sax1, Pax6* and *Ngn2* (Fig 1.2).

T (Bra) and *Sox2* balance the production of mesodermal and neural tissues by respectively promoting NMPs cells to acquire mesodermal or neural identities (reviewed in (Henrique et al., 2015)). *T (bra)* is transcribed in the NMPs domain and surrounding primitive streak, as well as their mesodermal descendants (Garriock et al., 2015). In combination with Wnt, *T (Bra)* promotes NMPs cells to become mesoderm, counteracting the neural activity of *Sox2* (Martin and Kimelman, 2008; Yamaguchi et al., 1999; Yoshikawa et al., 1997). This is observed in embryos lacking *T (Bra) (*or *Wnt3a),* in which the axis is truncated and the number of somites is reduced, and the neural tissue is expanded (Yamaguchi et al., 1999; Yoshikawa et al., 1997). On the other hand, *Sox2* is expressed in the NMPs and neural tube (Henrique et al., 2015), and serves as a pan-neural marker (Delfino-Machin et al., 2005; Miyagi et al., 2006). *Sox2* is involved in promoting neural identity in the bipotent NMPs (Chalamalasetty et al., 2014) and acts in conjunction with *T (Bra)* in maintaining the balance of neural and mesodermal progenitors. Reduction in *Sox2* expression in the NMPs promotes mesodermal fates (Yoshida et al., 2014), whereas its ectopic expression in the caudal paraxial mesoderm is sufficient to induce ectopic neural tissue (Chalamalasetty et al., 2014). In the NMPs, *Sox2* expression is under FGF/Wnt via a particular enhancer, the N1 enhancer (Takemoto et al., 2006). In the neural tube, however, *Sox2* regulation is under RA control working through a different enhancer (Cunningham et al., 2016; Iwafuchi-Doi et al., 2011; Meijer et al., 1990). Thus, despite FGF/Wnt and RA having antagonistic functions in promoting or preventing cell maturation, they both sustain *Sox2* transcription to maintain the neural identity of the cells.

Another important NMPs regulator is *Sax1* (*Nkx1.2*, in mouse). *Sax1* is also expressed in the NMPs and their progeny that becomes part of the neural tube (Delfino-Machin et al., 2005; Sasai et al., 2014). In the caudal neural tube, Sax1 is known to act downstream of FGF signaling in inhibiting differentiation and promoting floor plate induction (Sasai et al., 2014).

As progenitor cells begin their neuronal differentiation in the rostral transition zone, *Pax6* is activated (Bertrand et al., 2000; Pituello et al., 1999). Pax6 has two important functions in neuronal differentiation: initially, it provides neural identity to the cells exiting out of the stem zone, and then, it provides dorso-ventral patterning information to the cells in the mature neural tube (Bel-Vialar et al., 2007; Ericson et al., 1997). In addition to patterning, *Pax6* also promotes further differentiation by activating downstream differentiation markers, including *Ngn2* (Bel-Vialar et al., 2007). Loss of *Pax6* results in the reduction of *Ngn2* expressing cells and a concomitant reduction in the number of motor neurons. Conversely, forced expression of *Pax6* is sufficient to drive precocious differentiation as seen by ectopic expression of *Ngn2* in the caudal neural tube (Bel-Vialar et al., 2007).

Ngn2 is an important neurogenic factor that is involved in neural cell differentiation, and is expressed in motor neuron precursors and some dorsal interneuron precursors, where it promotes cell cycle exit and further differentiation into neurons (Lacomme et al., 2012; Parras et al., 2002; Scardigli et al., 2001).

1.5 Cdx transcription factors

Cdx are homeobox transcription factors known to integrate FGF-Wnt-RA signaling information during somitogenesis (reviewed in Deschamps and van Nes (2005)) . However, despite their expression in NMPs and their known function in spinal cord specification (Skromne et al., 2007), their role in spinal cord neurogenesis has not been investigated. In all the tissues where *Cdx* are transcribed, these genes regulate cell differentiation. This has been studied in greater detail in the trophectoderm (Strumpf et al., 2005) hematopoietic tissues (McKinney-Freeman et al., 2008; Wang et al., 2008), and the gut (Hryniuk et al., 2012). Significantly, in these last two tissues, Cdx dysregulation can lead to tissue hyper-proliferation and cancer (Saad et al., 2011; Scholl et al., 2007). Based on these evidences, Cdx could play similar functions in NMP tissue, integrating FGF-Wnt-RA signaling dynamics during the onset of spinal cord neurogenesis.

In all the vertebrates examined, the three Cdx family members, *Cdx1*, *Cdx2* and *Cdx4*, show a spatially nested expression domain along the rostro-caudal axis of the neural tube (Faas and Isaacs, 2009; Lohnes, 2003; Marom et al., 1997). This nested expression pattern, however, is not conserved across anamniotes and amniotes: in zebrafish and *Xenopus*, the rostro-caudal order of transcription is *Cdx4*, *Cdx1* and *Cdx2* (*Cdx1b* in zebrafish) (Cheng et al., 2008; Davidson et al., 2003a; Davidson and Zon, 2006; Reece-Hoyes et al., 2002), whereas in chicken and mouse the order is *Cdx1*, *Cdx2* and *Cdx4* (Deschamps and van Nes, 2005; Frumkin et al., 1991; Marom et al., 1997; Morales et al., 1996). The significance of this change in expression is not known, but may be associated with a switch in the tissue that gives rise to the primitive blood (I. Skromne, personal comm.). In chicken, *Cdx* genes are also expressed in a nested spatial and temporal

domain in region surrounding the primitive streak and later in the tail bud (Marom et al., 1997). *Cdx1* expression is first detected at stage HH4 caudal to Hensen's node (Frumkin et al., 1991). During primitive streak regression the expression expands rostral to the node, in epiblast cells surrounding the primitive streak. Finally, *Cdx1* transcription becomes restricted to the stem zone and by stage HH10 the expression fades away and disappears (Frumkin et al., 1991; Marom et al., 1997). *Cdx2* expression is also detected at stage HH4, in a region caudal to *Cdx1*. The expression then extends rostrally as body axis extended and by stage HH 10 it's expressed rostral to the node. *Cdx2* is also expressed in the transition zone briefly before fading away by stage HH13-14 (Marom et al., 1997). As the other family members, *Cdx4* expression is first detected at stage HH4 (Morales et al., 1996). Then, *Cdx4* expression extends rostrally during body elongation. In the spinal cord *Cdx4* extended all the way up to the second most recently formed somite, maintaining the same position as somites form and axis elongates (Fig. 3.1). The expression pattern is maintained till stage HH19-20, when it finally becomes undetected in the tail bud. Thus, among all *Cdx* genes in chicken, *Cdx4* is the one that is expressed for the longest duration during spinal cord formation.

Cdx play myriad roles during early development of embryos, although Cdx have been primarily studied in the context of *Hox* gene regulation and axial patterning (Hayward et al., 2015; Mazzoni et al., 2013; Nordstrom et al., 2006; Sanchez-Ferras et al., 2016; van den Akker et al., 2002; Young et al., 2009). Cdx are also involved in mesoderm formation (Davidson et al., 2003a; Davidson and Zon, 2006; van Nes et al., 2006; Young et al., 2009), trophectoderm development (Strumpf et al., 2005; Wu et al., 2010), gut morphogenesis (Hryniuk et al., 2012), hematopoiesis (Davidson et al., 2003a; Davidson

and Zon, 2006; McKinney-Freeman et al., 2008) and spinal cord development (Hayward et al., 2015; Shimizu et al., 2006; Skromne et al., 2007). As expected for genes with several functions, loss of Cdx activity causes several phenotypic defects including homeotic transformation (van den Akker et al., 2002), axis truncation (Chawengsaksophak et al., 2004; Savory et al., 2009), loss of spinal cord identity (Shimizu et al., 2006; Skromne et al., 2007), failure to form blood cells (Davidson et al., 2003a; Davidson and Zon, 2006), and loss of gut structures (Hryniuk et al., 2012). Most of these defects are caused by a failure of properly regulating the induction and subsequent maintenance of *Hox* transcription factors. Because of partially redundant functions, loss of single *Cdx* genes have less severe phenotypes compared to double and triple mutants (Davidson and Zon, 2006; Faas and Isaacs, 2009; van den Akker et al., 2002; van Rooijen et al., 2012). However, there are instances where individual Cdx member play specific function. For example, Cdx2 has specific functions not shared with other Cdx factors in hematopoiesis (Sanchez-Ferras et al., 2016), gut morphogenesis (Hryniuk et al., 2012) and trophectoderm differentiation (Strumpf et al., 2005).

Cdx function in CNS development

In the CNS, Cdx factors specify and pattern the spinal cord via *Hox* gene regulation. Loss of two *cdx* genes in zebrafish, *cdx1a* and *cdx4*, results in the transformation of spinal cord into hindbrain structures (Shimizu et al., 2006; Skromne et al., 2007); whereas in mice, *Cdx* triple mutants fail to develop neural tissue posterior to the otic vesicle (van Rooijen et al., 2012). Cdx are also involved in the collinear induction and subsequent maintenance of posterior spinal cord specific *Hox* genes (Hayward et al., 2015; Mazzoni et al., 2013).

In the aforementioned mouse triple mutants, loss of all *Cdx* genes also results in the loss of trunk and tail mesoderm, suggesting an involvement of these genes in the formation of all trunk and tail tissue derivatives (van Rooijen et al., 2012). Whether this is at the level of the NMPs or their progeny has yet to be determined.

Here I focus on deciphering the regulatory state dynamics involved in the onset of spinal cord neurogenesis, testing the central hypothesis that transcription factor Cdx integrates upstream FGF, Wnt and RA signaling information to regulate the transition of NMPs into neural progenitors. To address the role of Cdx in regulating spinal cord differentiation, my research focuses on one Cdx family member, *Cdx4*, as this gene is expressed in the nascent neural tube from early neurogenesis and its expression is maintained for the longest duration during embryonic development (Marom et al., 1997; Morales et al., 1996). In my thesis, I have characterized the role of Cdx4 in spinal cord neurogenesis by completing the two specific aims.

In specific aim 1, I tested the hypothesis that Cdx4 regulates neurogenesis by activating or repressing neural pluripotency and differentiation genes. I investigated the role of Cdx4 in regulating the transcription of marker genes that are known to be important in assigning the identity of cellular states in the caudal neural tube. My data show that Cdx4 drives expression of neural progenitor factor *Pax6* in the newly formed neural tube, in combination with RA signaling. My data also show that Cdx4 downregulates *Sax1*, a known marker of pluripotency. Together, my results suggest that Cdx4 drives differentiation by both inhibiting pluripotency and promoting differentiation. In addition, Cdx4 regulates neural identity by preventing *Ngn2* expression, the next step in the

differentiation pathway. Together, these findings indicate that *Cdx4* is at the core of the network that controls the stepwise acquisition of spinal cord identities by NMP cells.

In specific aim 2, I tested the hypothesis that Cdx4 act as a differentiation switch during the onset of spinal cord neurogenesis. Using mathematical modeling approaches, I investigated the role of *Cdx4* in coordinating upstream signaling information and regulating the proper spatio-temporal arrangement of cellular states. My data suggest that *Cdx4* regulates the pace of cell differentiation from NMP identity to neurogenic identity.

1.6 Figures

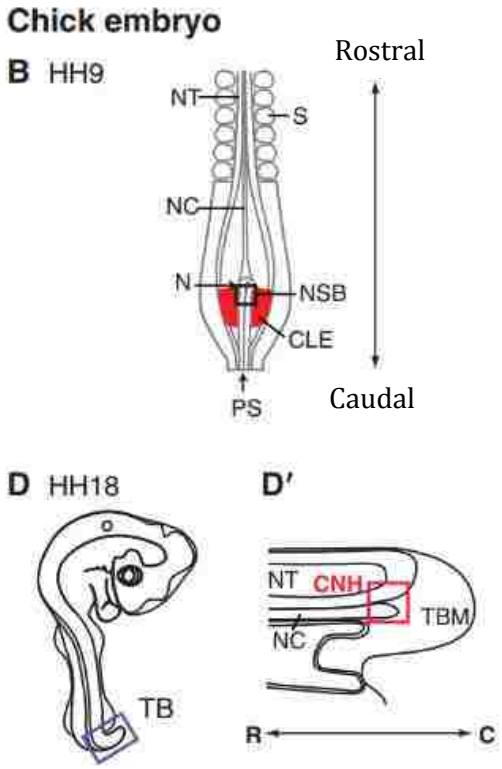

Figure 1.1: Location of NMP domain in chicken embryo. Reproduced from Wilson et al.(Wilson et al., 2009). Schematic shown the location of caudal lateral epiblast (CLE) and node streak border (NSB) in HH 9 embryo (A). The location of caudal neural hinge (CNH), a derivate of CLE and NSB, in the tail bud (B). CLE and NSB, and later CNH, are the source of bipotent NMPs in the chicken embryo.

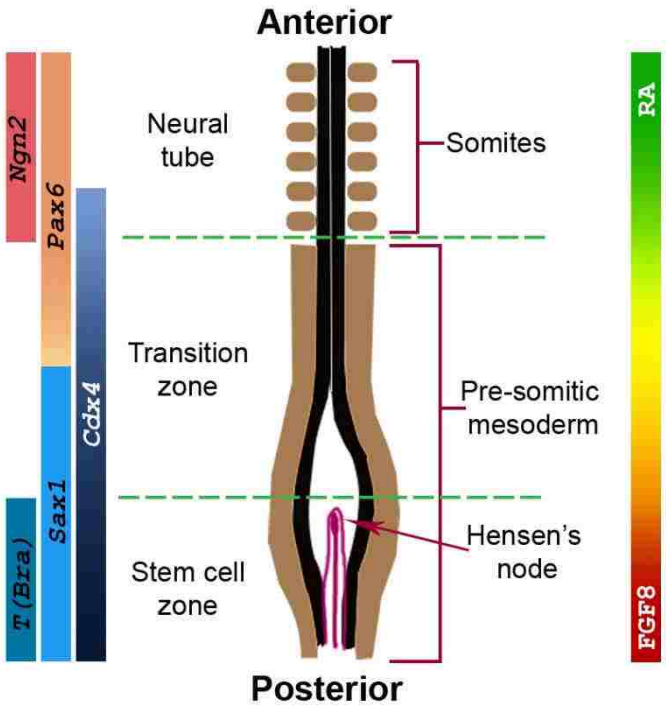

Figure 1.2: Signaling switch driving differentiation in caudal neural tube. Schematic representation of the caudal end of HH10 chicken embryo showing expression domain of key transcription factors including *Cdx4* (on left) and FGF8-RA signaling switch (on right) involved in their regulation. Subdivision of the neural tube into different regions is adapted from Olivera-Martinez et al.(Olivera-Martinez and Storey, 2007).

Chapter 2

METHODS

2.1 DNA constructs

Gene and gene constructs employed in this work where either obtained from other laboratories, or generated by me using standard molecular biology techniques and publicly available annotated sequences. A list of genes and constructs obtained from other laboratories is summarized in Table 2.1, and a list of genes and constructs generated by me is summarized in Table 2.2.

Table 2.1: Genes and constructs received from other labs.

Gene construct	**Purpose**	**Sources**	**References**
Pax6-pBS	*In situ* hybridization	Dr. Martyn Gouldin (Salk Institute, USA)	
Ngn2-pBS	*In situ* hybridization	Dr. Francois Medevielle (CBI, Toulouse, France)	(Bel-Vialar et al., 2007)
Pax6-pCIG	Electroporation		
EnRPax6-pCIG	Electroporation		

Chick-*T(Bra)*- pBS	*In situ* hybridization	Dr. Susan Mackem (NCI, USA)	(Liu et al., 2003)
mNkx1.2-pEF2	For generating mNkx1.2-pCIG	Dr. Yusuke Marikawa (U of Hawaii, USA)	(Tamashiro et al., 2012)
dnRAR-pCIG	Electroporation	Dr. Axia V. Morales (Cajal Institute, Spain)	(Martinez-Morales et al., 2011)

Ful legth Cdx4 for in situ hybridization and sub-cloning (Cdx4-pGEM-T-Easy). Full length Cdx4 (NM_204614.1) was cloned from reverse transcribed, total mRNA from chicken embryos at different stages of development (HH4-HH12; qScript cDNA Synthesis kit, Quantabio), using primers designed with the online program Primer BLAST (Table II). Fragment product of the correct size was TA cloned using pGem-T Easy Plasmid (Promega,). Cloning of the correct gene was confirmed by sequencing. This construct was used to generate in situ hybridization probe and as a template for additional construct.

Full length Cdx4 for chicken electroporation (Cdx4-pCIG). Full-length chicken Cdx4 was digested with SpeI and blunt ended with Mung Bean nuclease (NEB). Purified, linear Cdx4 was then digested with EcoRI. The purified Cdx4 fragment was then subcloned into pCIG previously digested with EcoRI-SmaI. This construct was used for over-expressing

wild type Cdx4 in chicken embryos by electroporation. pCIG contains nuclear GFP under IRES promoter for concomitant expression of GFP in electroporated cells (Megason and McMahon, 2002).

Constitutively active Cdx4 for chicken electroporation (VP16Cdx4-pCIG). The transactivator domain of VP16 was amplified from VP16-pCS2+ and fused to the C-terminal domain of Cdx4 containing the DNA binding homeodomain (corresponding to amino acids 119-364; renamed Cdx4-HD). Primers used for these amplifications are described in Table II. Chimeric VP16Cdx4 was then generated by PCR amplification from a mixture containing VP16 and Cdx4-HD fragments and VP16 forward and Cdx4-HD reverse primer. The segment was cloned into pGEM-T-easy and open reading frame confirmed by sequencing. VP16Cdx4 was then digested using ClaI-EcoRI and inserted into ClaI-EcoRI sites of pCIG.

Dominant negative Cdx4 for chicken electroporation (EnRCdx4-pCAGIG). Engrailed (EnR) repressor domain from EnR-pCS2+ was digested with XhoI and blunt ended with Mung Bean nuclease. After purification, the fragment was digested with EcoRI and re-purified. This EcoRI-blunt EnR product was ligated to a blunt ended Cdx4 fragment generated using SmaI (nucleotide site 328). As a final step, the chimeric construct was ligated to pCAGIG vector digested with EcoRI-EcoRV. Several clones were analyzed by sequencing to confirm correct orientation of the EnR and Cdx4 fragments, and the continuity of the open reading frame. pCAGIG contains GFP under IRES promoter for

concomitant expression of cytoplasmic GFP in electroporated cells. pCIG is derived from pCAGIG backbone, with addition of nuclear localization signal in from of GFP, making to GFP concentrate in nucleus (Matsuda and Cepko, 2004).

Table 2.2. Genes cloned in the lab with respective primers.

Gene construct	**Primers**	**Notes**
Cdx4	Forward: ACATGTATGTGAGTTCTCTCTTGG	Ta: 55^0 C
	Reverse: TGATCATTCTGAAACTATGAC	
VP16	Forward: ATCGATATGTCAAGGCCTCTCGAGTCGAC (ClaI site underlined.)	Ta: 50^0 C
	Reverse: TGTGTGCCAACCCCACCGTACTCGTCAATT	
Cdx4-HD	Forward: GAGTACGGTGGGGTTGGCACACAGCAGGTC	Ta: 55^0 C
	Reverse: TGATCATTCTGAAACTATGAC	
mNkx1.2	Forward: AT<u>ATCGAT</u>*CCACCATG*TTGGCATGGCAGG	Ta: 60^0 C

	(ClaI site underlined, Kozack sequence italicized.)	
	Reverse: GAGAATTCTCATAGGTGTGGAGCATAG (EcoRI site underlined.)	

Full length mNkx1.2 for chicken electroporation (mNkx1.2 pCIG). Mouse Nkx1.2 was PCR amplified from the mNkx1.2-myctag pEf2 construct (gift from Y. Marikawa), using the primers shown in Table II. The cloned segment was digested with ClaI and EcoRI included in the forward and reverse primers, respectively. Purified segment was then cloned into ClaI-EcoRI site of pCIG.

2.2 Chicken embryo incubation and harvesting

Fertilized broiler chicken eggs (Morris Hatchery, Inc.; Miami, FL) were incubated at 38.2° C in a humid chamber until reaching the appropriate stage of development. The embryos were staged according to Hamburger and Hamliton stages (Hamburger and Hamilton, 1951). Embryos post-electroporation were re-incubated until stipulated time for further analysis.

2.3 Chicken *in ovo* electroporation

Chicken embryos' neural tube were electroporated unilaterally at stage HH10-12 following standard protocols (Itasaki et al., 1999; Nakamura and Funahashi, 2001). Prior

to electroporation, India ink diluted in 1X phosphate buffer saline (PBS), microfiltered and autoclaved, was injected below the embryo to enhance contrast and facilitate embryonic manipulations. cDNAs encoding gene of interest intended for electroporation were cloned into pCIG expression vector. This vector contains a strong chicken β-actin promoter driving the expression of the gene of interest, followed by an Internal Ribosomal Entry Site (IRES), and a nuclear GFP (Megason and McMahon, 2002). The only exception was the cloning of EnRCdx4 into pCAGIG, a plasmid identical to pCIG except that it has a cytoplasmic, instead of nuclear, GFP (Matsuda and Cepko, 2004). Plasmids were diluted to a final concentration of 0.5 μg/μl in 1X PBS, with 50ng/ml Fast Green dye to aid in the visualization of the cocktail mix during neural tube injection. A few drops of Leibovitz's L15 media (Sigma-Aldrich) with 1X (100 U/mL) Pen/Strep (Sigma-Aldrich) were added on the top of the embryo to act as electrolyte and antibiotic. Electroporations were done using titanium electrodes and a square wave generator (ECM 800, Harvard apparatus) delivering 5 pulses of 21 V with 50 ms pulse duration and 1 s pulse interval (as described (Itasaki et al., 1999)). A drop of L15 media was again added prior to closing the shell with surgical tape (*3M*™ Blenderm™). Embryos positive for electroporation were assessed by the presence of GFP in the neural tube on one side. Only normal-looking embryos (e.g., not deformed) with good electroporation in the desired region (neural tube/transition zone/caudal neural plate depending on experimental requirements) were selected for further processing by *in situ* hybridization or immunohistochemistry. Analysis was focused on same axial level in all stage, transition zone (prospective thoracic level (Liu et al., 2001)) for stage HH 11-12 and thoracic level (somites 20-25 (Evans, 2003)) for stage HH 16-17.

2.4 Antisense RNA probe

Analysis of gene transcription was done by *in situ* hybridization. Dixgoxigenin (DIG) labelled antisense RNA probes against gene of interest were generated to detect gene transcripts. Briefly, construct encoding the gene of interest was linearized with the appropriate enzyme (Table III). The linearized construct was analyzed by gel electrophoresis and compared to undigested DNA and a DNA marker ladder. Linearized constructs were then purified and diluted to final concentration of 1 µg/µl in nuclease free water. Linearized DNA was then used as template for synthesis of RNA probe using appropriate RNA polymerase enzyme (Promega) (Table 2.3), using standard protocols (Wilkinson and Nieto, 1993). After transcription, DNase was added to the cocktail to remove template DNA and 1 µl of the synthesized probe was run on a gel along with DNA marker ladder to verify quality of probe (size and quantity). Verified probe was purified using RNA purification kit (QIAGEN) and store at -20°C until further use in hybridization buffer (see composition below).

Table 2.3. Enzymes used for RNA probe synthesis.

Gene	**Restriction enzyme**	**Polymerase**
Pax6	EcoRI	T7
Cdx4	EcoRI	Sp6
Sax1	EcoRI	T7

T(Bra)	KpnI	T3
Ngn2	XhoI	T3

2.5 *In situ* hybridization

Embryos harvested after electroporations were processed for *in situ* hybridization for the detection of gene transcripts, as described in (Wilkinson and Nieto, 1993). Briefly, harvested embryos were fixed with 4% paraformaldehyde diluted in PBS (PFA) at 4° C overnight. Fixed embryos were washed with 1X PBS and dehydrated and stored in 100% methanol (MtOH) at -20° C until further analysis. Dehydrated embryos were gradually hydrated using subsequent 10 minutes washes with 75% MtOH in PBS with 1% Tween-20 (PBT), 50% MtOH in PBT, 25% MtOH in PBT and finally 100% PBT, followed by two more washes in 1x PBT. Rehydrated embryos were treated with 1X (10 µg/ml) proteinase-K (Sigma Aldrich) in PBT for 15 mins. Proteinase-K treated embryos were fixed with 0.1% glutaraldehyde in 4% PFA for 20 mins. Fixed embryos were rinsed in hybridization buffer (50% formamide, 1.3 X SSC, 5mM EDTA, 100 µg/ml Heparin, .005% CHAPS, 0.2% Tween) followed with incubation in hybridization buffer for 2-3 hrs at 68° C. DIG-labeled RNA probe diluted in hybridization buffer was then added to replace the hybridization buffer. Embryos were incubated in this solution overnight at 68°C. Next day, the probe was replaced with two washes of 30 minutes each of hybridization buffer at 68°C. Embryos were then washed with 50:50 solution of Tris buffer saline with 10% Tween (TBST) and hybridization buffer mix for 20 mins at 68°C.

Embryos were then washed in 1X TBST thrice for 30 mins at room temperature. Embryos were then incubated in antibody-block buffer (5% heat inactivated goat serum and 1 mg/ml bovine serum albumin in 1X TBST) for 3 hrs at room temperature. Anti-DIG alkaline phosphatase-conjugated antibody (Roche) was diluted 1:5000 in block buffer and added to the embryos, which were then incubated at 4° C overnight. During the final day of the protocol, antibody treated embryos were washed with 1X TBST for several hours during which fresh TBST was replaced a minimum of three times. Finally before developing embryos were washed twice with 1X NTMT (0.1M NaCl, 0.05M $MgCl_2$, 0.1 Tris-HCl pH9.5, 0.2% Tween) for 10 mins at room temperature. Embryos were then developed in the dark in 1X NTMT solution containing 0.3 mg/ml nitro-blue tetrazolium salt (NBT, Thermo Scientific) and 0.117 mg/ml 5-bromo-4-chloro-3-indolyl-phosphate (BCIP, Biosynth) at room temperature until dark purple precipitate deposited revealing the areas of gene transcription. Post-development, embryos were washed with 1x TBST for 10 mins and then fixed in 4% PFA and stored at 4° C till further analysis.

2.6 Cryo-sectioning and Immunohistochemistry

Embryos harvested for immunohistochemistry (IHC) analysis were fixed with 4 % PFA for 3 hours at room temperature. Fixed embryos were washed with 1X PBS for an hour and incubated in 30% sucrose in 1X PBS overnight at 4° C to prevent desiccation during freezing step. Sucrose saturated embryos were placed in M-1 cryo-sectioning media (Thermo Scientific) in a plastic mold for 5 mins followed by freezing on dry ice. Frozen embryos were store at -80° C until processed for cryosectioning. Embryo were sectioned on cryostat (Leica CM1850). Consecutive 20 µm thick sections were collected on lysine

coated positively charged side of glass slides (Globe scientific). Collected samples were stored at -20° C until further processing.

Slides were stacked in Shandon Sequenza slide rack (Thermo Scientific) supported by Shandon coverplate for IHC analysis. Briefly, sections were washed with 1X PBS followed by wash with 1X PBS with 0.4% Triton (PBS-Triton), and blocked for one hour at room temperature blocking buffer (5% heat inactivated goat serum in PBS-Triton). Subsequently, appropriate primary antibody was added at required dilution (Table 2.4) in blocking buffer. Embryos were incubated with primary antibody at 4° C overnight. Next day, sections were washed 6 times with 1X PBS. Appropriate secondary antibody was added at required dilution (Table 2.5) in blocking buffer and incubated for an hour at room temperature. Embryos were then washed 6 additional times in 1X PBS, and left to dry at room temperature in dark. Mounting media (Vecta shield with/without DAPI) was added on the dried slides, which were than covered with cover-slips and sealed with nail polish. Processed slides were stored at -20° C.

Table 2.4. Primary antibodies

Name	Dilution	Source
Anti-mouse Pax6	1/300	Development Hybridoma Bank
Anti-mouse Pax7	1/300	Invitrogen
Anti-mouse Nkx6.1	1/250	Development Hybridoma Bank

Guinea pig anti-chick Ngn2	1/19200	Dr. Bennett Novitch (UCLA, USA) (Skaggs et al., 2011)
Anti-GFP Tag Rabbit polyclonal	1/500	AnaSpec Inc.

Table 2.5. Secondary antibodies

Name	Dilution	Source
Goat anti-mouse IgG (H+L) Alexa Flour 556	1/500	Invitrogen
Goat anti-guinea pig IgG (H+L) Alexa Flour 568	1/500	Invitrogen
Goat anti-rabbit mouse IgG (H+L) Alexa Flour 488	1/500	Invitrogen

2.7 Microscopy

Whole embryo images were taken in Zeiss stereo microscope (Carl Zeiss) with an AxioCam MRc digital color microscope camera (Carl Zeiss). Images of transverse section of neural tube were taken in AXIO Examiner Z1 (Carl Zeiss) compound microscope with an AxioCam MRc color camera, or on a Leica SP5 confocal microscope (Leica). Confocal images, thickness 2.304 μm, were processed with ImageJ (Schneider et al., 2012). Images were processed for figures using Photoshop for editing purposes including size and resolution adjustment.

2.8 Quantification of IHC data

To quantify changes in protein expression of candidate factor after electroporation, two strategies were employed. In the first strategy, protein (Pax6 or Ngn2) positive cells were counted on both electroporated and control side at the same dorso-ventral position, and the relative ratio of cells with and without protein on electroporated to control side was determined. Images were processed with ImageJ IHC toolbox plugin (Shu et al., 2013) before cell counting to select for cells above threshold level as determined by the program algorithm. A second strategy was taken to account for size deformation due to over-expression of genes. In this strategy, ratio of the mean fluorescence intensity of the electroporated side to that of the control side was determined by ImageJ. A total of 6 embryos per conditions were used for determining the significance of manipulations. Significance of difference between mean values of compared pairs was evaluated using two-tailed t-test (Microsoft Excel). Box-plus-scatter plot depicting distribution of data of each condition was plotted using MATLAB (MATLAB 2014b, The MathWorks Inc., Natick, MA, 2014).

2.9 Mathematical modeling

Transcriptional regulation of genes in the interaction network were defined by differentiation equations describing rate of change of mRNA and protein concentration in relation to concentration of regulating factors (Santillan, 2008; Sherman and Cohen, 2012; Shi et al., 2017). Differential equations representing interaction network were solved for numerical solution MATLAB solver. Parameters for differential equations

were either taken from published literatures or guessed in the range of parameters used in similar analysis in published literatures. (Detailed mathematical modeling method in chapter 4).

Chapter 3

CDX4 REGULATES THE ONSET OF SPINAL CORD NEUROGENESIS

3.1 Overview

During differentiation, cells transition through multiple discrete and labile states on their way to acquiring their final, specialized function. Each discrete state is defined by the totality of active transcription factors present inside the cell (Davidson et al., 2003b), and the transition between states is controlled by signaling factors outside the cell (Davidson et al., 2003b; Sandmann et al., 2007; Saunders and McClay, 2014). It is the cross-regulation between transcription and signaling components that promote the progressive acquisition of specialized functions while preventing dedifferentiation: transcription factors specify the cell's identity and ability to respond to signaling factors (competence), and signaling factors control the temporal activity of transcription factors to promote directional acquisition of specialized traits (Davidson, 2010; Davidson et al., 2003b). These interactions between transcription factors and signaling pathways form complex networks that have been challenging to dissect, hindering our understanding of the mechanisms regulating cell differentiation.

The vertebrate spinal cord is an ideal system to study the discrete steps in the differentiation of multipotent progenitor cells of the tail bud into neural progenitor fates. Not only is the tissue easily accessible, but the stepwise differentiation of cells occurs in a caudal-to-rostral direction whose configuration mirrors their temporal progression in differentiation: cells born earlier in development are more advanced in the differentiation

program and localize to more rostral regions that later born, more immature cells in caudal regions (Butler and Bronner, 2015; Diez del Corral and Storey, 2004; Wilson et al., 2009).

The spatiotemporal gradient of neural differentiation states in the spinal cord is generated and maintained by opposing gradients of the signaling factors FGF, Wnt, and Retinoic Acid (RA). *Fgf8* and *Wnts* (*Wnt3a* and *Wnt8c*) establish a caudal to rostral gradient that promote pluripotency by directly promoting *T (Bra)*, *Sox2*, *Cash4* and *Sax1* (*Nkx1.2*), and preventing *Pax6* and *Irx3* transcription (Bertrand et al., 2000; Diez del Corral et al., 2003). In contrast, RA secreted from somites establishes a rostral to caudal signaling gradient that promotes differentiation by inducing cells to exit the proliferation program, first by promoting transcription of neurogenic genes *Pax6* and *Irx3* (Diez del Corral et al., 2003; Pituello et al., 1999), and then by promoting transcription of the differentiation genes *Ngn1/2* and *NeuroM* (Diez del Corral et al., 2003). FGF/Wnt and RA opposing signaling activities are segregated to caudal and rostral regions of the nascent spinal cord through positive and negative interactions: FGF indirectly promotes differentiation by inducing RA production through a *Wnt8c*-mediated mechanism, but FGF also maintains RA production away from the pluripotency zone by directly inhibiting RA synthesis caudally (Kumar and Duester, 2014; Moreno and Kintner, 2004; Olivera-Martinez and Storey, 2007). These interactions are proposed to function as the signaling switch that drives the transition of cellular states in the caudal neural tube (Diez del Corral and Storey, 2004). While the signaling aspect of the differentiation switch have been well studied, the underlying transcription factor network driving the cell transition states in the nascent spinal cord is poorly understood.

In the NMPs domain and transition zones, Cdx stand out as a transcription factor that is under the simultaneous control of FGF, Wnt and RA signals (Deschamps and van Nes, 2005; Lohnes, 2003). In the spinal cord, *Cdx* genes are essential for tissue specification and rostrocaudal pattering (Hayward et al., 2015; Mazzoni et al., 2013; Shimizu et al., 2006; Skromne et al., 2007), controlling the initiation, establishment and maintenance of *Hox* domains of transcription. In the context of somitogenesis, Cdx is proposed to integrate the caudalizing signals FGF, Wnt and RA to generate the nested rostrocaudal distribution of *Hox* gene transcripts that patterns the spinal cord's primary axis (reviewed in Deschamps and van Nes (2005)). Whether Cdx also functions to integrate FGF, Wnt and RA signals in the caudal neural tube to regulate spinal cord neurogenesis is not known.

Here we show that Cdx4 plays a central role in regulating temporal progression of cellular states in the chicken caudal neural tube. Using transient gene expression strategies, we show that Cdx4 regulates several genes involved in the sequential differentiation of neural precursors, including *Sax1*, *Pax6* and *Ngn2*. Our result show that Cdx4 acts as a dual control switch during neurogenesis, inhibiting pluripotency in NMP cells while promoting acquisition of neural identity. Furthermore, we show that timely down-regulation of Cdx4 is needed for further neuronal cell differentiation. Our results support a novel role for Cdx factors in regulating the onset and progression of caudal neural tube neurogenesis.

3.2 Results

3.2.1 Spatio-temporal dynamics of *Cdx4* expression

To understand the role of Cdx4 in regulating onset of neurogenesis, I analyzed the spatio-temporal domain of *Cdx4* transcription. I harvested chicken embryos from various stages spanning from HH4 (20-24 hours post incubation) to HH22 (4 day post-incubation) (HH stages according to Hamburger and Hamilton (1951)). In all the stages analyzed, *Cdx4* expression was restricted to the caudal portion of the embryo (Fig. 3.1). At HH4, *Cdx4* was found to be expressed in the caudal half of the embryo in regions surrounding the primitive streak (Fig. 3.1 a). Expression was also observed at the posterior margin of the area opaca (Fig. 3.1a). No expression was detected in the Hensen's node (Fig 3.1 a). As Hensen's node regresses caudally from stage HH6 onwards, *Cdx4* expression appears and intensifies in Hensen's node and primitive streak (Fig 3.1 b). During stages HH7-10 (Fig. 3.1 c), a strong level of *Cdx4* expression was detected in the open neural plate and in the surrounding pre-somitic mesoderm (PSM). Relatively lower expression was detected in the PSM compared to the neighboring neural plate, and expression was completely absent in ventral midline of the neural plate (Fig 3.1 c). At these stages, a caudal high to rostral low gradient of *Cdx4* expression could be appreciated both in the neural plate and the PSM, with an anterior limit of the expression in the neural plate that localized to the second to last formed somite (Fig. 3.1 c). At stage HH12+ onwards, as the neural plate starts rolling over to form the neural tube and the primitive streak develops into tail bud, *Cdx4* expression domain remained constant in the tailbud, and nascent neural and mesodermal tissue (Fig. 3.1 d). From stage HH16 onwards, the area of expression shows

a gradual reduction finally becoming undetectable in the tail bud post stage HH22-23 (Fig. 3.1 e, f).

To explore the rostro-caudal (RC) gradient of *Cdx4* expression in neural region, I analyzed *Cdx4* domain of transcription in transverse sections (Fig. 3.2). The transverse sections not only confirmed that *Cdx4* transcription in neural tissues is higher caudally than rostrally, but also showed that *Cdx4* exhibits a dorsoventral (DV) gradient of transcription that has not been reported in previous studies. The analysis showed that in caudal most regions *Cdx4* is expressed throughout the medio-lateral neural plate (the future DV axis of neural tube), and that this expression becomes progressively restricted to the lateral/dorsal regions in more rostral regions of the tissue. In addition, *Cdx4* expression was absent in the dorsal roof region. The DV pattern dynamics can be more clearly observed as the length of the transition zone expands from stage HH10 to HH 15 (Fig. 3.2).

These observations show that *Cdx4* is transcribed in the NMPs domain harboring the neural tube progenitors and in the transition zone where early neural identity factors are turned on. Furthermore, these observations also show previously unreported *Cdx4* transcription dynamics along the DV axis of the neural tube at the time when DV identities begin to establish. These observations provide an impetus to explore the role of Cdx4 in early spinal cord neurogenesis.

3.2.2 *Cdx4* transcription shows dorso-ventral restriction in the caudal neural tube

Comparative analysis of *Cdx4* transcription to other DV neural tube markers revealed a correlation with *Cdx4* transcriptional down-regulation in ventral regions of the neural tube and the activation of DV patterning events (Briscoe et al., 2000; Diez del Corral et al., 2003; Novitch et al., 2001). To test the relationship between *Cdx4* dynamic DV transcription and neural tube DV patterning markers, I first analyzed the expression of *Cdx4* with respect to the expression of the dorsal neural tube marker *Pax7* (Briscoe et al., 2000; Diez del Corral et al., 2003), the dorsal to intermediate marker *Pax6* (Briscoe et al., 2000; Novitch et al., 2003) and the ventral marker *Nkx6.1* (Briscoe et al., 2000; Diez del Corral et al., 2003; Novitch et al., 2001). Dorsally, *Cdx4* expression overlapped with that of *Pax7* throughout *Cdx4*'s RC expression domain; and ventrally, *Cdx4* expression was downregulated concomitantly with the onset of *Nkx6*.1 expression (Fig. 3.3 A, B). In contrast, *Cdx4* and *Pax6* transcriptional domains overlapped to different extents depending on the RC level of the section (Fig. 3.3 C): in the caudal most region the caudal transition zone, *Cdx4* and *Pax6* expression co-localized, whereas in the rostral most region, *Cdx4* and *Pax6* expression overlapped only in the dorsal-most portion of the *Pax6* expression domain. The finding that in more rostral regions of the neural tube the transcription of *Cdx4* becomes gradually restricted to dorsal regions suggested a possible involvement of Cdx4 in DV patterning of the neural tube.

3.2.3 Cdx4 does not regulate dorso-ventral patterning of the neural tube

To test *Cdx4* involvement in promoting dorsalization or preventing ventralization of the neural tube cells, I over-expressed wild type *Cdx4* in the neural tube of stage HH11-12 embryos and analyzed changes in the expression domains of DV markers *Pax7*, *Pax6,* and *Nkx6.1* 24 hours post-electroporation (hpe). In this experimental paradigm, *Cdx4* expression was artificially maintained at high levels in the neural tube at times when it is normally down regulated. High levels of *Cdx4* expression did not change *Pax7* and *Nkx6.1* transcription domain (Fig. 3.4 a, a, c, c'). However, over-expression of *Cdx4* caused sustained *Pax6* expression in dorsal cells and ectopic expression in ventral cells (Fig. 3.4 b, b'). This result suggests that Cdx4 is not a general regulator of DV gene transcription, but a specific *Pax6* transcriptional regulator.

3.2.4 Cdx4 regulates *Pax6* transcription in neural progenitor cells

In addition to its function in DV cell specification, Pax6 has an earlier role in the maturation of neural progenitor cells in the nascent neural tube (Bel-Vialar et al., 2007). To investigate the role of Cdx4 in regulating *Pax6* transcription during neural progenitor cell maturation, I investigated whether Cdx4 was sufficient to activate *Pax6* in the nascent neural tube, in a region where *Pax6* is not yet transcribed in wild type embryos. Embryos were electroporated with *Cdx4* in the transition zone, grown for 8 hours only, and analyzed for premature *Pax6* activation by *in situ* hybridization. No changes in *Pax6* transcription were observed in *Cdx4* electroporated cells compared to contralateral control cells (Fig. 3.5 A: a, a'). This was in contrast to the activation of *Pax6* by *Cdx4* in

the mature neural tube, where embryos were allowed to grow for 24 hours after electroporation (Fig. 3.4 b, b'). Several explanations can account for the delayed activation of *Pax6* by *Cdx4* including that *Cdx4* requires the presence of additional co-factors or the elimination of repressors to activate *Pax6* transcription.

To test if Cdx4 dependent activation of *Pax6* depends on co-factors present in the mature neural tube, I bypassed this potential need by generating a chimeric Cdx4 in which the endogenous caudal activation domain of Cdx4 was replaced with the transcriptional activation domain of the herpes simplex virus VP16 protein: VP16Cdx4 (Sadowski et al., 1988)). Chimeric VP16Cdx4 have shown to reproduces Cdx functions in *Hox* gene regulation assays, independently of the presence or absence of regulatory signals (e.g., FGF; (Bel-Vialar et al., 2002; Faas and Isaacs, 2009)). VP16Cdx4 over-expression in the transition zone caused the activation of *Pax6* transcription as early as 8 hpe (Fig. 3.5 A: b, b'). In addition, I also observed caudalization of *Pax6* in some embryos (n=4/6 by ISH, n=4/6 by IHC Fig. 3.4 B: b, b'). Together, these results suggest that the Cdx4 can activate *Pax6* transcription in the caudal neural tube but only in particular permissive conditions.

To test if endogenous Cdx4 is necessary for *Pax6* activation in the transition zone, I outcompeted endogenous Cdx4 from DNA binding sites by over expressing a dominant negative form of Cdx4 in which the transcription activation domain of the protein was replaced with the transcriptional repressor domain of the *Drosophila* Engrailed protein (Han and Manley, 1993). This chimeric form of Cdx4 has been shown to repress the expression of downstream targets of Cdx in *Xenopus* assays (e.g., *Hox* genes) (Bel-Vialar et al., 2002; Isaacs et al., 1998). Overexpression of dominant negative EnRCdx4 resulted in loss of *Pax6* in the transition zone as early as 8 hpe (Fig. 3.5 A: c, c'). These results

suggest that Cdx4 is necessary for *Pax6* activation in the transition zone. However, together with the gain of function experiments, these results also suggest that Cdx4 activation of *Pax6* transcription require additional cofactors.

3.2.5 Cdx4 activation of *Pax6* depends on retinoic acid

One possible factor that could regulate Cdx4 activity in the transition zone is retinoic acid (RA). RA is synthesized in the somites flanking the neural tube (Molotkova et al., 2005), from where it diffuses to the transition zone to activate *Pax6* transcription (Pituello et al., 1999). To test whether RA is required for Cdx4 dependent *Pax6* activation, I analyzed the effect of simultaneously increasing Cdx4 activity while eliminating RA signaling on *Pax6* expression. As shown by others (Novitch et al., 2003), inhibition of RA pathway by over-expressing a dominant negative RA receptor (dnRAR) resulted in the downregulation of *Pax6* (Fig 3.6 A: d, d'). In this background, *Cdx4* overexpression did not rescue *Pax6* transcription (24 hpe; Fig 3.6 A: e, e'). By contrast, in the presence of RA signaling, Cdx4 overexpression is able to activate *Pax6* (Fig 3.6 A: a, a'). This suggests that RA signaling provides the permissive environment for Cdx4 to activate *Pax6*. In addition, *VP16Cdx4* overexpression rescued *Pax6* expression even in the absence of RA (Fig 3.6 A: f, f') signaling. This suggests that the Cdx4's failure to activate *Pax6* in the absence of RA is not due to its inability to bind to *Pax6* regulatory region. Together, my results suggest that Cdx4 activation of *Pax6* transcription in the transition zone is dependent on RA.

3.2.6 Cdx4 inhibits Pax6-dependent induction of the neural differentiation gene *Ngn2*

Despite Pax6 being active in both the transition zone and the neural tube, it only activates neural differentiation genes in the neural tube (Bel-Vialar et al., 2007). What prevents Pax6 premature activation of neural differentiation genes in the transition zone? I addressed this question by focusing on the regulation of the neurogenic factor *Ngn2* for two reasons: First, *Ngn2* transcription is under direct Pax6 regulation (Scardigli et al., 2003), and second, *Ngn2* transcription domain in the caudal-to-rostral axis is immediately anterior to *Cdx4* transcription domain (Fig 3.7 B). Thus, it is possible that Cdx4 activity is incompatible with *Ngn2* transcription. To test the possibility that Cdx4 is a negative regulator of *Ngn2*, I over expressed *Cdx4*, *VP16Cdx4* and *EnRCdx4* in the neural tube. All constructs caused downregulation of *Ngn2* expression despite the fact that *Cdx4* and *VP16Cdx4* also induced Pax6 (Fig 3.7 A: a, a'; b, b'). This result supported the idea that Cdx4 represses *Ngn2*. To further test this possibility I co-expressed *Cdx4* and *Pax6*. While Pax6 on its own was able to ectopically activate *Ngn2* (Fig 3.7 A: d, d') (Bel-Vialar et al., 2007), it can no longer do so in the presence of Cdx4 (Fig 3.7 A: e, e'). Together, these results suggest that Cdx4 is a negative regulator of *Ngn2* transcription, and of neuronal differentiation.

3.2.7 Cdx4 inhibits pro-neural cell's pluripotency in the NMPs domain

Cdx4 is transcribed at high levels in the stem zone of the caudal neural plate, where it overlaps with the transcription of two pluripotency marker genes *T (Bra)* (NMP marker;

(Henrique et al., 2015; Yamaguchi et al., 1999)), and *Sax1* (known as *Nkx1.2* in mouse, a marker of newly differentiated progenitor neural cells; (Delfino-Machin et al., 2005; Sasai et al., 2014)). In mouse, the Cdx factor Cdx2 have been shown to be necessary for sustained *T (Bra)* expression (Savory et al., 2009). To investigate Cdx4 function in the regulation of the caudal stem zone of the neural tube, I analyzed the expression of *T (Bra)* and *Sax1* in embryos electroporated with different *Cdx4* constructs. Neither gain nor loss of Cdx4 function affected *T (Bra)* transcription (Fig 3.8 A), suggesting that Cdx4 does not regulate *T (Bra)*. However, over expression of *Cdx4* and *VP16Cdx4* resulted in loss of *Sax1* in the neural tube (Fig 3.8 B: a, a'; b, b'), suggesting that neural progenitor cell identities are under Cdx4 regulation. Given that both Cdx4 and VP16Cdx4 are transcriptional activators, this result suggests that Cdx4 repression of *Sax1* is likely to be indirect. One likely candidate to mediate this activity is *Pax6*, as it is induced by Cdx4 and directs cells towards differentiation. Even though *Cdx4* over-expression didn't expand *Pax6* expression in caudal neural tube, I wanted to rule out the possibility that VP16Cdx4 represses *Sax1* via *Pax6* activation. However, *Pax6* over expression did not change *Sax1* transcription in the caudal neural tube (Fig 3.8 C). Furthermore, EnRCdx4 also down regulated *Sax1* transcription (Fig 3.8 B: c, c'), suggesting loss of function of Cdx4 also results in downregulation of *Sax1*. Together, these results suggest that, through unknown and indirect mechanisms, Cdx4 represses *Sax1* and neural pluripotency.

3.2.8 Feedback regulation of *Cdx4* transcription by pluripotency and differentiation genes establish a gene network that regulates neural cell progenitor maturation

So far my data shows that Cdx4 inhibits transcription of the pluripotency marker gene (*Sax1)* and activate the transcription of early (*Pax6*), but not late (*Ngn2*), differentiation marker genes. In order to determine whether feedback regulation controls *Cdx4* transcription in the nascent neural tissue, I examined if over expression of *Sax1* and *Pax6* causes changes in *Cdx4* transcription. First I analyzed the role of Sax1 in regulating *Cdx4*. To over-express *Sax1*, I used the mouse version of the gene, *mSax1 (mNkx1.2)*, that was shown to act as a repressor (Tamashiro et al., 2012) and has been previously used to study the role of Sax1 in chicken embryo (Sasai et al., 2014). Over expression of *mSax1* didn't affect *Cdx4* transcription (Fig 3.9 A: b, b') in the transition zone 8 hpe, suggesting Sax1 is not involved in *Cdx4* regulation. I also tested for Sax1's regulation of *Pax6*, as *Sax1* and *Pax6* domain abuts in the transition zone. As previously suggested (Sasai et al., 2014), over expression of *mSax1* down regulated *Pax6* transcription (Fig 3.9 A: c, c'). Using *mSax1* I was able to test for Sax1 autoregulation in chicken. Over-expression of *mSax1* resulted in downregulation of endogenous *Sax1* (Fig 3.9 A: a, a') suggesting Sax1 inhibits itself by a negative autoregulation.

I next examined the role of Pax6 regulation of *Cdx4* in the transition zone. Over-expression of *Pax6* in this region resulted in *Cdx4* down regulation (Fig 3.9 B: a, a'), suggesting that Pax6 represses *Cdx4* in the region of overlap. Consistent with this result, dominant negative *EnRPax6* over expression resulted in upregulation of *Cdx4* (Fig 3.9 B: b, b'). Given that the activator Pax6 represses *Cdx4* and the dominant negative construct EnRPax6 activates *Cdx4*, these results suggest that the negative feedback regulation of

Pax6 on *Cdx4* is indirect. It is unlikely that the downstream target of Pax6, *Ngn2*, mediates this regulation because the expression domain of *Cdx4* and *Ngn2* do not overlap (Fig 3.3 A; Fig 3.7 C).

Together, these results show evidence for cross talk among transcriptional regulators responsible for the maturation of neuronal progenitor cells in caudal neural tube. My results also support the evidence for a core role of Cdx4 in regulating downstream transcription factor response to the overlying signaling information.

3.3 Discussion

Here I showed that Cdx4 plays a central role of coordinating signaling information in regulating downstream transcriptional response during the onset of spinal cord neurogenesis in early embryonic stages. This proposed role of Cdx4 is independent of its role in rostro-caudal patterning. By using gain and loss of function strategies, my data specifically highlighted several points of gene interaction. (1) Cdx4 promoted maturation of pro-neural cells in the NMPs domain by downregulating pluripotency marker *Sax1*. (2) Cdx4, in combination with RA, further promoted differentiation in the cells exiting the NMPs domain by activating *Pax6* transcription. (3) Cdx4 indirectly inhibited further differentiation of *Pax6*+ cells by inhibiting *Ngn2*. (4) Finally the crosstalk between *Sax1*, *Pax6* and *Cdx4* refines the transcriptional response of cells to signaling factors. Together, this data supports a key role for Cdx4 operating as a differentiation switch, regulating the transition of caudal spinal cord cells from pluripotent to neurogenic state.

3.3.1 Role of Cdx4 in neurogenesis as a differentiation switch

Cdx4 is expressed in a dynamic RC-DV gradient at the caudal end of the embryo (Fig 3.2), overlapping various cellular states involved in early neurogenesis. At the caudal most end, *Cdx4* is transcribed in NMP cells that are self-renewing and pluripotent, and can give rise to both mesoderm and neuroectoderm (Wilson et al., 2009). These cells are defined by transcription of the genes *T* (*Bra*) and *Sox2* (Henrique et al., 2015). In contrast, at the rostral end of the expression domain, *Cdx4* is transcribed in cells expressing early neural identity markers. Rostral to the *Cdx4* expression domain, cells express the differentiation marker *Ngn2*. My results support the idea that across its domain of expression, Cdx4 interact with factors involved in onset of spinal cord neurogenesis.

At the caudal end of the embryo, NMP cells differentiate to give rise to growing spinal cord tissue and surrounding mesoderm. NMP cells express the mesodermal marker *T (Bra)* and the neural marker *Sox2*. According to current models, *T (Bra)* and *Sox2* cross regulation maintains NMP status in dynamic equilibrium (Henrique et al., 2015; Martin and Kimelman, 2012). A tilt in the equilibrium leading to accumulation of *T (Bra)* would lead to cells acquiring mesodermal fate, whereas a tilt favoring *Sox2* transcription would lead the cells to acquire a neural fate (Gouti et al., 2015; Henrique et al., 2015).

Recent evidence suggests that Cdx factors might also be involved in maintaining the balance of NMP cells. *Cdx2* mutant mice, compared to wild type, exhibit early axis truncation with deficiencies in mesodermal and ectodermal tissue after somite 5 (Chawengsaksophak et al., 2004; Savory et al., 2009). In this respect, *Cdx2* null mutants are similar to *T (Bra)* null mutants (Chawengsaksophak et al., 2004). Indeed, loss of *Cdx2*

lead to reduction in *T (Bra)* expression domain post E9.5 (Savory et al., 2009). Conversely, *Cdx* triple mutants exhibit a complete loss of *T (Bra)* in the stem zone, suggesting a redundant function of Cdx in maintaining *T (Bra)* expression (van Rooijen et al., 2012). Even though Cdx2 binding sites were found on *T (Bra)* locus, Cdx dependent *T (Bra)* regulation has been suggested to occur via Cdx2 modulation of *Wnt3a* expression (Savory et al., 2009). In the current study, however, Cdx4 activity manipulation did not change the expression domain of *T (Bra)*. Overexpression of *Cdx4* or *VP16Cdx4* did not upregulate *T (Bra),* suggesting Cdx4 is not sufficient to induce *T (Bra)* (Fig 3.8 A). Conversely, loss of function via EnRCdx4 did not lead to downregulation of *T (Bra)* expression. This could be a result of Cdx functional redundancy as other Cdx members were not altered. Also, as the Cdx dependent regulation of *T (Bra)* is suggested via modulation of Wnt3a signaling (Savory et al., 2009), given the observation that cells at the caudal end were sparsely electroporated, any change in *Wnt3a* expression wouldn't have been sufficient to downregulate *T (Bra)*.

NMP cells also express pluripotency marker *Sax1 (Nkx1.2* in mice*)*. *Sax1* expression is maintained in the neural committed cells as they leave the NMP domain and become part of the neural plate. By contrast, newly differentiated mesodermal fated cells do not express *Sax1*, suggesting *Sax1* is a neural specific marker. While *Sax1* has been consistently used as a marker for pluripotent cells (Bertrand et al., 2000; Delfino-Machin et al., 2005; Sasai et al., 2014), its function in promoting pro-neural fate in the caudal neural tube has not been investigated. However, a recent study suggested that Sax1 acts a repressor and is involved in mediating upstream FGF signaling in inhibiting differentiation and promoting floor plate competence and induction (Sasai et al., 2014).

In the caudal transition zone, *Sax1* expression is nested within the *Cdx4* expression domain. My data showed that Cdx4 negatively regulates *Sax1* (Fig 3.8 B). Significantly, Cdx4 repression of *Sax1* was indirect, as VP16Cdx4, the constitutively active form of Cdx4 also repressed *Sax1*. Surprisingly EnRCdx4, the constitutive repressor form of Cdx4 also repressed *Sax1* suggesting that loss of function of Cdx4 also downregulated *Sax1*. One possibility that will explain both constitutive active and repressive forms of Cdx4 resulting in the same phenotype is that Cdx4 regulates *Sax1* by activating its activator (for example *Wnt3a* (van Rooijen et al., 2012)) and also its inhibitor (currently unknown). My speculation is that in the caudal stem zone Cdx4 dependent repression is not dominant due to high concentration of signaling factors FGF/Wnt that induces both *Sax1* and *Cdx4* (Bel-Vialar et al., 2002; Bertrand et al., 2000; Diez del Corral et al., 2002; Nordstrom et al., 2006; Tamashiro et al., 2012). High levels of FGF/Wnt signaling are either able to repress the Cdx4 dependent repressor of *Sax1* or outcompete its activity. However, in the caudal transition zone Cdx4 dependent repression is able to outcompete FGF/Wnt dependent *Sax1* activation leading to *Sax1* downregulation in the transition zone.

It is important to mention that despite the downregulation of *Sax1* in neural plate in Cdx4 overexpression experiments, there was no change in the expression domain of *T (Bra),* as discussed earlier. This suggest that Cdx4 is not directly involved in determining the size of NMP domain and might be playing an indirect role in balancing neural and mesodermal specification. Further research would explicate if Cdx promotes neural or mesodermal fates in the NMPs or both.

Cdx4 dependent downregulation of *Sax1* in the pro-neural cells located in the caudal transition zone has two implications, downregulating pluripotency and promoting differentiation. Sax1 has been shown to inhibit *Pax6* and *Irx3* expression in caudal neural tube (Sasai et al., 2014), thereby indirectly promoting expression of floor plate specification factors. By downregulating *Sax1*, Cdx4 primes the neural progenitor cells to begin their differentiation by getting rid of the repression, thus rendering the neural tube competent to respond to differentiating signals. Cdx4's role in furthering differentiation of pro-neural cells also involves the activation of *Pax6* (Fig 3.6). This activity only takes place in the rostral portion of the transition zone because Cdx4 activation of *Pax6* transcription is dependent on RA signaling. Hence, Cdx4 promotes acquisition of neural identity by two mechanisms, by downregulating pluripotency by indirectly repressing *Sax1*, which otherwise inhibits *Pax6*; and by directly activating *Pax6*.

As mentioned above, Cdx4's regulation of *Pax6* is dependent on RA and thereby restricted at the rostral transition zone. Multiple mechanisms have been proposed to explain lack of *Pax6* expression at the caudal end. Firstly, FGF signaling has been suggested to inhibit *Pax6* via higher-order chromosomal modification resulting in the *Pax6* locus being inaccessible to activators (Patel et al., 2013). This could explain Cdx4's inability to turn on *Pax6* in the caudal stem zone as it is unable to bind to the *Pax6* locus. However, as observed, VP16Cdx4 was able to prematurely activate *Pax6* in the caudal transition zone suggesting that locus inaccessibility is not the only reason for *Pax6* inhibition. Secondly, Sax1 is a known inhibitor of *Pax6* in the newly differentiated pro-neural cells. However, my results showed that while *Cdx4* overexpression downregulates *Sax1*, this downregulation is not concomitant with *Pax6* activation in *Sax1*- cells. The

discrepancy between Cdx4 and VP16Cdx4 ability to activate *Pax6* suggest that in addition to open chromatin and absence of Sax1, Cdx4 also requires a co-factor in order to activate *Pax6*.

In the presence of RA, Cdx4 was able to activate *Pax6* similar to VP16Cdx4 (Fig 3.9). RA has been implicated in opening up the *Pax6* locus by antagonizing FGF signaling (Patel et al., 2013). In addition, the *Pax6* locus also contain retinoic acid response elements (RAREs) (Cunningham et al., 2016), suggesting RA-RAR and Cdx4 cooperate at the promoter levels to activate *Pax6*. Cdx factors are known to regulate *Hox* gene activation via chromatin remodeling (Mazzoni et al., 2013), suggesting another possibility that Cdx4, in the presence of RA, can open repressive chromatin structure, thus opening the *Pax6* locus for regulation. Thus while it is unclear how RA modulates Cdx4 activity in the transition zone, epigenetic modification is the most probable candidate.

The final step in our model proposes that Cdx4 prevents the further differentiation of cells promoted by Pax6. Pax6 promotes cell differentiation by activating several downstream targets, including *Ngn2*. In the neural tube surrounded by somites, *Ngn2* is expressed in a subset of *Pax6*+ cells where it promotes cell cycle exit and further differentiation (Lacomme et al., 2012). This expression of *Ngn2* in the intermediate domain of neural tube is under direct Pax6 regulation (Scardigli et al., 2003), as suggested by lowered *Ngn2* expression in *Pax6* mutants compared to wild type mice (Bel-Vialar et al., 2007). In the neural tube domain where *Cdx4* and *Pax6* overlap, *Ngn2* is not transcribed (Fig 3.7 B). My experiments demonstrated that Cdx4 can repress *Ngn2* transcription (Fig 3.7), suggesting that Cdx4 primes the cells for differentiation but does

not let them differentiates just yet. As *Cdx4* expression gets dorsally restricted, Pax6 is now able to activate *Ngn2* in the ventral neural tube regions. This is evident from ventral expression of *Ngn2* in the early neural tube (Fig 3.7 B). As Cdx factors are known to act as transcriptional activators, the negative regulation of *Ngn2* seems to be indirect. Indirect regulation could also provide a time delay between *Cdx4* elimination and *Ngn2* activation.

3.3.2 Mechanism of Cdx4 downregulation in rostral transition zone

Several possible mechanism, acting in conjunction, can be invoked to explicate the progressive downregulation of *Cdx4* from the ventral neural tube. (1) My experiments showed that *Pax6* overexpression lead to loss of *Cdx4* (Fig 3.9 B). By contrast, *EnRPax6* overexpression lead to upregulation of *Cdx4* (Fig 3.9 B), suggesting Pax6 regulation of *Cdx4* is indirect and probably by prompting expression of a *Cdx4* inhibitor. However, loss of *Pax6*, as observed in *Sax1* overexpression experiments (Fig 3.9 A), did not change Cdx4 expression domain implying Pax6 is not sufficient to downregulate *Cdx4* and could be cooperating with additional factors that are responsible for *Cdx4* repression. (2) RA could also be involved in *Cdx4* downregulation as RA signaling antagonizes FGF/Wnt signaling in the caudal neural tube (Diez del Corral et al., 2003). Additionally, RA has also been shown to directly inhibit *cdx4* expression in zebrafish (Lee and Skromne, 2014). Furthermore, *Pax6* being a downstream RA target (Novitch et al., 2003) suggest that RA dependent *Cdx4* inhibition could also involve Pax6 dependent mechanism. (3) Since, *Cdx4* downregulation in ventral neural tube is concomitant with activation of ventral neural tube identity factor *Nkx6*.1 (Fig 3.3), and *Nkx6*.1 being a direct SHH target

(Briscoe et al., 2000), then SHH signaling could also be another potential repressor of *Cdx4*. In summary, signaling information in the mature neural tube downregulates *Cdx4* expression in rostral transition, thereby promoting further differentiation of neural cells.

Altogether, my data suggest the mechanism for sequential turning on or off of genes involved in early neurogenesis in the caudal spinal cord, with Cdx4 at its core. My data proposes a model where the RC gradient of *Cdx4* drives sequential maturation of cells from NMP state to neural state, where its downregulation is required for further progression into neurogenic state.

3.3.3 Integration of signaling and transcription factor models during spinal cord neurogenesis

The proposed GRN (Fig 3.10), with Cdx4 at its core, involved in progression of cellular states in caudal neural tube could be acting under the signaling switch proposed by Diez del Corral (2003) and Olivera-Martinez (2007). High concentration of FGF/Wnt signaling in the caudal stem zone leads to activation of *T (Bra)*, Sax1 and *Cdx4*. With the decrease in FGF/Wnt signaling strength in the transition zone Cdx4 is able to downregulate *Sax1*. Wnt8c is responsible for activating *Raldh2* in the somites, where Wnt8c is able to overcome FGF repression of *Raldh2*. RA synthesized in somites then diffuses caudally into the neural tube, and promotes differentiation of competent cells in the rostral transition zone. Cdx4 is responsible for initial activation of *Pax6* in combination with RA; however, in the neural tube surrounded by the somites, RA can maintain *Pax6* expression in a Cdx4 independent manner. In the rostral transition zone, Pax6 activation drive cells to acquire neural identity. However, the presence of Cdx4

prevents them from turning on *Ngn2* and further differentiating. Once *Cdx4* starts clearing from the ventral neural tube, *Pax6*+ cells start upregulating *Ngn2* and acquire neurogenic identity.

Altogether, FGF-Wnt-RA provides spatial information to the maturing neural cells, in addition to driving transition in signaling factors. The transcription network in the NMP cells responds to this spatio-temporal information and regulates the pace of differentiation in the maturing neural cells.

3.4 Figures

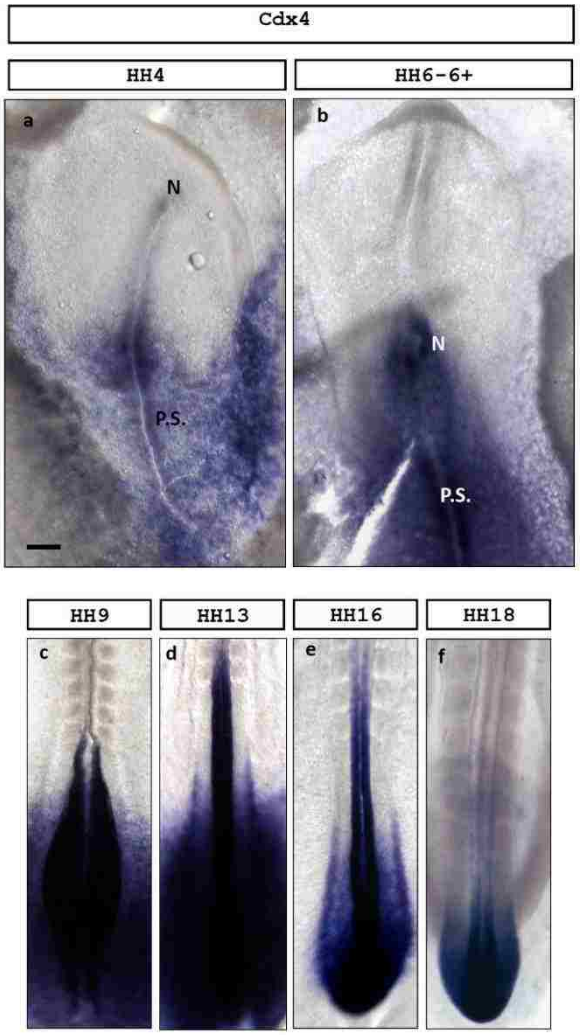

Figure 3.1: *Cdx4* is transcribed in region encompassing early neurogenic events. *Cdx4* transcription is restricted at the caudal end of the embryo throughout its expression duration. *Cdx4* is detectable in chicken embryo around stage HH4 (a). At HH6-6+ (b) *Cdx4* is transcribed in the primitive streak (P.S.) region including the Hensen's node (N). *Cdx4* transcription domain includes caudal later epiblast, node-streak border and transition zone; regions that are involved in early neurogenic events as shown for HH9 (c) and HH13 (d). As neural tube rolls up to form tail bud, *Cdx4* expression is still maintained in the NMP domain as shown for HH16 (e) and HH18 (f). Scale bar 200µm.

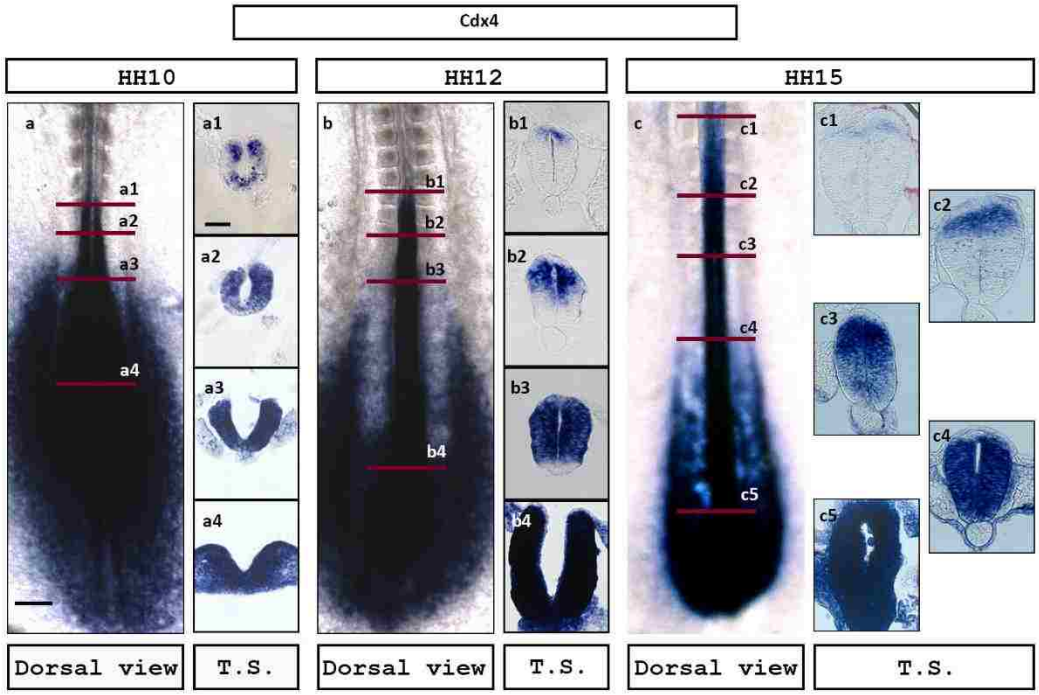

Figure 3.2: *Cdx4* transcription exhibit rostro-caudal (RC) and dorso-ventral (DV) dynamics. *Cdx4* is transcribed in a caudal-high to a rostral-low gradient in the neural tube. At the caudal end, *Cdx4* is transcribed throughout the medio-lateral (a4) or dorso-ventral (b4,c5) extent of the neural tube. *Cdx4* transcription is progressively restricted in the dorsal end of the neural tube at the rostral end of the expression domain (a1,b1,c1). Scale bar 200µm (whole mount); 40µm (transverse sections). Red bars represent RC axial position of transverse section on the right of whole mount image.

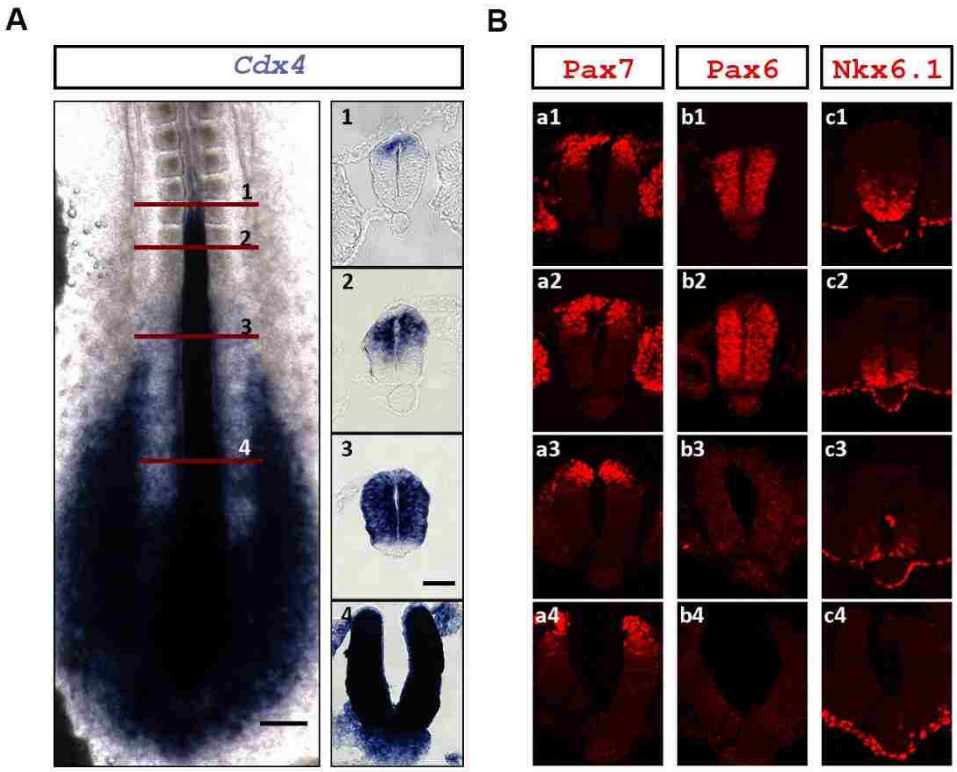

Figure 3.3: *Cdx4* dorso-ventral (DV) transcription dynamics overlap with expression of dorso-ventral patterning factors. Rostro-caudal (RC) expression of Cdx4 in HH11 wild type embryo. Sections on the left depict Cdx4 expression domain along the DV axis at depicted RC levels (A). Red bar represent the RC axial level of transverse sections on the right of whole mount view. Expression of known DV patterning factors along the equivalent position on the RC axes as for the sections in A (B). Cdx4 DV expression overlaps with that of dorsal patterning factor Pax7 (B: a1-a4), while it is complementary to ventral patterning factor Nkx6.1 (B: c1-c4). There is partial overlap with the expression of intermediate factor Pax6 (B: b1-b4). Scale bar 200µm (whole mount); 40µm (transverse sections).

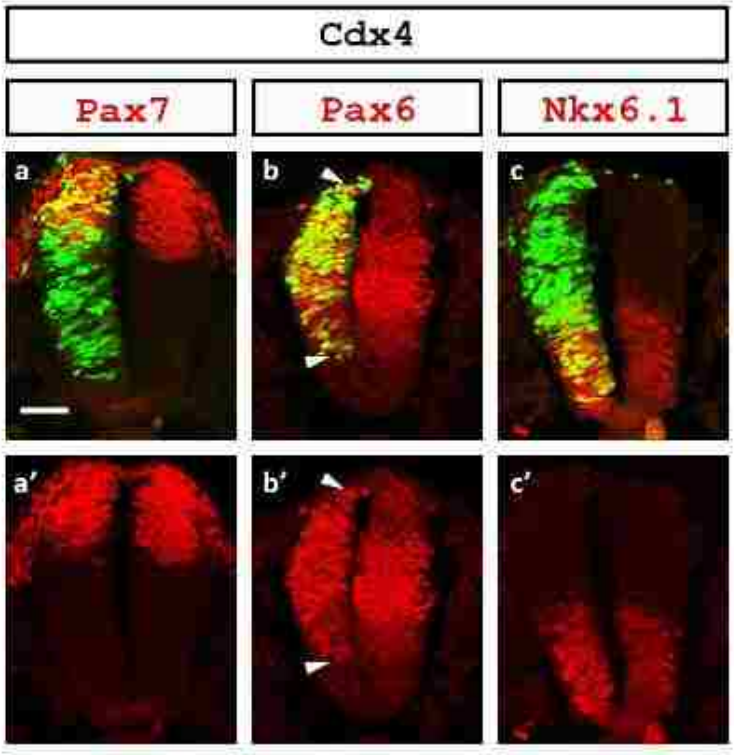

Figure 3.4: Cdx4 does not regulate onset of DV patterning. Ectopic *Cdx4* over-expression in a mature neural tube failed to change the overall DV patterning (a, c). However, *Cdx4* over-expression resulted in expansion of *Pax6* expression in cell-autonomous manner suggesting Cdx4 is a *Pax6* activator (b) (n=6/6). White arrows point to ectopic domain of *Pax6* expression in electroporated side. Electroporated cells are shown with green nucleus (co-expression of GFP) and red nucleus depict the mentioned factor's expression as analyzed with immunohistochemistry. Embryos were electroporated at HH11-12 and analyzed 24 hours post-electroporation (hpe). Scale bar 40μm.

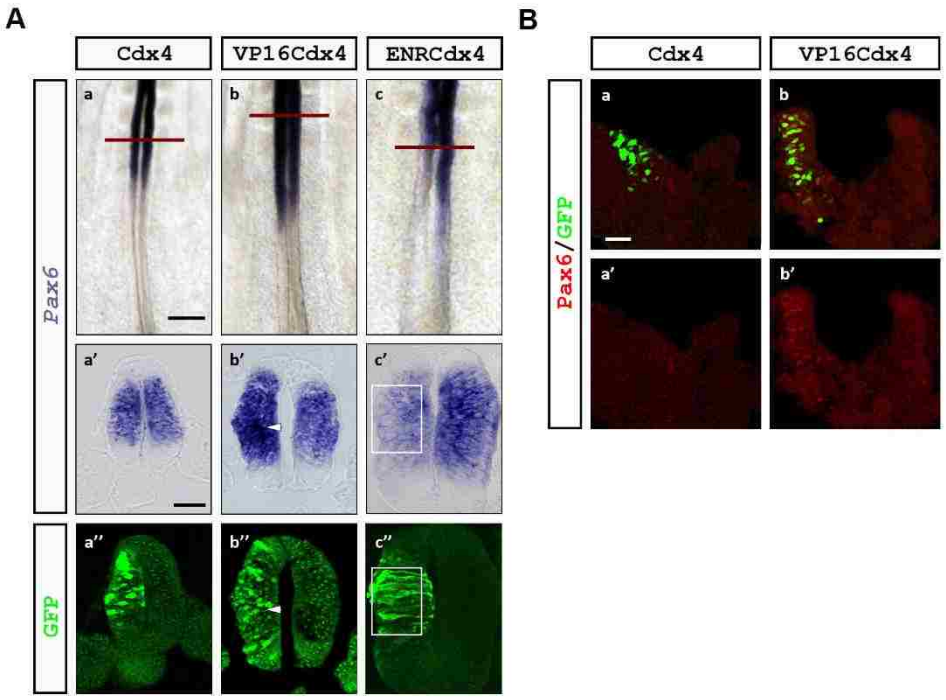

Figure 3.5: Cdx4 is not sufficient for Pax6 activation. *Cdx4* over-expression failed to change *Pax6* in the transition zone (A: a, a'; B: a, a') (n=6/6). Constitutive activated *VP16Cdx4* however resulted in over-expression of *Pax6* in the electroporated side (A: b, b', B: b, b') (n=6/6) and in some cases (n=4/6 in both *in situ* hybridization (ISH) and immunohistochemistry (IHC) analysis) resulted in premature activation of *Pax6* in posterior neural tube. Constitutive repressor *EnRCdx4* resulted in downregulation of *Pax6* expression in the neural tube (A: c, c') (n=6/6). Expression of *Pax6* on manipulation of Cdx4 activity is analyzed with ISH in A and IHC in B. Green cells represent GFP+ cells electroporated cells in both A and B. Embryos were electroporated at HH 10-11 and analyzed 8 hpe. Red bar represent axial level of transverse section in A. In A, white arrow represent ectopic expression of *Pax6* (A: b', b") and white box represent loss of *Pax6* expression in normal domain (A: c', c"). Scale bar 200µm (whole mount); 40µm (transverse sections).

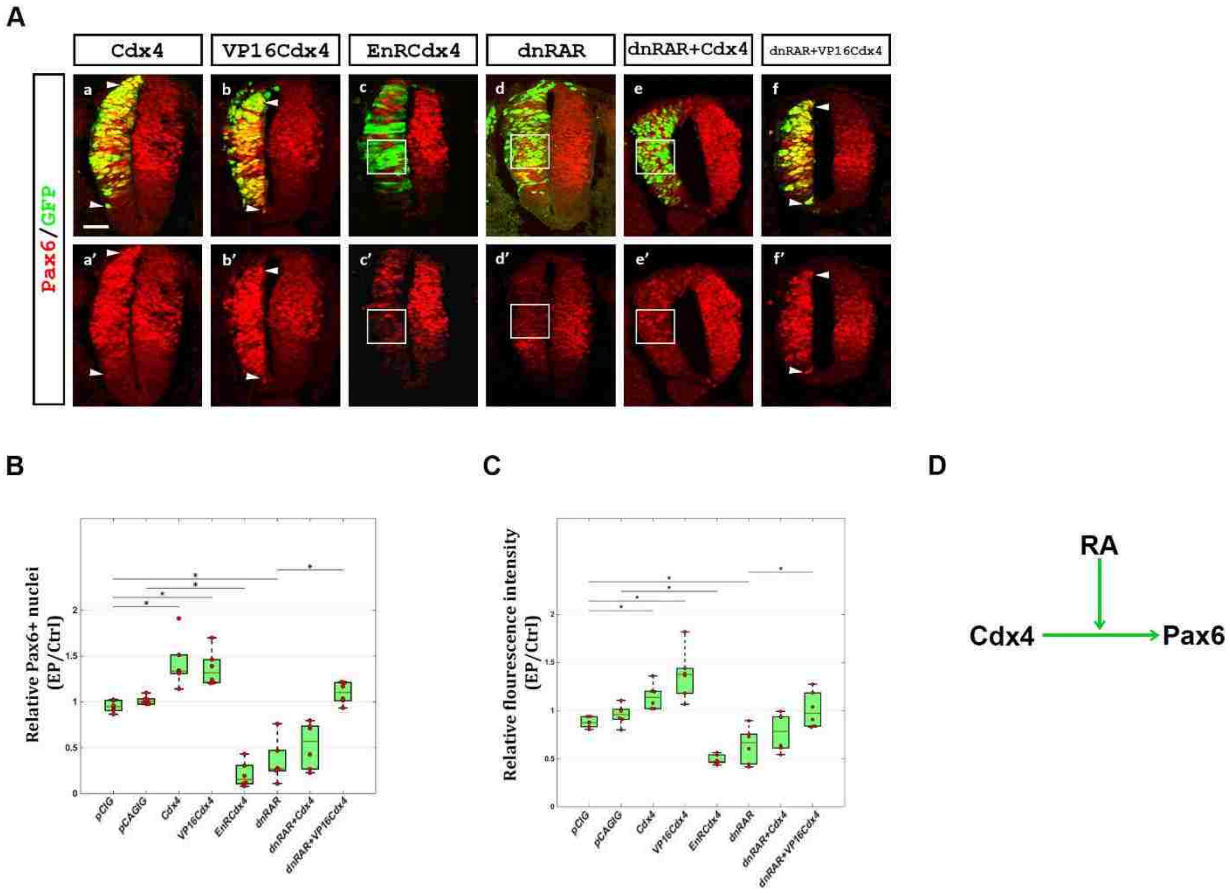

Figure 3.6: Cdx4 requires RA to activate *Pax6* transcription. Ectopic *Cdx4* expression increases *Pax6* DV expression domain cell autonomously (A: a, a') as shown previously (Fig. 3.4). Ectopic constitutive activated *VP16Cdx4* induces *Pax6* expression similar to the ectopic expression of *Cdx4* (A: b, b') (n=6/6). Ectopic constitutive repressor *EnRCdx4* represses *Pax6* transcription (A: c, c') (n=6/6). RA is required for *Pax6* transcription (A: d, d'; and (Novitch et al., 2003)) (n=6/6). Ectopic *Cdx4* failed to activate *Pax6* in loss of function RA background (A: e, e') (n=6/6). However, *VP16Cdx4* expression was able to activate *Pax6* in RA signal deficient background (A: f, f') (n=6/6), suggesting RA is required for Cdx4 dependent *Pax6* activation. Embryos were electroporated at HH11-12 and analyzed 24 hpe. White arrows represent ectopic

expression of *Pax6* and white box represent loss of *Pax6* expression in normal domain. Scale bar 40µm. Quantification (B and C) of experiments as shown in figure A. Box-scatter plot representing ratio of *Pax6* positive cells on electroporated side to that on the contralateral control side (B). Box-scatter plot representing ratio of mean fluorescence intensity of electroporated side to that of the contralateral control side (C). Cell count and mean intensity measurement were conducted using ImageJ. Comparisons between conditions were analyzed for statistical significance with two tailed t-test (p value <0.05) (Microsoft Excel). Significance of comparison is shown with a bar and a star. Summary figure (D).

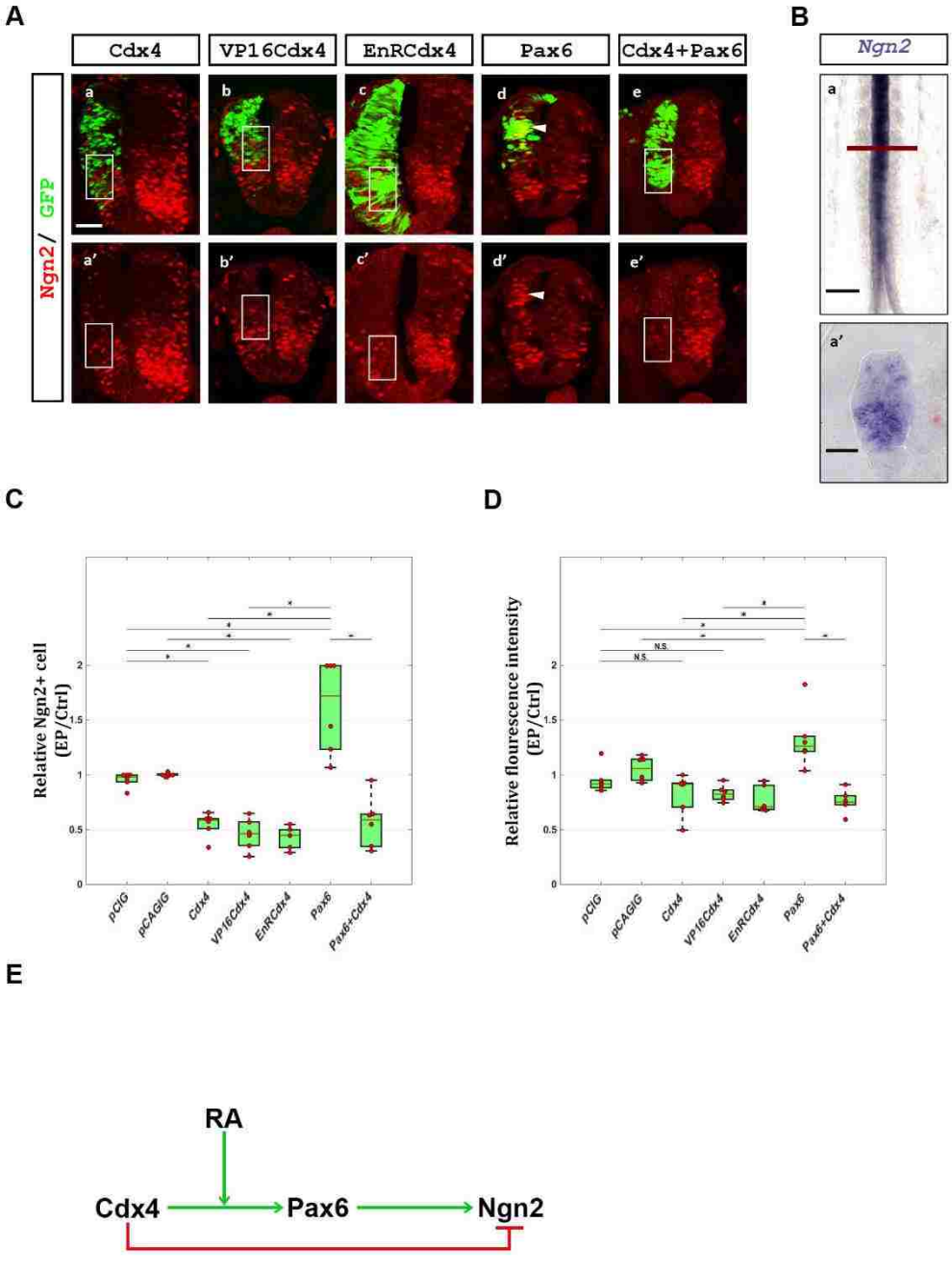

Figure 3.7: Cdx4 represses transcription of the neural differentiation *Ngn2* even in the presence of the neurogenic activator Pax6. Cdx4 and constitutive active VP16Cdx4

inhibit *Ngn2* (analysis by IHC, A: a, a', b, b') (n=6/6), despite these constructs activating *Pax6* (Fig. 3.6 A). EnRCdx4 represses *Ngn2* (A: c, c') (n=6/6) as it represses *Pax6* (Fig. 3.6 A). Pax6 induces *Ngn2* (A: d, d') (n=6/6). Cdx4 prevents Pax6 dependent induction of *Ngn2* (A: e, e') (n=6/6). White arrows represent ectopic expression of *Ngn2* and white box represent loss of *Ngn2* expression in normal domain. RC domain of *Ngn2* expression by ISH (B: a). DV domain of *Ngn2* expression at the RC level marked by red bar (B: a'). Scale bar 200μm (whole mount); 40μm (transverse sections). Quantification of experiments (C and D) as shown in figure A. Box-scatter plot representing ratio of *Ngn2* positive cells on electroporated side to that on the contralateral control side (C). Box-scatter plot representing ratio of mean fluorescence intensity of electroporated side to that of the contralateral control side (C). Cell count and mean intensity measurement were conducted using ImageJ. Comparisons between conditions were analyzed for statistical significance with two tailed t-test (p value <0.05) (Microsoft Excel). Significance of comparison is shown with a bar and a star. Summary figure (E).

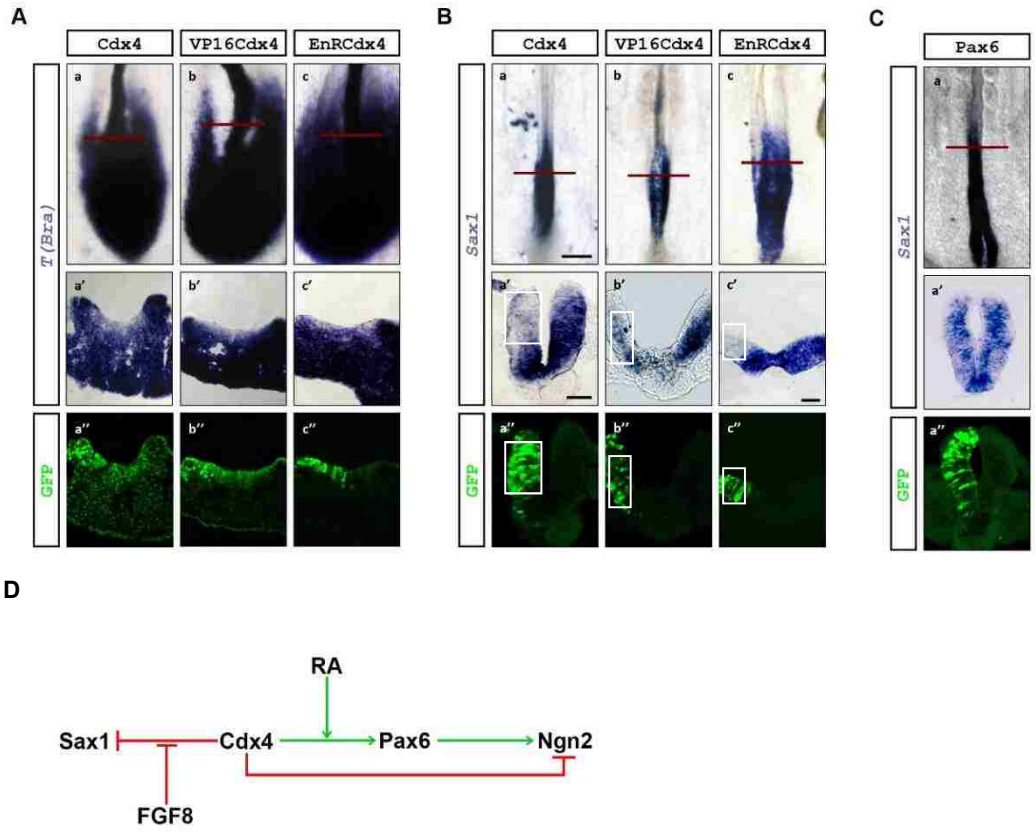

Figure 3.8: Cdx4 inhibits pluripotency. Cdx4 has no effect on *T (Bra)* expression. Cdx4 (A: a, a'), VP16Cdx4 (A: b, b') and EnRCdx4 (A: c, c') doesn't change expression of *T (Bra)* in NMPs (n=6/6). Cdx4 has inhibits *Sax1* expression indirectly. Cdx4 (B: a, a') and VP16Cdx4 (B: b, b') (n=6/6) both inhibit *Sax1* expression in the NMPs and posterior transition zone suggesting indirect inhibition by Cdx4. However, EnRCdx4 (B: c, c') also downregulate *Sax1* similar to Cdx4 activity (n=6/6). However, Pax6 has no effect on *Sax1* expression (C: a, a') (n=6/6), suggesting anterior boundary of *Sax1* is not determined by Pax6. White box represent loss of *Sax1* expression in normal domain. RC level of transverse section marked by red bar. Scale bar 200µm (whole mount); 40µm (transverse sections). Summary figure (D).

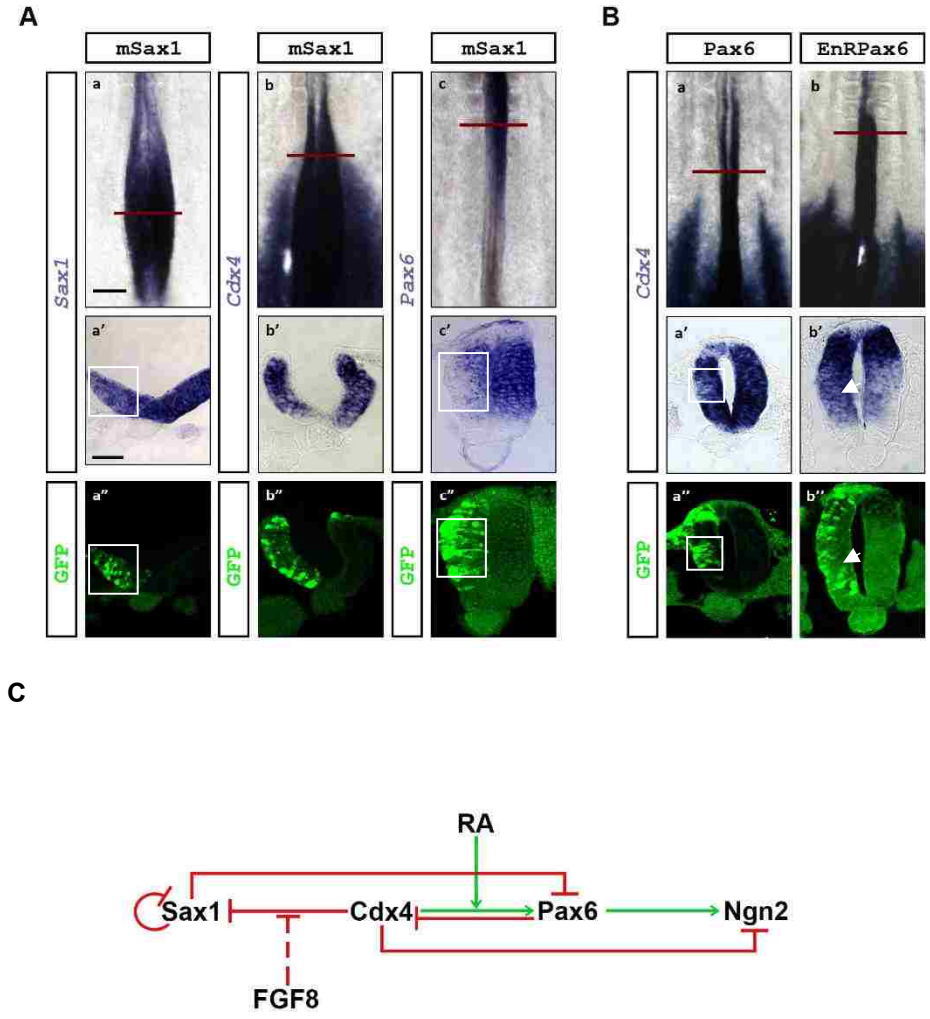

Figure 3.9: Feedback from Sax1 and Pax6. Sax1 inhibits its own expression (A: a, a') (n=6/6) providing negative autoregulation. Sax1 has on effect on *Cdx4* expression (A: b, b') (n=6/6), however Sax1 inhibits *Pax6* expression (A: c, c') (n=6/6) probably determining the posterior limit of *Pax6*. Pax6 inhibits *Cdx4* (B: a, a') (n=6/6) providing a negative feedback to the circuit, although the regulation in probably indirect as EnRPax6 activates *Cdx4* expression (B: c, c') (n=6/6). White box represent loss of expression in normal domain and white arrow represent ectopic expression. RC level of transverse section marked by red bar. Scale bar 200µm (whole mount); 40µm (transverse sections). Summary figure (C).

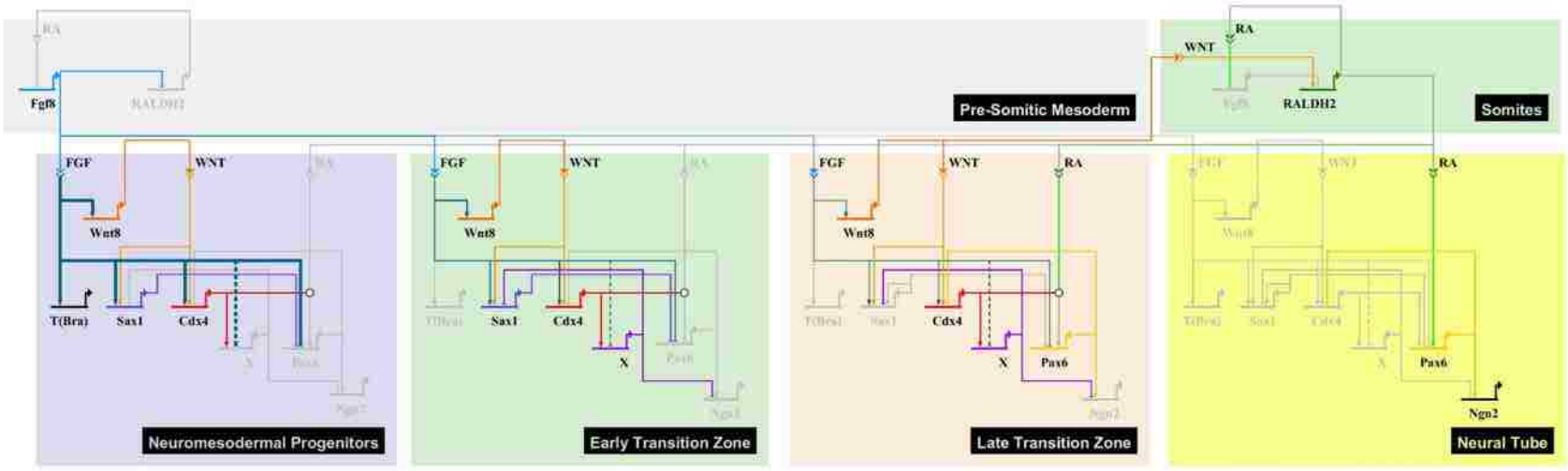

Figure 3.10: Gene regulatory network regulating the onset of spinal cord neurogenesis. Overlying FGF8, WNT8C and RA signaling information drives transition of cellular states during onset of spinal cord neurogenesis. Cdx4 is at the core of GRN that coordinates upstream signaling information into downstream transcriptional response.

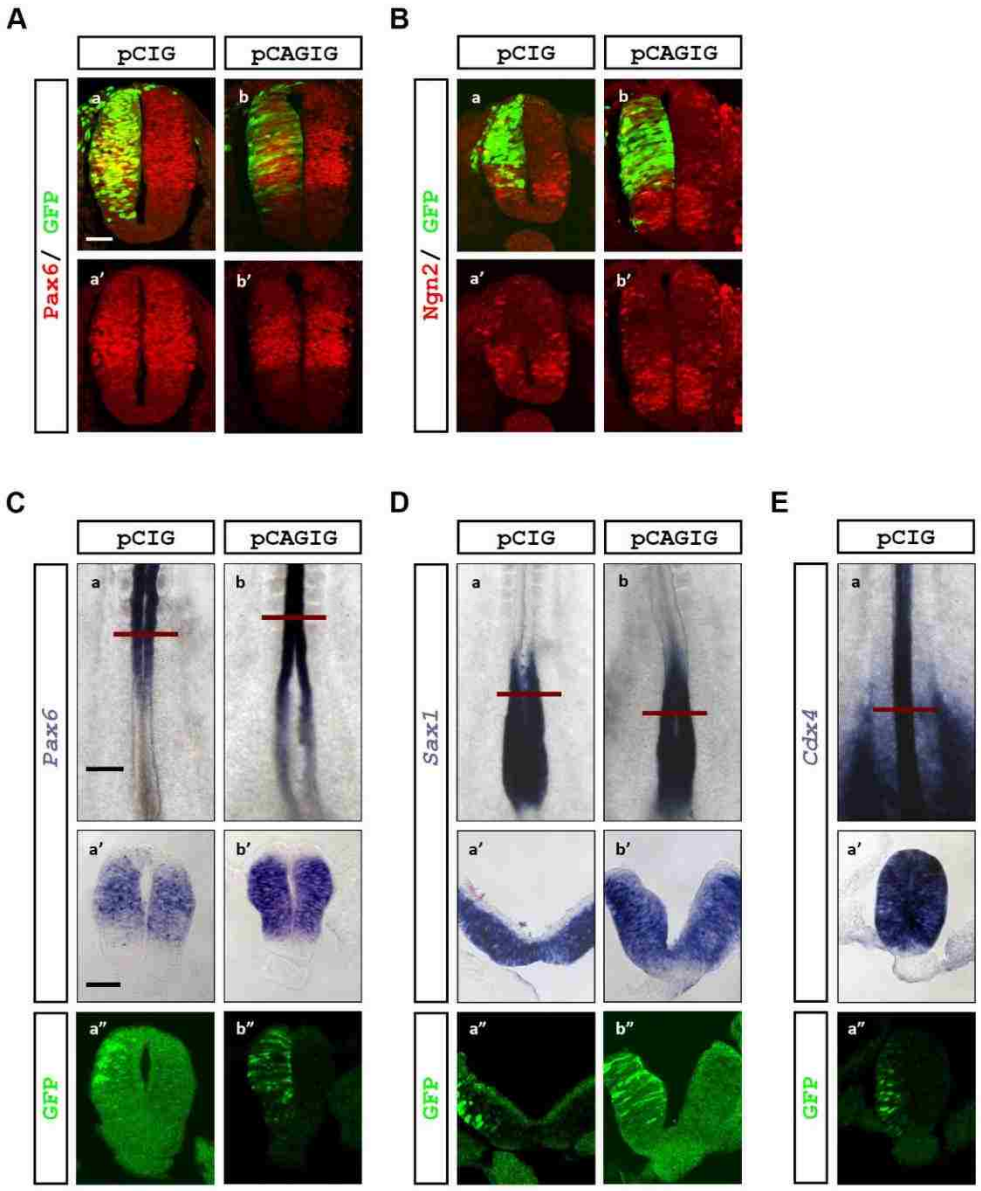

Figure 3.11: GFP over-expression doesn't affect wild type expression of factors investigated. pCIG (nuclear GFP) and pCAGIG (cytoplasmic GFP) ectopic expression didn't change *Pax6* (A: IHC analysis, C: ISH analysis), *Ngn2* (B), *Sax1* (D) and *Cdx4* (E) expression compared to contralateral control side (n=6/6).*Cdx4* expression analysis for pCAGIG over-expression wasn't done as none of the pCAGIG backbone construct were analyzed for *Cdx4* expression. Red bar shows RC level of transverse section. Scale bar 200µm (whole mount); 40µm (transverse section)

Chapter 4

A MATHEMATICAL MODEL FOR SPATIO-TEMPORAL RESOLUTON OF CELLULAR STATES IN THE CAUDAL NEURAL TUBE

4.1 Overview

4.1.1 Gene regulatory network

Experiments help in understanding the role candidate factor plays in specific developmental process, usually by testing if specific components are necessary (loss of function experiments) and/or sufficient (gain of function experiment) for that process to occur. As such, these experiments generate qualitative data representing the requirement of the candidate factor in the process studied. Qualitative data thus generated from various similar experiments focusing on different factors involved in a particular developmental process can be compiled to construct a regulatory module representing the hierarchy and cross-regulation among these factors in the context of that particular developmental process. Such a regulatory module is normally depicted as a gene regulatory network (GRN) (Davidson, 2010; Davidson et al., 2003b; Erwin and Davidson, 2009).

A GRN is a representation of a set genes that are part of a circuit. In a GRN, genes are interconnected to other genes via regulatory relationships. These relationship could be positive (activator) or negative (repressor) (Davidson, 2010; Davidson et al., 2003b; Erwin and Davidson, 2009). Each gene drives and/or represses the expression of a subset

of other genes, making that gene an upstream regulator and the set of genes regulated as its downstream targets. This upstream regulator and downstream targets represent the hierarchical aspect of the GRN. The downstream targets then could act as upstream regulators of a further set of genes, thus expanding the network. Downstream targets can interact with each other and can also influence the expression of its upstream regulator by a positive or negative feedback. Other more complex regulatory relationships also exist in a gene regulatory network; including coherent feedforward, incoherent feedforward, extended positive feedback, extended negative feedback, mutual activators, mutual repressors, etc (Alon, 2007; Davidson et al., 2003b; Erwin and Davidson, 2009; Hinman and Davidson, 2007; Mazzoni et al., 2013). These hierarchical cross-regulatory relationships drive a cell's identity along a path as determined by the GRN that is active in the cell. The changes in the cell's identity, as determined by the gene regulatory network, play out in a temporal or a spatio-temporal domain as seen during various developmental process (Davidson et al., 2003b).

GRN, by definition, shows a map of interactions between components, and hence, the information presented is a static snapshot of genes that are involved in a process and the regulatory relationships among them. This static information is useful in understanding the molecular architecture of the process. However, the GRN lacks the information about the quantitative aspect of the interactions. It also fails to provide the dynamic aspect of genetic networks where relations evolve over time. The nature of interaction and the dynamic behavior, together are crucial in understanding how the regulatory module functions during the temporal progress of the developmental process.

4.1.2 Mathematical modeling

Mathematical modeling provides an important tool to help simulate and analyze the temporal or spatio-temporal characteristics of GRNs. One of the useful and popular ways to model the GRN is to use continuous ordinary (ODE) or partial (PDE), differential equations (Karlebach and Shamir, 2008; Polynikis et al., 2009), because of their applicability to represent the law of mass action dynamics of the various mRNA and proteins involved in the GRN (Parmar et al., 2015). With differential equations, regulatory relationship are represented with set of equations, in which the rate of change of concentration of one factor depends on the concentration of other factor(s) as described in the GRN. Such mathematical relationships usually result in a non-linear differential equation system, which are hard to solve analytically; however, the system of equations can be solved numerically using available software such as MATLAB, MATHEMATICA, etc.

4.1.3 GRN regulating the onset of spinal cord neurogenesis

Signaling information from antagonistic FGF-RA gradients drives the expression of marker genes for pluripotency (*T (Bra), Sax1*), transition (*Pax6*) and differentiation (*Ngn2*) domains of the neural tube during onset of neurogenesis (Diez del Corral and Storey, 2004; Gouti et al., 2015). However, prior to my work, little information was available on how signaling factors regulate transcription factors during the onset of spinal cord neurogenesis. My data proposes a novel role of Cdx4 in integrating signaling information and conveying it transcriptional information during spinal cord neurogenesis.

My functional data show that Cdx4 is at the core of a GRN that regulates differentiation of neural progenitor cells. In the rostral portion of the caudal neural plate, Cdx4 activates the expression of the neural factor *Pax6* while simultaneously repressing the Pax6 dependent neurogenic factor *Ngn2*. In contrast, in the caudal portion of the caudal neural plate, Cdx4 represses the expression of the pluripotency marker gene *Sax1*. To test the functionality and robustness of the GRN revealed experimentally, I have built up a GRN (Fig 3.10) that I propose is active in the caudal neural tube to drive multipotent NMP cells into neurogenic cells.

The goal of modeling the GRN is to understand the dynamics of the system and to shed light on the temporal changes cells undergo during the spinal cord neurogenesis. To address this goal, the overall aims of the modeling are: 1) to test to what extent the proposed model matches experimental observations, 2) to estimate the strength of regulatory relationships that will result in a stable and robust GRN and 3) to perform theoretical experiments to understand the role of signaling and molecular switches.

To systematically test the GRN, first I analyzed the signaling switch occurring over a static spatial domain, the caudal neural plate; and second I analyzed the transcriptional factor dynamics occurring under the given signaling factor dynamics. Here I report that, under appropriate conditions, the signaling and transcription factor network recapitulates the spatio-temporal dynamics as observed in wild type embryos.

4.2 Methods

Transcriptional regulation of genes in the interaction network were modeled by differential equations describing the rate of change of mRNA and protein (Santillan, 2008; Sherman and Cohen, 2012; Shi et al., 2017), as follows

mRNA dynamics:

$$\frac{dM}{dt} = \alpha_m H_1 - \beta_m M H_2$$

Protein dynamics:

$$\frac{dP}{dt} = \alpha_p M H_3 - \beta_p P H_4$$

where,

α_m = Transcription rate constant. β_m= mRNA decay rate constant. α_p= Translational rate constant. β_p= protein decay rate constant.

M and *P* are mRNA and protein concentrations, respectively.

H_1 , H_2, H_3, H_4; are Hill functions describing regulatory interaction by upstream factors.

Hill function describing activation is of the form:

$$H_i = \frac{\left(\frac{A}{A_c}\right)^n}{1 + \left(\frac{A}{A_c}\right)^n}$$

where *A* is the concentration of activator protein, A_c is the Hill constant and *n* is the Hill coefficient of cooperativity.

Multiple activators can be described with the equation

$$H_i = \frac{\left(\frac{A1}{A1_c}\right)^{n1} + \left(\frac{A2}{A2_c}\right)^{n2}}{1 + \left(\frac{A1}{A1_c}\right)^{n1} + \left(\frac{A2}{A2_c}\right)^{n2}}$$

The Hill function describing repression is of the form:

$$H_i = \frac{1}{1 + \left(\frac{R}{R_c}\right)^{m}}$$

where R is the concentration of repressor protein, R_c is the Hill constant and m is the Hill coefficient of cooperativity.

Multiple repressors can be described with the equation

$$H_i = \frac{1}{1 + \left(\frac{R1}{R1_c}\right)^{m1} + \left(\frac{R2}{R2_c}\right)^{m2}}$$

Finally, a regulation where both an activator and a repressor act together can be represented with the equation:

AND configuration: Where activator and repressor can bind on separate regulatory regions.

$$H_i = \frac{\left(\frac{A}{A_c}\right)^{n}}{1 + \left(\frac{A}{A_c}\right)^{n}} \; x \frac{1}{1 + \left(\frac{R}{R_c}\right)^{m}}$$

OR configuration (Competitive inhibition): Where activator and repressor competes for a regulatory region.

$$H_i = \frac{\left(\frac{A}{A_c}\right)^n}{1 + \left(\frac{A}{A_c}\right)^n + \left(\frac{R}{R_c}\right)^m}$$

In case of a diffusing molecule, a diffusion term, $\mu \frac{d}{dx^2}$,was added on the left side of the equation (μ is diffusivity coefficient, *x* is the spatial dimension).

Differential equations representing the interaction network were numerically solved using MATLAB solver. Partial differential equations showing interactions among factor with diffusing molecules were solved using MATLAB pdepe solver. Ordinary differential equations were solved using MATLAB ode45 solver. MATLAB was also used to plot the simulations of the equation systems.

4.3 Model of the signaling switch driving neuronal differentiation

Regulatory interactions between FGF, Wnt and RA signaling factors have been experimentally determined by other groups (Diez del Corral et al., 2003; Olivera-Martinez and Storey, 2007). While several FGF and Wnt factors are transcribed within and around the caudal neural plate (Lunn et al., 2007; Olivera-Martinez and Storey, 2007), for simplicity, I am focusing my model on the ones shown to have most influence on the system: FGF8 and Wnt8c (Olivera-Martinez and Storey, 2007).

Fgf8 is transcribed in the caudal stem zone (Fig 4.1 A), where it inhibits *Raldh2* transcription (no RA production), and promotes *Cyp26a* transcription (high RA degradation) (Diez del Corral and Storey, 2004). In the caudal stem and transition zone, FGF8 also activates *Wnt8c* transcription (Olivera-Martinez and Storey, 2007). Wnt8c

then induces *Raldh2* transcription in the region where activation outcompetes FGF8-mediated repression (Olivera-Martinez and Storey, 2007). RA produced by RALDH2 diffuses from *Raldh2* expressing cells and inhibits *Fgf8* transcription (Diez del Corral and Storey, 2004; Kumar and Duester, 2014). Together these interactions give rise to an extended negative feedback loop (Fig 4.2 A). My model also considers positive autoregulation of *Raldh2* by RA, as in developing embryos once activated *Raldh2* expression is maintained in the somites even in the absence of inducing Wnt8c signal.

4.3.1 Equations

In order to understand how the proposed regulatory relationships can act as a switch in a spatial domain, I modeled the proposed interactions (Fig 4.2 A) using partial differential equations. The model simulates these interaction in a moving spatial domain that is static with respect to the caudal stem zone (Fig 4.1 B). Regulatory relationships between interacting molecules are modelled using Hill's equations (see Methods). Below are the equations that mathematically describe the interactions between FGF8, Wnt8c and RA.

Fgf8 transcription

Fgf8 mRNA is synthesized exclusively in the caudal stem zone. As the embryo extends, the caudal stem zone moves caudally. The caudal movement of the stem zone leaves a trail of *Fgf8* transcripts in cells that exit the caudal stem zone. These cells no longer transcribe *Fgf8,* but the transcripts persists due to long half-life of *Fgf8* mRNA (Dubrulle and Pourquie, 2004). *Fgf8* transcription is restricted to the caudal stem zone, because of

high concentration of RA in rostral regions that acts as a strong *Fgf8* repressor. To simulate how increase in level of RA leads to decrease in *Fgf8* domain and vice versa, I have assumed a constant exponential input to drive *Fgf8* transcription that doesn't depend on RA. RA however can negatively regulate *Fgf8* transcription at different axial positions, and can bring it down to zero in the rostral regions.

The constant input recapitulates *Fgf8* transcription in the wild type embryos. *Fgf8* mRNA half-life is around 2 hours (Dubrulle and Pourquie, 2004), thus the rate constant of degradation with 2 hours of life is (0.693/120) around 0.006 min^{-1}. Since the speed of elongation is 3μm/min (from somite 5^{th} to somites 13^{th}) (Denans et al., 2015), the rate constant with respect to the spatial reference is 0.002 μm^{-1}.

Constant input:

$$F_0 = 0.06e^{-.002x} \quad (1)$$

Fgf8 mRNA transcription:

$$\frac{dF_m}{dt} = \alpha_{Fm} F_0 \left(\frac{1}{(1+(R/R_{FR})^r)}\right) - \beta_{Fm} F_m \quad (2)$$

FGF8 translation:

FGF8 is synthesized by the exponential distribution of *Fgf8* mRNA. Further, FGF8 diffuses from cells where it is transcribed thus expanding the domain of FGF signaling beyond its domain of transcription (Fig 4.1 A, B).

$$\frac{dF}{dt} = -D_F \frac{d^2F}{dx^2} + \alpha_{Fp} F_m - \beta_{Fp} F \quad (3)$$

(Parameter values for rate constant of synthesis and degradation and diffusion coefficient are described in section 4.3.2)

Wnt transcription

In the current model, *Wnt8c* transcription is under FGF8 regulation. Wnt8c produced from *Wnt8c* also diffuses but to a lesser extent, as represented by a low diffusion coefficient.

Wnt8c mRNA transcription:

$$\frac{dW_m}{dt} = \alpha_{Wm}\left(\frac{(F/F_{FW})^a}{(1+(F/F_{FW})^a)}\right) - \beta_{Wm}W_m \quad (4)$$

Wnt8c translation

$$\frac{dW}{dt} = -D_W\frac{d^2W}{dx^2} + \alpha_{Wp}W_m - \beta_{Wp}W \quad (5)$$

Raldh2 transcription

Raldh2 is synthesized by Wnt8c in the rostral domain where Wnt8c activation overcomes FGF8 dependent inhibition. RA is produced by RALDH2 in somites, from where it diffuses caudally into undifferentiated neural and mesodermal tissues. At the caudal end of the embryo, RA is degraded by CYP26A, whose transcription is under FGF8 regulation.

Raldh2 mRNA transcription

$$\frac{dR_m}{dt} = \alpha_{Rm}\left(\frac{(\frac{W}{W_{WR}})^a+(\frac{R}{R_{RR}})^a}{\left(1+(\frac{W}{W_{WR}})^a+(\frac{R}{R_{RR}})^a\right)}\right)\left(\frac{1}{(1+(F/F_{FR1})^r)}\right) - \beta_{Rm}R_m \quad (6)$$

RA production (as modeled by RALDH2 translation)

$$\frac{dR}{dt} = -D_R \frac{d^2R}{dx^2} + \alpha_{Rp} R_m - \beta_{Rp} R(1 + \beta_{FR} \frac{(F/F_{FR}2)^a}{(1+(F/F_{FR}2)^a)}) \quad (7)$$

4.3.2 Parameters

Most parameter values of transcription rate constants, mRNA degradation rate constants, translation rate constants and protein degradation rate constants for the signaling network are experimentally undetermined. For these values the parameter is set to a value as used in other published models (Tiedemann et al., 2012). In case where parameter value has been experimentally determined, values within the determined range has been used.

Fgf8 mRNA:

For *Fgf8* transcription, the transcription rate constant is set to α_{Fm} = 1/min as it is not determined experimentally. *Fgf8* mRNA half-life in chickens has been suggested to be around 3-4 hours (Dubrulle and Pourquie, 2004). In my model, β_{Fm} = 0.006/min with half-life around 2 hours.

FGF8 protein:

FGF8 translation and degradation rates have not been experimentally determined. FGF8 diffusion coefficient has been experimentally suggested to be around 2 μm^2/sec (Muller et al., 2013).

α_{Fp} = 0.3/min β_{Fp} = 0.005/min

D_F = 120 μm^2/min (2 μm^2/sec)

Wnt8c mRNA:

In my model, Wnt8c transcription depends only on FGF8. In chicken embryo, *Wnt8C* expression domain extend beyond *Fgf8* mRNA domain (Fig 4.2 A), all the way up to the FGF8 signaling domain (Fig 4.2 B). FGF8 and *Wnt8c* domain overlap, suggesting that FGF8 is a strong activator of *Wnt8c*, as *Wnt8c* can be activated by a very low level of FGF8 at the rostral end. By contrast, *Wnt8c* mRNA level in the caudal stem zone is one-third of the *Fgf8* mRNA level (Olivera-Martinez et al., 2014), which suggest that transcription rate constant of *Wnt8c* is low, making it saturate at lower value compared to *Fgf8*.

α_{Wm} = 0.1/min β_{Wm} = 0.03/min

Wnt8c protein:

Wnt8c translation and degradation rate constant are experimentally undetermined. Wnts are known to have restricted diffusion domain, represented by a smaller diffusion coefficient, 0.1 μm^2/sec (Eroshkin et al., 2016).

α_{Wp} = 0.3/min β_{Wp} = 0.01/min D_W = 10 μm^2/min

Raldh2 mRNA:

Parameters for *Raldh2* transcription are experimentally undetermined.

α_{Rm} = 1/min β_{Rm} = 0.03/min

RA:

Parameters for RALDH2/RA production are experimentally undetermined. However, RA is a smaller molecule compared to FGF8, and has been suggested to diffuse faster than FGF8 (18 μm^2/sec) (White et al., 2007).

α_{Rp} = 0.3/min β_{Rp} = 0.025/min D_R = 1200 μm^2/min

β_{FR} = 6

Hill constants

The value of Hill constant is the concentration of enzyme at which rate of reaction, catalyzed by the enzyme, is half of the maximum possible rate. Hence, Hill constant act as the measure of interaction strength. Its hypothetical range is from zero to infinity, with values closer to zero signifying very small amount of enzyme is required to achieve maximum rate of reaction and vice versa. In case of transcription factor regulations, Hill constant closer to zero signify that the factor is a strong regulator (activator or repressor) of the reaction process and higher values of Hill constant signify a weak regulation by the factor (Fig 4.3). A strong activator/repressor will drive activation/repression faster compared to a weak activator/repressor (Fig 4.3 A and C). In addition, a strong activator/repressor will be active at a lower concentration than a weak activator/repressor to achieve the same change (Fig 4.3 B and D).

As the interaction strength of signaling factors FGF8, Wnt8c and RA in regulating each other's dynamics have not been experimentally determined, I varied the Hill constants to understand the behavior of the system.

There are six parameters that describe the interaction among signaling factors in the model. The four parameters that are important in determining the FGF8-Wnt8c-RA interactions are F_{FR1} (FGF8 dependent repression of *Raldh2*), F_{FR2} (FGF8 dependent degradation of RA), W_{WR} (Wnt8c dependent activation of *Raldh2*) and R_{RF} (RA dependent inhibition of *Fgf8*). The remaining two parameters are F_{FW} (FGF8 dependent activation of *Wnt8c*) and R_{RR} (RA dependent positive auto-regulatory feedback on *Raldh2)*.

4.3.3 System behavior

To understand the system's behavior in term interaction strengths, I varied the Hill constants while keeping the rate constants unchanged. The parameters for rate constants of synthesis and degradation would also affect the steady state behavior; however, in the present study the focus is on the interaction strengths and not the production dynamics. These manipulations resulted in different steady state signaling profiles. The profiles generated can be classified into four broad behaviors as FGF-dominant, FGF/RA balanced, RA-dominant, and aberrant.

FGF8 dominance

The model simulates how the system will behave with a given initial exponential *Fgf8* transcript gradient in a spatial domain, generated as a result of the caudal movement of the stem zone which is the source of *Fgf8* transcription.

If FGF8 dependent repression of *Raldh2* transcription outweighs RA dependent repression of *Fgf8* transcription (as described by Hill constant listed in Table4.1), the system doesn't show appreciable *Raldh2* transcription (Fig 4.4). Such a system would lead to maintenance of pluripotent stem progenitor cells without differentiation.

Table 4.1 Hill constant values for various behavior exhibited by the system

Hill constants	**FGF8 dominance**	**FGF8-RA balance**			**RA dominance**	**No RA feedback**	
		Somites	**Equidistant**	**Stem zone**		**Aberrant**	**Oscillations**
F_{FW}	10	10	10	10	10	10	10
W_{WR}	1	1	1	.5	.2	1	10
F_{FR1}	1	1	2	3	5	2	50
F_{FR2}	2	2	8	10	15	20	50
R_{RF}	10	1	1	.5	.2	1	50
R_{RR}	50	50	50	50	50	300	1000

FGF8-RA balance

Under appropriate interaction conditions; FGF8, Wnt8c and RA signaling factors settle to a stable steady state profile. This steady state suggests that the activating and repressive interactions of the system have reached an equilibrium, and if other conditions don't change (for example: speed of caudal movement), then the differentiation front, as defined by the region of overlap of FGF8 and RA (Goldbeter et al., 2007), will continue to move caudally along with the stem zone at the same speed. The location of the differentiation front could be closer to the somites (Fig 4.5 A, B, C), equidistant (Fig 4.5 D, E, F), or closer to the stem zone (Fig 4.5 G, H, I) depending upon the interaction strengths (Table 4.1). The position of differentiation front determines the steepness of signaling gradients. This in turn will affect regulate the spatio-temporal dynamics of downstream transcription factors.

RA dominance

The third typical behavior shown by the system is where the system starts with an initial *Fgf8* mRNA gradient and ends with high, broad RA distribution (Table 4.1 and Fig 4.6). This behavior simulates the possibility where RA driven differentiation overtakes the caudal stem cell zone. In this scenario, the system starts with a stem cell zone and as time progress the differentiation front move closer and closer to the stem cell zone finally overtaking the stem zone. As the differentiation front moves closer to the caudal end, the size of the stem cell zone decreases progressively and in the end a fully differentiated

region is left. Importantly, this is the mechanism by which axial elongation is thought to cease in embryos (Cunningham et al., 2016; Olivera-Martinez et al., 2012).

Aberrant behaviors

Under certain sets of Hill constants, the system settles into mRNA and protein profiles that are not exhibited in natural systems. These behaviors of the system are classified into aberrant behaviors.

Negative feedback loops can result in system oscillation due to the fact that the inducer drives the expression of its own inhibitor (Novak and Tyson, 2008; Pigolotti et al., 2007). In this system, the FGF8-Wnt8c-RA signaling interaction is a form of an extended negative feedback loop, where FGF8 drives production of Wnt8c that, in turn, drives the production of RA. RA inhibits FGF8, the indirect activator of RA. Hence in principle, FGF8-Wnt8c-RA network should oscillate under appropriate conditions. In our simulation, the oscillations are prevented by the auto-regulatory positive feedback of RA on *Raldh2*. The auto-regulatory positive feedback simulates differentiation once appropriate level of factor has been induced, or certain threshold of differentiation has been achieved. Furthermore, it prevents FGF8 from turning itself back on.

In the case when I decrease the strength of RA feedback, the system starts to oscillate under a certain parameter range or shows an aberrant peak of activity in the spatial domain (Fig 4.7).

My simulations of the system show that the FGF8-Wnt8c-RA interaction network as postulated by Olivera-Martinez et al. (Olivera-Martinez and Storey, 2007) could indeed

give rise a signaling switch that could travel caudally with the caudal elongation of embryonic axis. However, the behavior of the switch depends on the interaction parameters, which regulates the position and the speed of the differentiation font.

4.3.4 Robustness

The system showed wide range of behaviors as explained above depending upon the interaction strengths, suggesting that the system doesn't have one steady state for all conditions. The steady state depends upon the interaction strength keeping the production and degradation constant unchanged.

In order to test the robustness of the system, I then tested the range of interaction parameters, which lead to a similar response. Varying the value of interaction parameters within a range of ± 20% produced a similar steady state mRNA and protein profiles (Table 4.2 and Fig. 4.8).

Table 4.2: Stability of signaling profile.

Hill constants	**Value**		
	-20%		**+20%**
F_{FW}	8	10	12
W_{WR}	.8	1	1.2
F_{FR1}	.8	1	1.2
F_{FR2}	1.6	2	2.4

R_{RF}	.8	1	1.2
R_{RR}	40	50	60

I also explored the possibility of the bistability of the system. Bistability is the phenomenon where a system settles to two different stable steady state depending upon the initial conditions. FGF8-RA interaction are shown to behave in a bistable manner as shown by Goldbeter et al. (Goldbeter et al., 2007) . In our case, however, even with varied initial conditions, the system failed to exhibit bistability. This could be due to the non-overlap between expression of *Fgf8* and *Raldh2*, which are the source of FGF8 and RA, respectively. Due to strong mutual repression between *Fgf8* and *Raldh2*, there expression domains are separated, resulting into lesser overlap between FGF8 and RA domains, as compared to simulations by Goldbeter.

4.4 Transcriptional switch model for describing differentiation

My experimental data provides a framework for a transcriptional network driving the gradual maturation and differentiation of tail bud NMPs into spinal cord progenitor cells. Here I use that data to generate a mathematical model of the transcription network that respond to signaling dynamics identified by other groups (Diez del Corral et al., 2003; Olivera-Martinez and Storey, 2007), and that provides spatio-temporal identities to a cell as it transits from NMP state to neurogenic state. The goal behind this exercise is to generate a model with predictive value that would allow us to explore characteristics of

the system, such as cross-regulatory relationships and interaction strengths, of the network.

To understand the transcriptional factor dynamics, I used the signaling factor profile generated in the above simulation as the input. I chose the profile generated in Fig 4.5.E (Fig 4.9 A) for two reasons. First, the profile generated by this system closely resembles that of the signaling factors' domain at stage HH 11-12 (Fig 4.1 A). Second, all the experiments evaluating the role of Cdx4 in neurogenesis were done at stage HH10-12 (Chapter 3).

The transcription switch simulations focus on modeling cells that exit the NMP domain and progressively acquire more differentiated states as they transit from the caudal end rostrally (left to right movement in graphs; Fig 4.9.B). For simplicity, the cells are assumed not to undergo any cell division during their journey from NMP state to the neurogenic state. Further, as the caudal stem zone continues to move caudally, the cell of interest is at rest. However, from the point of view of the caudal stem zone the cell moves rostrally with time. Hence the spatial signaling information, from point of view of the cell, is perceived as temporal information. The temporal change in signaling information drives temporal changes in transcription factors expression. Cells exiting out the NMP domain go through the same changes in the transcription factor expression as they are under the same signaling input. As these cells are arranged spatially in order of their birth, from the caudal NMPs to the rostral differentiated cells, the temporal changes in transcription factors give rise to spatial changes in profiles (Fig 4.9.B).

In simulating the transcription network, I focused on monitoring the changes in expression levels of several transcription factors that marks the state of pluripotency (*T*

(Bra), Sax1), early and late differentiation (*Pax6 and Ngn2*), and my gene of interest, *Cdx4*. In addition to these factors, I included factors *X* and *Y* to modulate the indirect regulation of Cdx4 and Pax6, respectively, as suggested by my experimental data (chapter 3). The table below gives the combination of transcription factors as they relate to the progressive restriction of cell identity from NMP to neurogenic state (Fig 4.9 B).

Table 4.3: Temporal identity of cell (In spatial order, from early to late)	
Cellular state	**Transcription factors**
Neuromesodermal progenitor (NMP)	$Bra^{+}Sax1^{+}Cdx4^{+}$
Caudal Transition zone	$Sax1^{+}Cdx4^{+}$
Rostral transition zone	$Cdx4^{+}Pax6^{+}$
Post-mitotic neural progenitors	$Pax6^{+}Ngn2^{+}$

4.4.1Mathematical description of the transcription network

FGF8 is involved in activating genes including *T (Bra)* and *Cdx4* at the caudal end (Bel-Vialar et al., 2002; Boulet and Capecchi, 2012). Wnt8c is involved in the activation of *Sax1* (Tamashiro et al., 2012) and *Cdx4* (Nordstrom et al., 2006). *Sax1* in turn inhibit itself (Fig 3.9A; (Tamashiro et al., 2012)) and is indirectly inhibited by Cdx4 (Fig 3.8 B). *Pax6* is activated by Cdx4, and that activation depends on presence of RA (Fig 3.6). RA also independently activate *Pax6* (Fig 3.6; (Novitch et al., 2003)). In addition, Sax1 inhibits *Pax6* (Fig 3.9A). Pax6 is the sole activator *Ngn2* (Fig 3.7) (Bel-Vialar et al.,

2007), which is inhibited indirectly by Cdx4 (Fig 3.8 B). *X* is the downstream of Cdx4 and is responsible for Cdx4 dependent inhibition (Fig 3.7; Fig 3.8 B) and is presumed to be inhibited FGF8, thus it is unable to repress *Sax1* in the NMP domain. Similarly, *Y* is downstream of Pax6 and responsible for Pax6 dependent inhibition of *Cdx4* (Fig 3.9 B). Y is also assumed to be inhibited by FGF8.

4.4.2 Equations

F, W and R are values of FGF8, Wnt8c and RA proteins as described by the signaling dynamics described in the previous section. The output levels of the signaling network are used as inputs in the transcription network.

T (Bra)

mRNA

Synthesis activated by FGF8.

$$\frac{dT_m}{dt} = \alpha_{Tm}\left({(F/F_{FT})^a}\Big/{(1+(F/F_{FT})^a)}\right) - \beta_{Tm}T_m \quad (8)$$

Protein

$$\frac{dT}{dt} = \alpha_{Tp}T_m - \beta_{Tp}T \quad (9)$$

Sax1

mRNA

Synthesis activated by Wnt and inhibited by factor X (which is Cdx4 dependent; Fig 3.8 B) and negative auto-regulation from its own protein (Fig 3.9 A; (Tamashiro et al., 2012)).

$$\frac{dS_m}{dt} = \alpha_{Sm}\left({(W/W_{WS})^a}\Big/{(1 + (W/W_{WS})^a + (S/S_{SS})^r + (X/X_{XS})^r)}\right) - \beta_{Sm}S_m \quad (10)$$

Protein

$$\frac{dS}{dt} = \alpha_{Sp}S_m - \beta_{Sp}S \quad (11)$$

Cdx4

mRNA

Synthesis activated by FGF and Wnt (Bel-Vialar et al., 2002; Keenan et al., 2006; Nordstrom et al., 2006; Pilon et al., 2006); and inhibited by factor Y (which is Pax6 dependent; Fig 3.9 B)

$$\frac{dC_m}{dt} = \alpha_{Cm}\left({(F/F_{FC})^a + (W/W_{WC})^a}\Big/{(1 + (F/F_{FC})^a + (W/W_{WC})^a + (Y/Y_{YC})^r)}\right) - \beta_{Cm}C_m \quad (12)$$

Protein

$$\frac{dC}{dt} = \alpha_{Cp} C_m - \beta_{Cp} C \quad (13)$$

Factor X

mRNA

Synthesis activated by Cdx4. Since Cdx4 dependent *Sax1* repression doesn't work in caudal stem zone, I have assumed that *X* is inhibited by FGF8.

$$\frac{dX_m}{dt} = \alpha_{Xm} \left({(C/C_{CX})^a} \Big/ {(1 + (C/C_{CX})^a + (F/F_{FX})^r)} \right) - \beta_{Xm} X_m \quad (14)$$

Protein

$$\frac{dX}{dt} = \alpha_{Xp} X_m - \beta_{Xp} X \quad (15)$$

Pax6

mRNA

Synthesis activated by Cdx4- RA complex (Fig 3.7) and independently by RA; and inhibited by and Sax1 (Fig 3.9A) (Sasai et al., 2014).

$$\frac{dP_m}{dt} = \alpha_{Pm}\left(\left.(C/C_{CP})^a\right/(1 + (C/C_{CP})^a + (S/S_{SP})^r)\right)\left(\left.(R/R_{RP})^a\right/(1 + (R/R_{RP})^a)\right) - \beta_{Pm}P_m \quad (16)$$

Protein

$$\frac{dP}{dt} = \alpha_{Pp}P_m - \beta_{Pp}P \quad (17)$$

Factor Y

mRNA

Synthesis activated by Pax6, and inhibited by FGF8.

$$\frac{dY_m}{dt} = \alpha_{Xm}\left(\left.(P/P_{PY})^a\right/(1 + (P/P_{PY})^a + (F/F_{FY})^r)\right) - \beta_{Ym}Y_m \quad (18)$$

Protein

$$\frac{dY}{dt} = \alpha_{Yp}Y_m - \beta_{Yp}Y \quad (19)$$

Ngn2

mRNA

Synthesis activated by Pax6 and inhibited by factor X (which is Cdx4 dependent) (Fig 3.7) (Bel-Vialar et al., 2007).

$$\frac{dN_m}{dt} = \alpha_{Nm}\left({(P/P_{PN})^a}\Big/{(1 + (P/P_{PN})^a + (X/X_{XN})^r)}\right) - \beta_{Nm}N_m \quad (20)$$

4.4.3 Parameters

Rate constants

The parameter values of transcription rate constant, mRNA degradation rate constant, translation rate constant and protein degradation rate constant; for the transcription factors are experimentally undetermined. Hence, all the values are kept similar based on values used in published models (Kiparissides et al., 2011; Tiedemann et al., 2012), with one exception, Cdx4. The exception was made for Cdx4 because Cdx proteins are known to be stable for long time (Gaunt et al., 2005), hence β_{Cp} was set to 0.05/min.

Constant for mRNA synthesis/degradation: α_{im} = 1/ min β_{im}= 0.03/min

Constant for protein synthesis/degradation: α_{ip} = 1/ min β_{ip}= 0.2/ min

Hill coefficients

Hill coefficients for activation and repression are ‘a’ and ‘r’, respectively, as used in the signaling model. Homeobox transcription factors, for example Pax6, are known to bind as dimer (Briata et al., 1999; Papadopoulos et al., 2012; Singh et al., 2000; Yamamoto et al., 1999). Other homeobox transcription factors in the proposed GRN are Sax1 and

Cdx4. Hence they are predicted to bind as dimers too (Gregory et al., 2006). Therefore, for sake of simplicity, Hill coefficients for all transcription factors are set to 2.

Hill constants

As described earlier, Hill constant describe the strength of interaction between factors. In case of a signaling factors driving expression of a transcript factor, Hill constant acts as a threshold at which the signaling factor induces transcription factor expression. Higher value of Hill constant will result into higher threshold, thus making the transcription factor expressed only in the region where signaling factor is abundant. Hill constant values also suggest the time required for activation or repression (Fig 4.3). In terms of temporal changes in identity, high Hill constants would also lead to strong activation and faster turning on of target genes (Fig 4.3.B). Following this logic, the opposite is also true: lower Hill constant for a repressive interaction leads to strong inhibition and hence lesser overlap between transcription domains of a repressor and its target (Fig 4.10).

4.4.4 System behavior

I varied the Hill constants to investigate the characteristics of the transcription network that would recapitulate spatio-temporal resolution of cellular states as seen in wild type embryos. Production and degradation dynamics also play important roles in determining the expression domains of factors. However the focus in the current study is to understand the interaction strengths and not how the production dynamics are involved in determining transition in cellular states, which otherwise would increase the number of

variables, further complexing the analysis . Hence rate constants were remain unchanged throughout the simulations.

An overview of the network suggests that the spatial dynamics of the signaling factor network would be sufficient to drive the transcription network and give rise to the correct spatio-temporal generation of fates. As FGF8 concentration is high on the left side of spatial domain and RA is high on the right side of spatial domain, transcription factors regulated by each should be present only on their respective side. In the middle the cross-repressive interaction should be able to achieve the observed transition in cellular state.

However, if all the interactions in the network are equally strong (Hill constants =1 Fig 4.11 B) or equally moderate (Hill constants =20, Fig 4.11 C), than the network doesn't result in proper spatial resolution of temporal states seen in wild type embryos. Only a subset of interaction strengths give rise to correct spatial order of identities, one such set is listed in Table 4.4 (Fig 4.12 A)

Table 4.4: Hill constant for correct spatio-temporal of cellular states.

Hill constants	**Description**	**Value**
F_{FT}	FGF8 dependent activation of T *(Bra)*	1000
F_{FC}	FGF8 dependent activation of *Cdx4*	1
F_{FX}	FGF8 dependent repression of *X*	1
F_{FY}	FGF8 dependent repression of *Y*	1
W_{WS}	Wnt8c dependent activation of *Sax1*	50
W_{WC}	Wnt8c dependent activation of *Cdx4*	50

S_{SS}	Sax1 dependent repression of *Sax1*	100
S_{SP}	Sax1 dependent repression of *Pax6*	20
C_{CX}	Cdx4 dependent activation of *X*	20
C_{CR}	Cdx4-RA complex dependent activation of *Pax6*	10
R_{RP}	RA dependent activation of *Pax6*	10
X_{XS}	X dependent repression of *Sax1*	1
X_{XN}	X dependent repression of *Ngn2*	1
P_{PY}	Pax6 dependent activation of *Y*	5
P_{PN}	Pax6 dependent activation of *Ngn2*	20
Y_{YC}	Y dependent repression of *Cdx4*	5

4.4.5 Robustness

I evaluated the robustness of the interaction network with respect to Hill constant values. Once again as the focus of the study is on the interaction strengths, the rate constants of production and degradation were unchanged. The system resulted in comparable spatio-temporal resolution of transcription domains within the tested range of ± 30% (Fig 4.12 B, C), suggesting the robustness of the system to disruptions in interaction kinetics.

Next, I tested the response of the transcription network to the noise in overlying signaling information. As the signaling factors are the only source of spatial information, a robust system should be able to withstand small noise in the signaling information. Extrinsic noise could result from heterogeneity of signaling molecule concentration around

neighbor cells and their binding to receptor molecules on the cell's surface. Particularly the noise would be significant at domains where multiple signaling factors overlap. In the simulations, both periodic disturbance (Fig 4.13 C, D) and random noise (Fig 4.13 E, F) were very much tolerated by the transcription network without any distortions in the spatio-temporal resolution of the cellular states. This suggest that transcription network has built in robustness to the extrinsic noise.

Finally, I evaluated the role of signaling gradients in determining the spatio-temporal resolution. Signaling information is important in driving dynamics in downstream transcription network. Thus dynamics of signaling information should have an important role in dynamics of the cellular state. Replacing the exponential gradient of all the signaling factors (Fig 4.14 A, B) with linear gradients (Fig 4.14 C, D) or with a Boolean switch (Fig 4.14 E, F) resulted in loss of proper resolution of transition zone identity. This suggests that the signaling factors encode the spatial information which otherwise is absent in the transcription network. A change in the spatial information will result in different read out by the transcription network.

4.4.6 Role of individual transcription factors

My model proposes the central role of Cdx4 as the coordinator of upstream signaling information and downstream targets. To test the role of Cdx4 in the transcription network *in silico*, I evaluated the transcription profile generated with *Cdx4* over-expression (Fig 4.15 B), loss of *Cdx4* (Fig 4.15 C) and with noise in *Cdx4* (Fig 4.15 D). Gain of *Cdx4* downregulated *Sax1* and *Ngn2* transcription, similar to what I described in the embryo

(Fig 3.7 A; Fig 3.8 B). Conversely, loss of *Cdx4* leads to overlap in expression domains of *Sax1*, *Pax6* and *Ngn2*. In *in ovo* experiments loss of function was carried out by means of a repressive form of Cdx4 rather than a genetic knockout. Hence there are discrepancies between the loss of Cdx4 simulation output and phenotypes obtained from EnRCdx4 over-expression experiments. Gene knockout could be performed in future to test the out of the model for equivalence with loss of *Cdx4* in natural system. Both over-expression and loss of *Cdx4* simulations suggest the role of Cdx4 in proper segregation of transition zone and neural tube identities. I also investigated the robustness of the system by introducing noise in the transcription of *Cdx4*. In this model, noise was well tolerated, but it did affect temporal levels of *Sax1* and *Ngn2* (Fig 4.15 D), two downstream targets of Cdx4 that are negatively regulated by it.

4.5 Discussion

Here I simulated mathematically the interactions of the gene regulatory network identified experimentally in chapter 3 (Fig 3.10). The simulations emphasized the role of the transcription network in reading, interpreting and executing spatial information given by the signaling factors in driving transitions of cellular states.

4.5.1 Signaling factor simulation recapitulates signaling dynamics observed in natural systems

My simulations showed the various behaviors the FGF8-Wnt8c-RA system can exhibit under different interaction conditions. However, only a subset of those behaviors is

equivalent to what is observed physiologically, thus restricting the possible interaction to a specific parameter space. Two important behaviors exhibited by the signaling system were 1) FGF8-RA balance (Fig 4.5) or 2) RA dominance (Fig 4.6), leading to stable steady state profiles. FGF8-RA balance refers to the interaction strengths that result in a system where cross-repression reaches an equilibrium and neither FGF8 nor RA take over the system. In the absence of RA takeover, there will always be a pocket of stem cells that will continue to divide and add cells to the elongating axis. In natural systems, such behavior will yield to long body axis unless a termination mechanism is turned on. The FGF8-RA balance system could explain the elongated axis of some vertebrates, such as snakes, that has numerous vertebrae and a long neural tube form. The second behavior of the system, RA dominance, is the process by which the spatial field of cells starts as an undifferentiated region with RA domain gradually overtaking it, causing the cells to differentiate, and eliminating all precursor cells that could elongate the body axis. This simulation exhibited progressive restriction of the undifferentiated zone, as seen in chicken embryos (Fig 3.1). The time duration of RA takeover could also decide the length of the body axis, as faster RA takeover will lead to shorter body axis and vice versa.

One unexpected observation in the signaling factor interactions was the absence of a bi-stability switch. Double negative feedback loops such as the one between FGF and RA have been shown to exhibit multiple stable steady state under appropriate conditions (Ferrell, 2002). In the signaling switch, FGF8 represses RA, which in turn represses FGF8, hence satisfying the double negative condition. However, the present model fails to show bistability. This is significant considering that the mutual repression model

proposed by Godlbeter (Goldbeter et al., 2007) for FGF8-RA exhibited bistability. In Goldbeter model, for the same set of parameters, the starting initial concentration of FGF8 and RA determine whether the system settled on a stable FGF8 dominant or RA dominant steady state (Goldbeter et al., 2007). The model also showed that the strong mutual repression results in wider domain of bistability. In case of weaker mutual repression or only one factor (FGF8 or RA) being stronger repressor than the other, the system didn't show bistability.

So, what are the possible reasons for the presence and absence of bistability between Goldbeter's and the model proposed here? There are few but significant discrepancies between the present model and the Goldbeter's model. Goldbeter's model considered a constant level of *Fgf8* and *Raldh2* transcripts overlapping in the spatial domain, that was unaffected by FGF8-RA cross repression. Overlap of mRNAs meant that signaling factors also overlapped and interacted throughout the domain. As the cross repression acted only at the level of synthesis of signaling molecules from the constant mRNAs, a suitable trigger (different initial condition) could switch the system from FGF8 dominant to RA dominant steady state, that could then be sustained by the mRNA present in that spatial domain. In the present model, however, strong repression leads to mutual exclusion of expression domains of *Fgf8* and *Raldh2* in the spatial space (Fig 4.5). The domain of signaling molecules did overlap in the determination front, due to diffusion of molecules from the region of synthesis. Only in the determination front could signaling molecules interact. However, the domain of FGF8-RA overlap was smaller compared to the overall spatial domain of simulation. Hence any bistable steady state in the determination front would be destroyed by the signaling molecules diffusing from

surrounding tissues over time, leading to only one steady state solution. Weaker repression could increase the overlap between transcription domains, however, as Goldbeter model suggested, that condition will less likely to result in bistability.

The second possible reason for the absence of bistability is the positive feedback of RA on *Raldh2*. In the current model, the autoregulatory feedback model the situation where after a threshold level of RA has been synthesized, RA is able to maintain its own expression even with strong FGF8 repression, thus maintaining the differentiated state of the cells. However, autoregulatory positive feedback doesn't rule out bistability (Moss Bendtsen et al., 2015). But in the current model, with the decrease in strength of autoregulatory positive feedback the system started exhibiting oscillatory behavior, suggesting that the positive feedback plays a role in preventing switch like behavior.

4.5.2 Interaction strengths dictate the interpretation of signaling information

Strength of cross-regulatory interactions (Hill constants) are important in determining the output of the signaling information. In other words, systems can use same signaling information to drive different physiological outputs by playing with the interaction strengths of the transcription regulation. As observed in simulations (Fig 4.11; Fig 4.12), varying the Hill constants resulted into different spatio-temporal dynamics of the transcription network under the same signaling information.

The interaction strength is a measure of the threshold of regulatory factor required for transcription factor regulation (Fig 4.3; Fig 4.10). A possible way of modulating the threshold is via modulating strength of the enhancer. A weak enhancer requires a greater

amount of regulator to be active, hence a higher Hill constant. Conversely, a strong enhancer is active even with low amounts of regulator due to its lower Hill constants. By utilizing enhancers of different strength or by varying the strength of an enhancer, transcription factor expression dynamics could be varied in a natural system (Miyagi et al., 2006; Simmons et al., 2001; Woodcock et al., 2013).

In living systems, one of the ways of modulating strength of an enhancer is by epigenetic regulation (Calo and Wysocka, 2013). Chromatin modification, by masking/unmasking enhancer regions, modulates the ability of transcription factors to bind to regulatory regions (Doyle et al., 2014; Kim et al., 2004; Patel et al., 2013; Plachetka et al., 2008). Also epigenetic modification of histone residue can modulate the activity of enhancers (Stonestrom et al., 2015; Wu et al., 2011; Zhang et al., 2012). Another possible way of regulating the strength of enhancer interaction is the presence of cofactors (McClellan et al., 2013; Merino et al., 2015). In fact, a combination of chromatin and cofactors determines the enhancer activity during development (Fry and Farnham, 1999; Voss and Hager, 2014). Altogether, the data about regulatory strengths could be tested *in vivo* to validate the model and further refine the parameter set.

4.5.3 Transcriptional network recapitulates NMP to neurogenic state transition as seen in caudal neural tube

Results from *in silico* experiments also reemphasize the role of Cdx4 in coordinating upstream signaling factors and downstream transcription network. In the present model, Cdx4 plays a determining role in generation of caudal transition zone (*Sax1+ Pax6-*

Ngn2-) and rostral transition zone (*Sax1- Pax6+ Ngn2*-). In the *Cdx4* manipulation simulations (Fig 4.15), *Cdx4* overexpression resulted in loss of *Sax1* and *Ngn2* suggesting that Cdx4 promotes acquisition of rostral transition identity, and inhibits both caudal transition identity and neurogenic identity. As in the present model RA limits Cdx4's regulation of *Pax6*, over loading the system with Cdx4 didn't expand its caudal domain of expression. Conversely, loss of *Cdx4* resulted in expansion of *Sax1* and *Ngn2* domains rostrally and caudally, respectively; suggesting the role of Cdx4 in separating caudal transition zone from neurogenic zone. In these conditions, changes in *Pax6* domain weren't significantly altered, even in the absence of Cdx4, because RA was able to activate *Pax6*. However, due to expansion of *Sax1* and *Ngn2* the rostral transition identity was lost. Both gain and loss of *Cdx4* simulations suggest that Cdx4 is involved in establishing rostral transition zone (*Sax1-Pax6+Ngn2*-) that separates caudal transition zone (*Sax1+Pax6-Ngn2-,*) from neurogenic zone (*Sax1-Pax6+Ngn2+*), hence regulates the pace of differentiation.

4.6 Figures

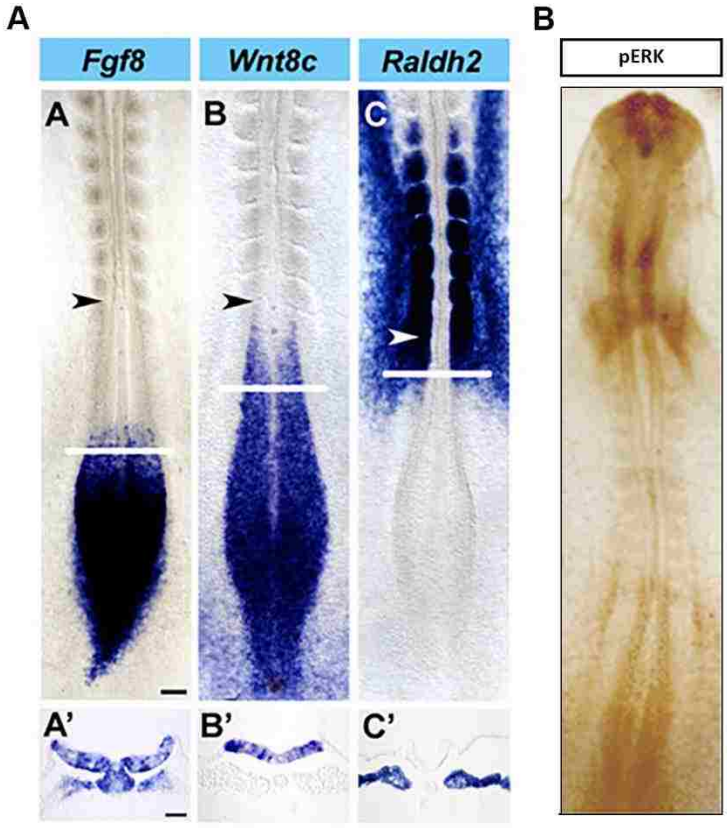

Figure 4.1: Expression domains of signaling factors. *Fgf8*, *Wnt8c* and *Raldh2* expression domain (A) in the caudal end of the embryo at stage HH10 as shown in Olivera-Martinez et al.(2007). *Wnt8c* expression overlaps with *Fgf8* expression at the caudal end and with *Raldh2* expression at the rostral end of the embryo. No overlap exist between expression domain of *Fgf8* and *Raldh2*. Domain of active FGF8 signaling as shown by expression of phosphorylated ERK (B). Image reproduced from (Lunn et al., 2007)

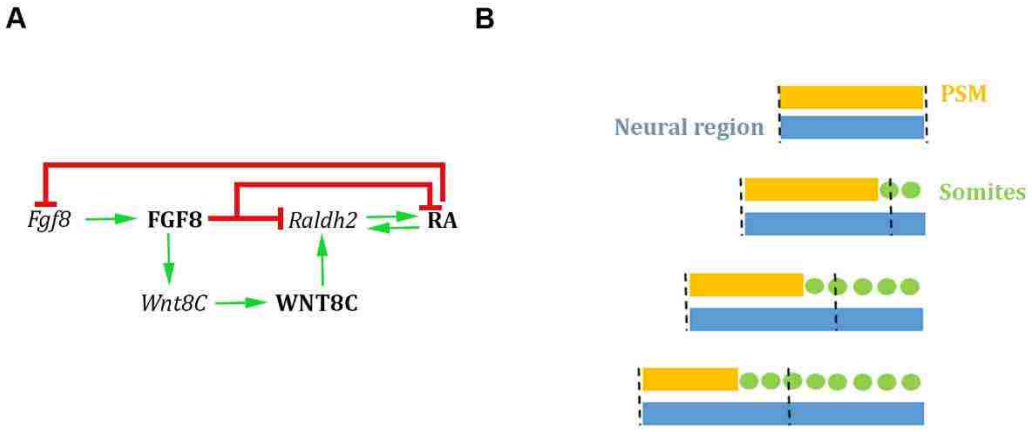

Figure 4.2: FGF8-Wnt8c-RA signaling interaction at the caudal end of the embryo. Interaction network (A) representing the regulatory relationships among FGF8-Wnt8c-RA mRNA, proteins and products as described in Olivera-Martinez, (2007) and Diez del Corral et al. (2003). Conceptual definition of the spatial domain (B, dotted line) where the interaction are simulated. This spatial domain is static with respect to the caudal zone, which move caudally at a constant speed.

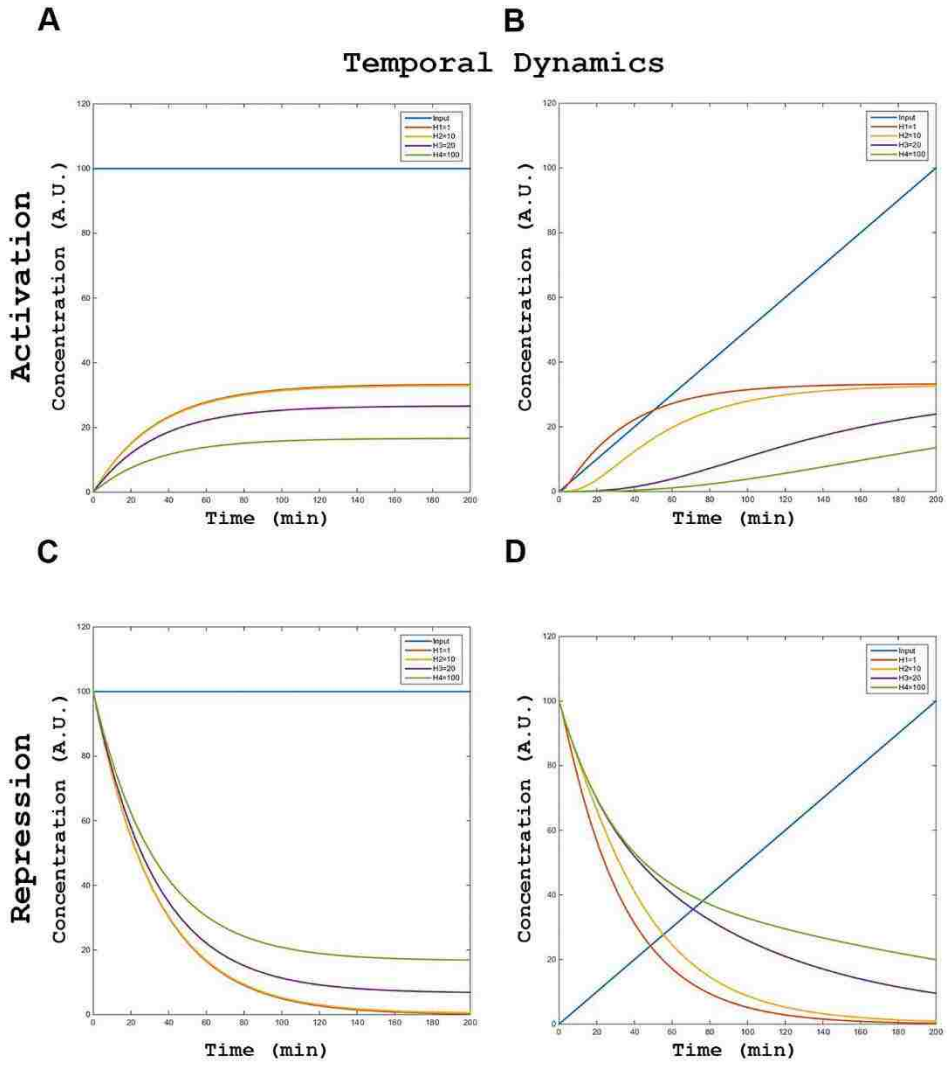

Figure 4.3: Hill constant determine the strength of activating/repressive interactions. For a constant amount of activator (A), downstream targets with lower Hill constant (H1=1 vs H4=100) have higher rate of production with a higher value of final concentration. In the case of graded input of activator (B), downstream targets with lower Hill constant are activated first. For a constant amount of repressor (C), downstream targets with lower Hill constant have faster decline in concentration with a lower value of final concentration. In the case of graded input of repressor (D), downstream targets with

lower Hill constant are repressed first. Blue: Input. Red: Hill constant (H1) =1. Orange: Hill constant (H2) =10. Purple: Hill constant (H3) =20. Green: Hill constant (H4) =100.

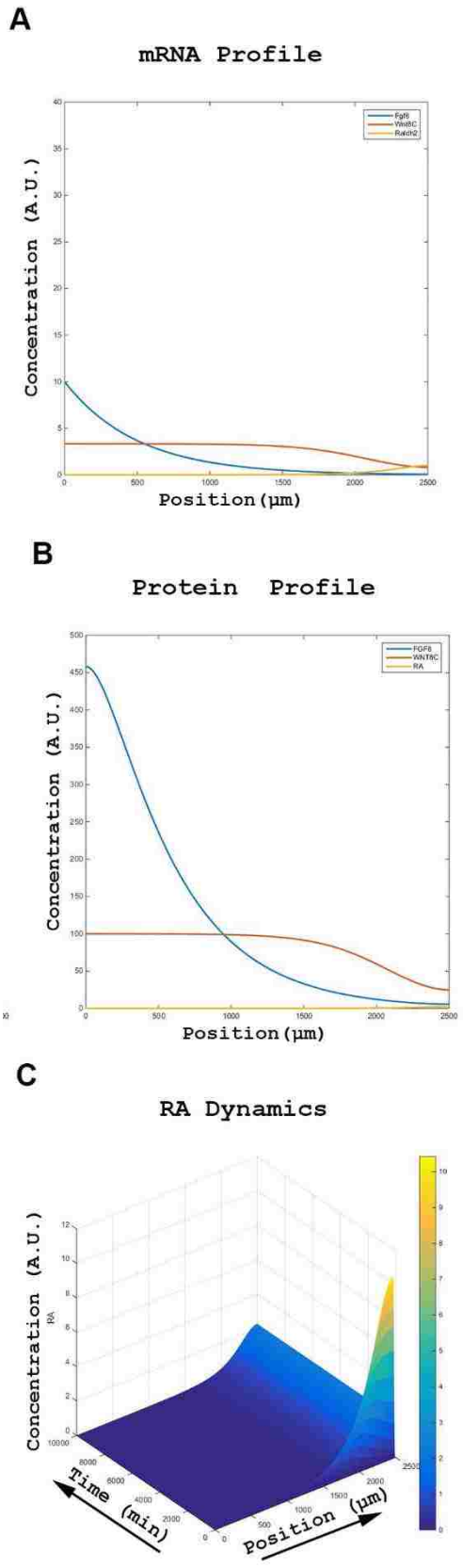

Figure 4.4: FGF8 dominance prevents *Raldh2* to achieve enough levels to start differentiation process. mRNA profile showing *Fgf8* and *Wnt8c* expression and very low expression of *Raldh2*. Protein profile showing FGF8 and Wnt8c domains (B). RA dynamics (C) over space and time. Strong inhibition of RA synthesis by FGF8 prevents RA accumulation. Blue: *Fgf8*/FGF8. Red: *Wnt8c*/Wnt8c. Orange: *Raldh2*/RA.

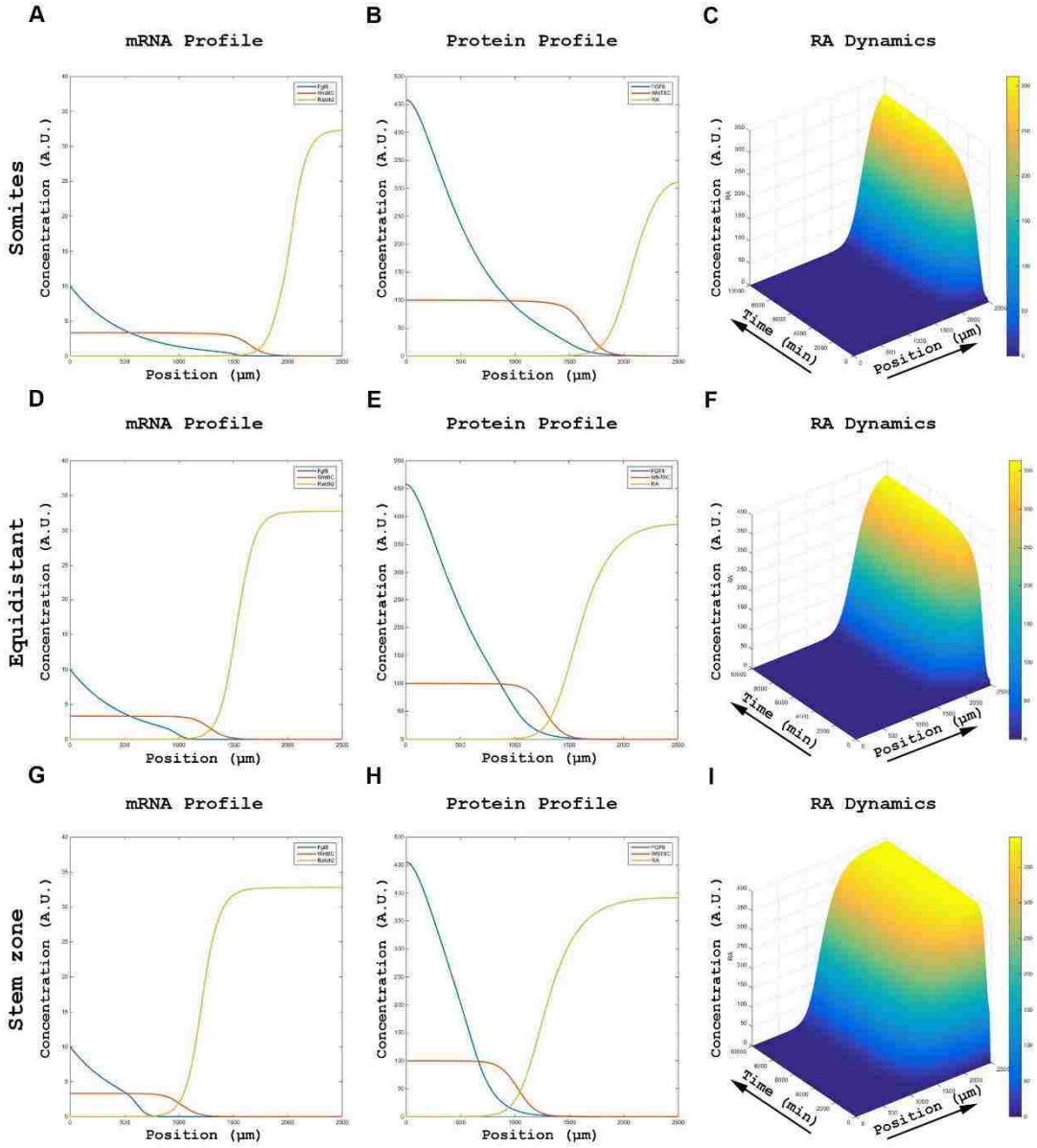

Figure 4.5: FGF8-RA balance give rise to a steady state differentiation switch. Profiles of FGF8, Wnt8c and RA mRNA (A, D, and G), protein (B, E, and H) and RA dynamics (C, F, and I) under conditions where the differentiation front is closer to somites (A-C), equidistant (D-F) or closer to stem cell zone (G-I). The domain of overlap of FGF8 and RA determines the differentiation font.

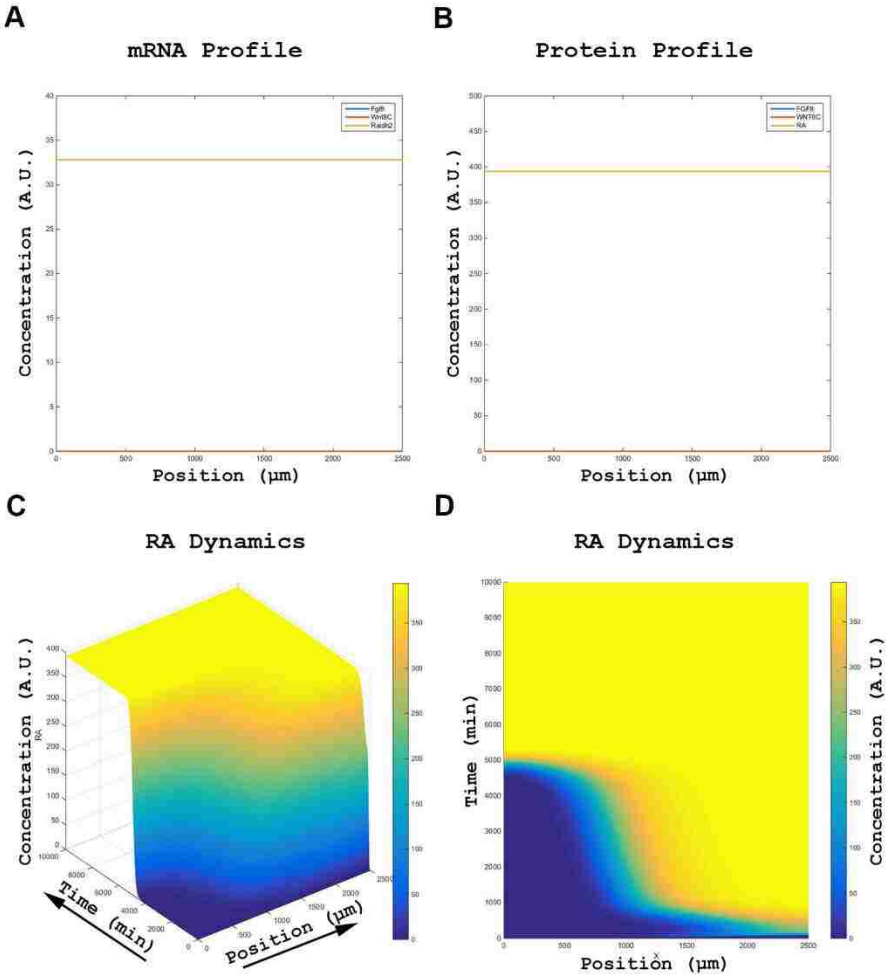

Figure 4.6: RA dominance over *Fgf8* leads to differentiation taking over stem zone. mRNA (A) and protein (B) profile showing the end result of simulation under the condition where RA inhibition of *Fgf8* overcomes FGF8 inhibition of *Raldh2*. RA dynamics (C) over space and time. RA domain progressively expands moving the differentiation font closer and closer to the stem zone. (D) 2-D view of RA dynamics in (C).

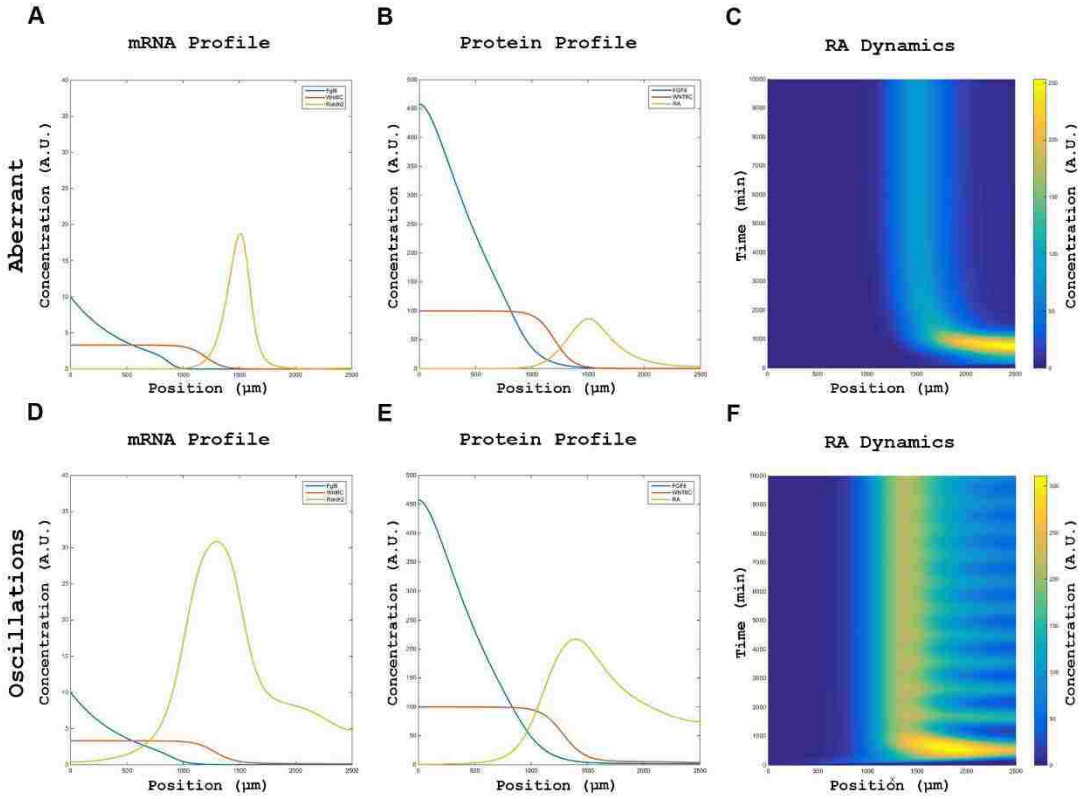

Figure 4.7: System behaviors not observed in natural systems. Peak of RA activity in the spatial domain that is not observed in physiological conditions (A). In the absence of RA autoregulation, the system can also show oscillatory behavior (B).

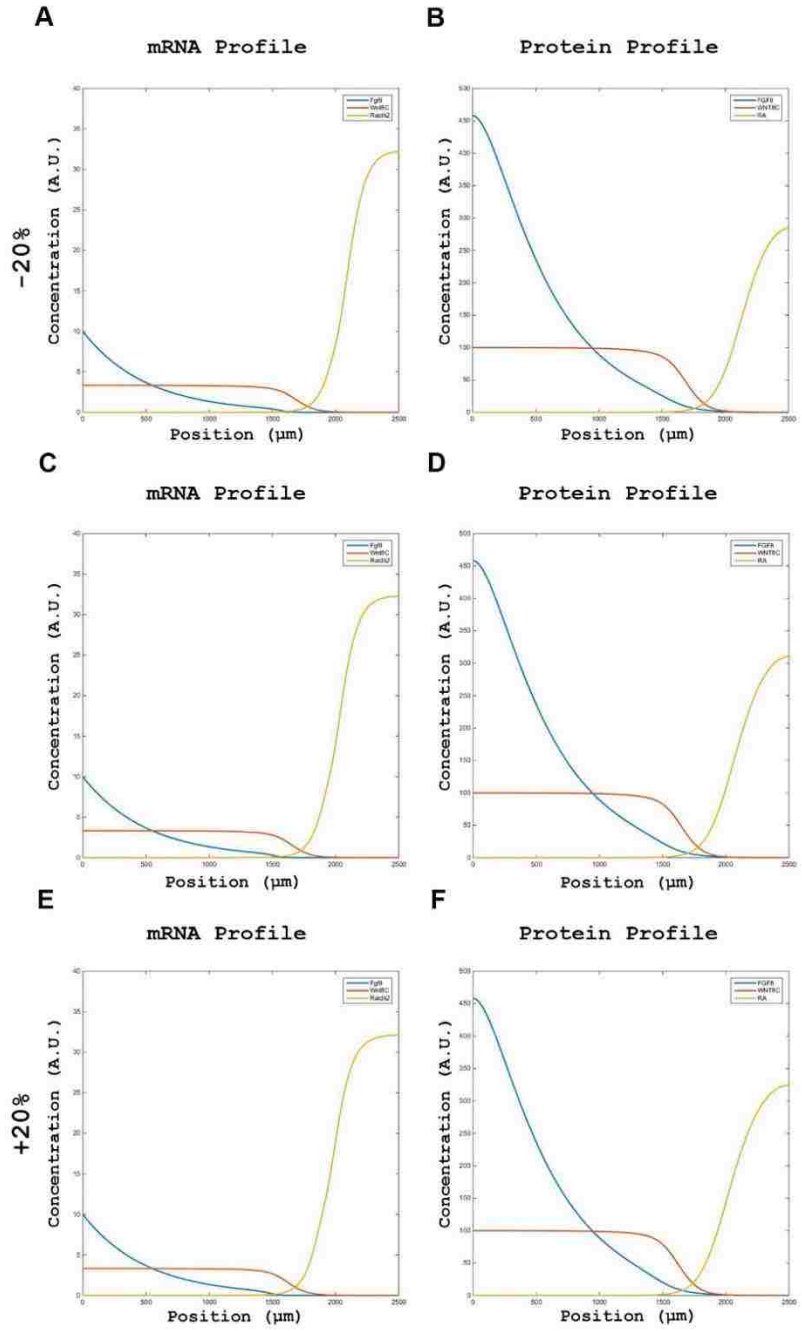

Figure 4.8: Stability of the signaling profile. The interaction network is stable to moderate changes in interaction strengths. Within a range of 20% change in Hill constant, the mRNA (A, C, E) and protein (B, D, F) steady states profiles are almost similar.

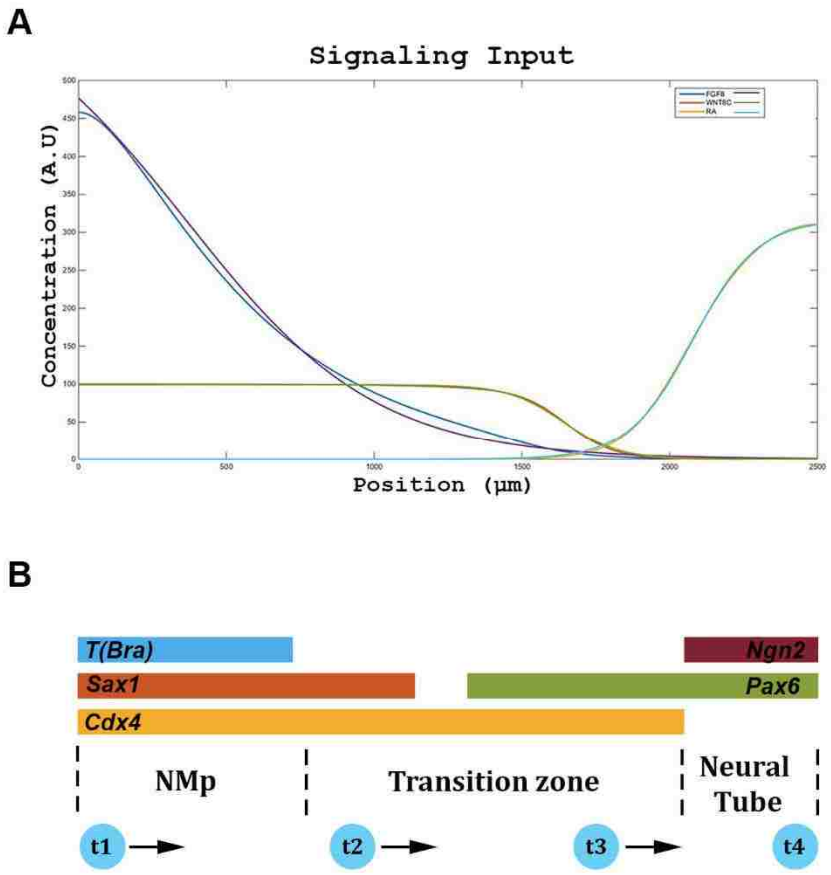

Figure 4.9: Spatial signaling information drives spatio-temporal cell identity dynamics. Profiles of FGF8 (blue), Wnt8c (red) and RA (orange) values obtained after simulation of the signaling network compared with profiles of FGF8 (Purple), Wnt8c (Green) and RA (Sky blue) values obtained from equations generated by MATLAB curve fitting plug-in. Expression domains, caudal/left to rostral/right of transcription factors involved in spinal cord neuronal maturation, as determined by the FGF-Wnt-RA signaling network (B). As cells exit out of the NMP domain, they acquire more rostral identities as time progresses (t1>t2>t3>t4). Hence the temporal order of identities acquired by the cell results into the spatial order of state in the caudal neural tube.

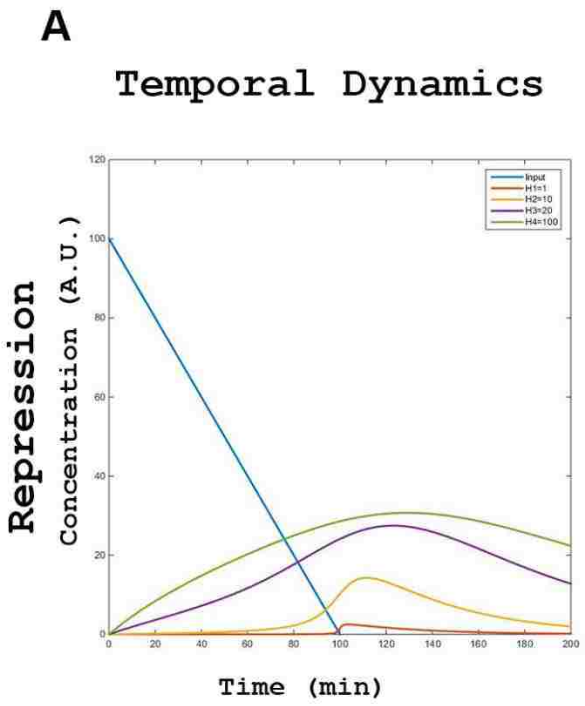

Figure 4.10: Hill constant determines the temporal activation of downstream targets in response to a graded repressor input. In response to an inhibitor degrading over time, downstream targets with higher Hill constant (H4=100 VS H1=1) are activated earlier compared to targets with lower Hill constants. In other word, targets with higher Hill constants need more repressor for inhibition, compared to targets with lower Hill constants. Blue: Input. Red: Hill constant (H1) =1. Orange: Hill constant (H2) =10. Purple: Hill constant (H3) =20. Green: Hill constant (H4) =100.

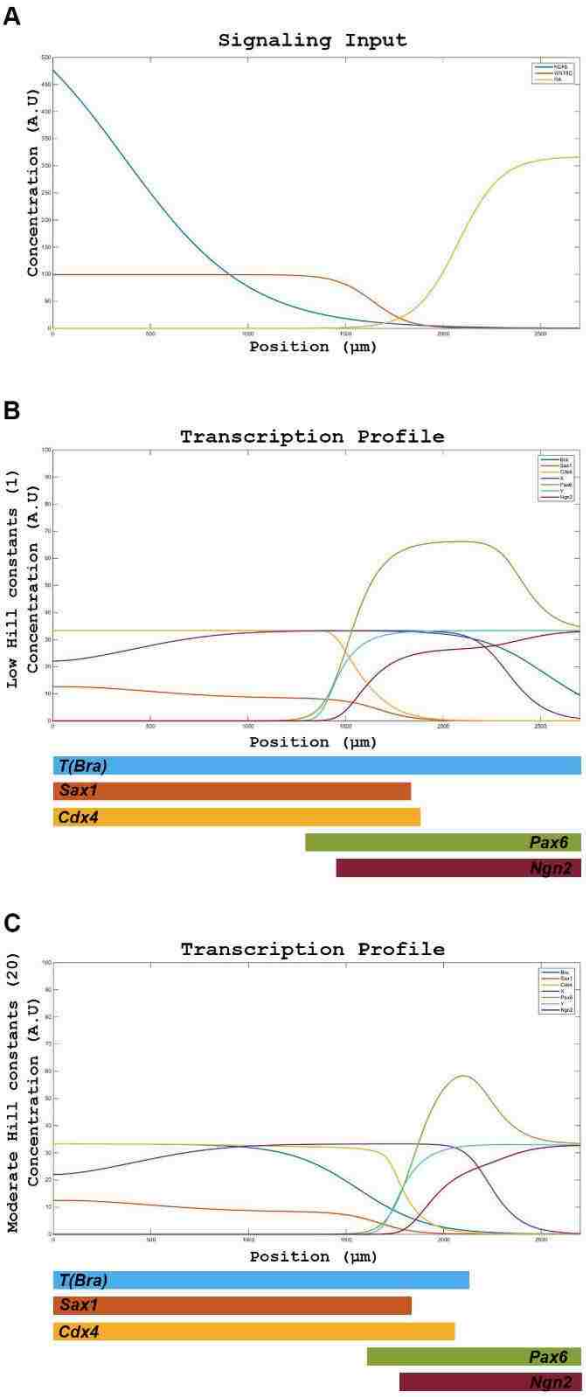

Figure 4.11: Transcription network determine the interpretation of signals. In response to the same signaling input (A), transcription network involving strong interaction (B) reacts differently than a transcription network with moderate interaction (C), even when their network architecture is the same.

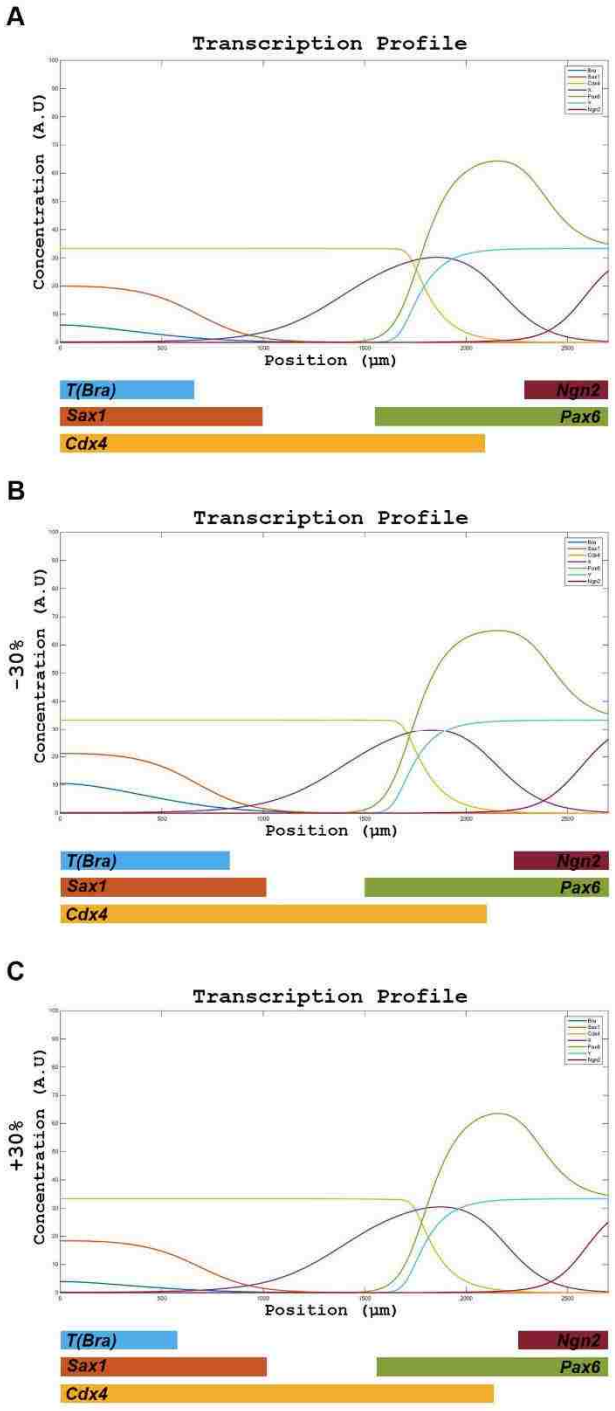

Figure 4.12: Transcription network recapitulates embryonic expression domains. For a subset of interactions the transcription network reproduces the spatial temporal order of transcription factor domains as observed in the wildtype (A). The spatio-temporal order of transcription factors remained comparable to the original order when the interaction strengths were changed by -30% (B) or +30% (C) of original value.

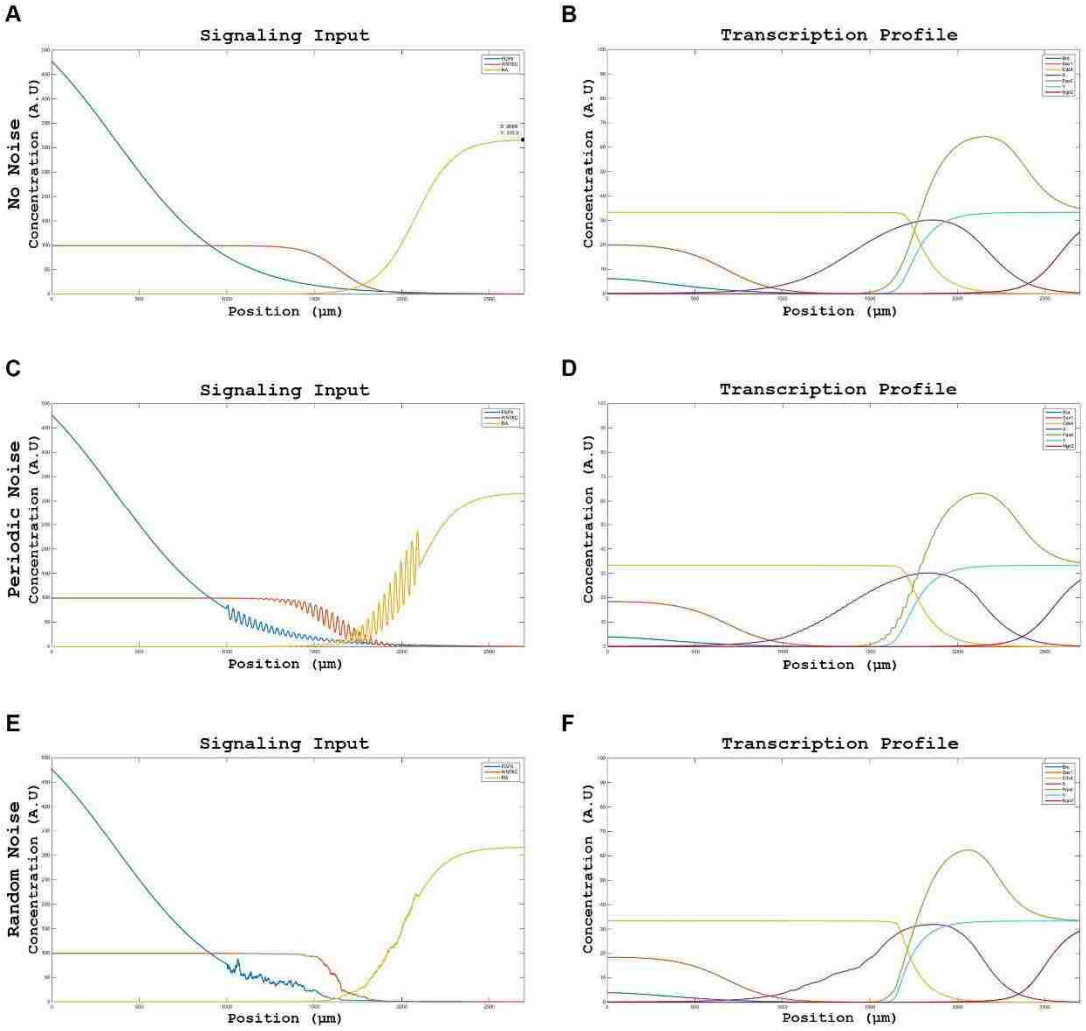

Figure 4.13: Transcription network is robust, withstanding noisy signaling information. The transcription network generated similar transcription expression profiles in response to noise. Expression profiles of signals (A, C, E) and transcription (B, D, F) factors when no noise (A, B), periodic noise (C, D) or random noise (E, F) is introduced into the system. While expression profile of transcription factors did not change in response to signaling noise, the signaling noise was translated into transcriptional noise.

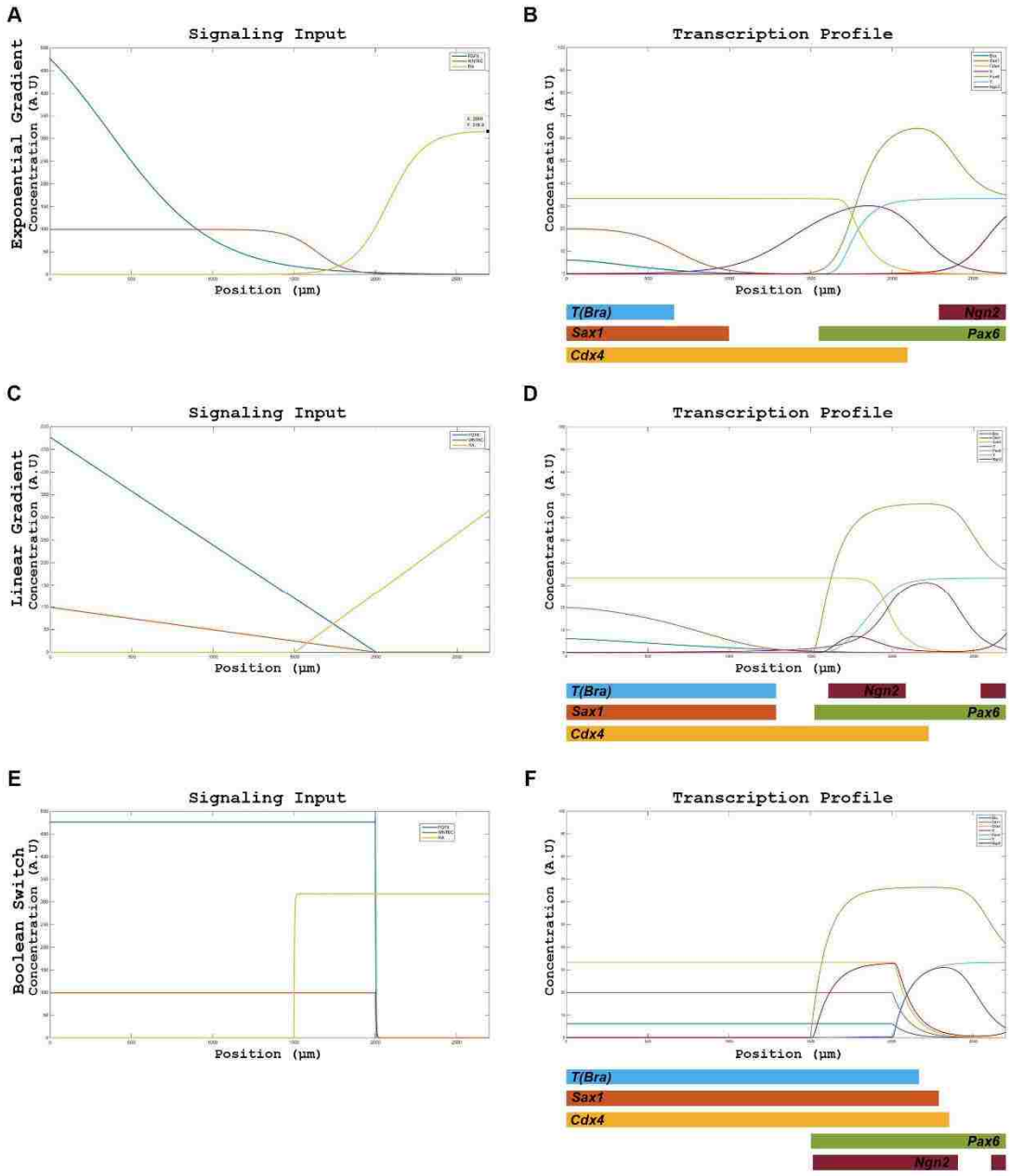

Figure 4.14: Spatial distribution of transcription factors is derived from the spatial profile of the signaling gradients. Signaling factors imprint spatial information onto the transcription network. The transcription network reads the spatial information and reacts accordingly. Simulations of exponential gradients (A, B), linear gradients (C, D) or Boolean information (E, F) leads the same transcription network to different spatial outputs.

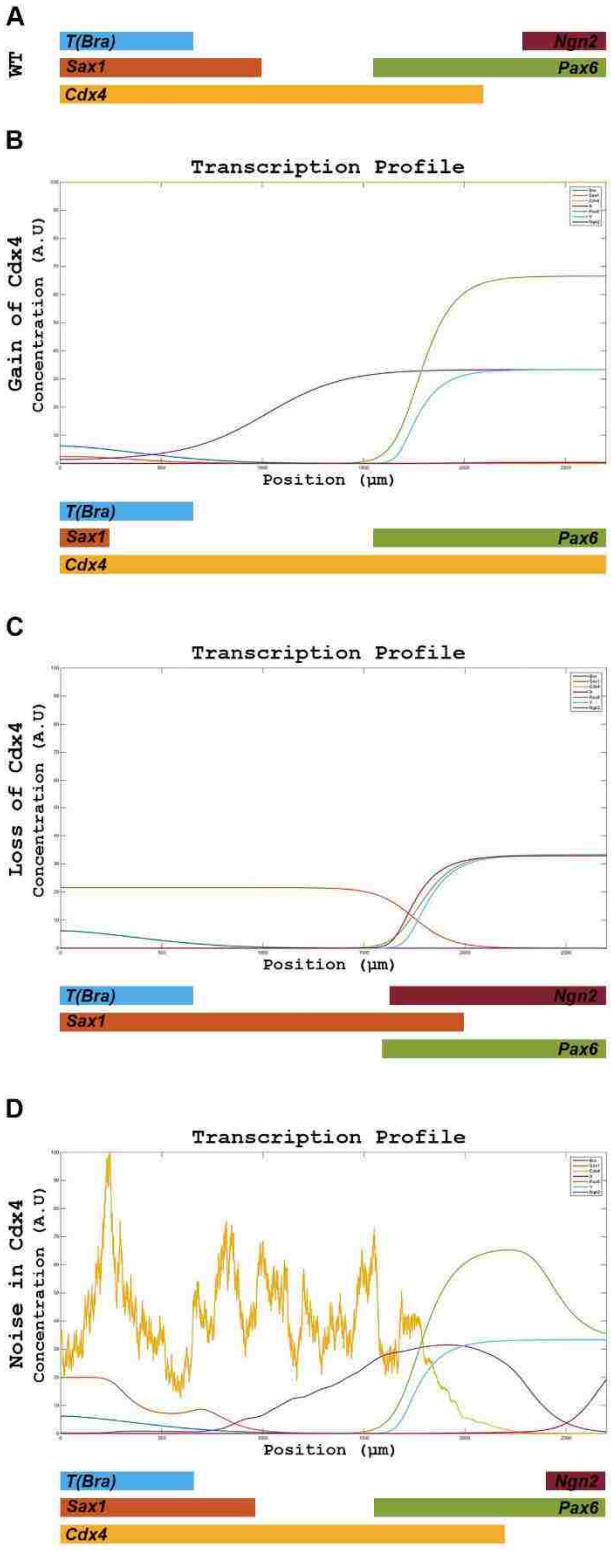

Figure 4.15: Cdx4 plays role in segregating spatio-temporal identities. Cdx4 is required for generation of transition zone identities. Gain of function leads to expansion of rostral transition zone (*Sax1- Pax6+ Ngn2-*) domain caudally (A). Conversely, loss of Cdx4 lead to loss of both caudal transition zone (*Sax1+ Pax6- Ngn2-*) and rostral transition zone (B). In addition, both pre-neural and neurogenic cells markers overlapped in a small domain, suggesting precocious differentiation (B). Both in (A) and (B) *T (Bra)* domain remain unaffected. Noise in Cdx4 was well tolerated by did lead to noise in downstream target Sax1, with which Cdx4 domain overlaps considerably (C).

Chapter 5

DISCUSSION

5.1 Cdx in spinal cord neurogenesis

The current study describes a novel function of Cdx factors in spinal cord neurogenesis. My results showed that Cdx4 is involved in transcription regulation of factors that mediate early stages of maturation of neural progenitors, from their origin in the NMP cell pool at the caudal end, to the acquisition of neurogenic identities and their incorporation in the closed neural tube. Cdx4, through the direct activation of some and indirect repression of other transcription factors, coordinates the gradual loss of pluripotency and acquisition of differentiation states by cells, hence spatio-temporally separating neurogenic events. In the transition zone, Cdx4 inhibits *Sax1* caudally and promotes *Pax6* rostrally. Due to the requirement of RA for *Pax6* regulation, *Pax6* activation is restricted in the rostral half of the transition zone. Significantly, however, Cdx4 also prevents the premature differentiation of newly generated *Pax6*+ cells by preventing activation of *Ngn2*, thus delaying later maturation steps (Chapter 3). Together, these data generate a network of transcription factor interactions that, in computer simulations, recaptures the cellular events observed during spinal cord differentiation (Chapter 4).

Cdx function in regulating the progressive differentiation of spinal cord progenitor cells is different from its previously described functions in spinal cord specification (Skromne et al., 2007) and patterning (Bel-Vialar et al., 2002; Mazzoni et al., 2013; Nordstrom et

al., 2006). Previous studies in our laboratory have demonstrated a crucial role of Cdx in suppressing hindbrain and promoting spinal cord identities (Skromne et al., 2007). In zebrafish, loss of the two members of Cdx family, *cdx1a* and *cdx4,* results in the loss of spinal motor and sensory neurons and an expansion of hindbrain neuronal populations into the trunk and tail of the embryo (Skromne et al., 2007). Interestingly, this role of cdx was independent of *hox* gene activation, as 5' *hox* gene overexpression didn't rescue loss of spinal cord in *cdx* double mutant zebrafish embryos. In contrast, overexpression of *cdx4* in the hindbrain induces neurons to acquire spinal cord identity (Skromne et al., 2007). Similar results have been reported in mice: in embryos that are triple mutants for *Cdx1, Cdx2 and Cdx4*, the spinal cord fails to form (van Rooijen et al., 2012), whereas in embryos over-expressing *Cdx1*, spinal cord neurons are observed in the hindbrain region (Charite et al., 1998). This suggested that Cdx factors play a partially redundant role in spinal cord specification, a function that is evolutionarily conserved.

5.2 Cdx role in coordinating FGF-Wnt-RA signaling information

In regulating spinal cord neurogenesis, Cdx coordinates FGF, Wnt and RA signaling information that other studies have shown to direct spinal cord cell maturation (Diez del Corral et al., 2003; Olivera-Martinez and Storey, 2007). My results showed that with respect to maturation of spinal cord progenitors, Cdx acted antagonistically to FGF-Wnt signaling in the caudal end. FGF-Wnt signaling directs activation of pluripotency marker *Sax1* (Diez del Corral et al., 2002; Tamashiro et al., 2012), in addition to activating *Cdx4* that, my results showed, represses *Sax1* (Fig 3.8B). Hence, while FGF-Wnt signaling promotes pluripotency, the downstream target Cdx4 antagonizes pluripotency and primes

the cells towards their differentiation pathway. Thus, in controlling *Sax1* transcription, Cdx4 provides a feedforward that is antagonistic to FGF-Wnt activity. A similar antagonism was observed in the regulation of *Pax6*, where FGF represses *Pax6* (Bertrand et al., 2000) while Cdx4 promoted its induction (Fig 3.5; Fig 3.6) In contrast, Cdx4 cooperates with RA in promoting *Pax6* transcription and differentiation. In all, Cdx4 acts antagonistically to the inducing FGF-Wnt signaling and synergistic to RA signaling in promoting sequential maturation of cells.

Interestingly, however, Cdx factors cooperate with FGF-Wnt but not RA during spinal cord specification and patterning, which is the opposite of what my results suggest for spinal cord cell maturation. In regulating spinal cord patterning, Cdx factors act downstream of FGF and Wnt signaling in activating caudal 5' *Hox* genes to bestow identity to brachial and thoracic regions of the spinal cord (Bel-Vialar et al., 2002; Marletaz et al., 2015; Nordstrom et al., 2006; Shimizu et al., 2006). Cdx factors also inhibit rostral identities by repressing 3' *Hox* genes that are in turn activated by RA signaling (Lee and Skromne, 2014; Marletaz et al., 2015; Skromne et al., 2007). Hence, Cdx factor cooperate with FGF-Wnt and antagonize RA signaling during patterning of the hindbrain and spinal cord.

Thus, Cdx factors coordinate the signaling information from the FGF-Wnt-RA factors in a contrasting manner depending upon the functional context during spinal cord development. One possible explanation could be that the access of Cdx factors to the regulatory regions is controlled by the signaling information. This is evident in the case of *Pax6* transcription, where FGF signaling leads to higher order chromosomal silencing of *Pax6* (Patel et al., 2013). Recent evidence shows that FGF signaling leads to

translocation of the *Pax6* locus to nuclear boundary, which has been associated with chromatin inactivity (Patel et al., 2013). Downregulation of FGF signaling leads to removal of higher order chromatin modifications that were previously blocking access of regulators to the *Pax6* locus. The other possible speculation could be the availability of cofactors that are regulated by signaling information, as in the case of Cdx regulation of intestinal differentiation. During intestinal stem cell maturation, CDX2 has been shown to associate with Wnt signaling transcription factor TCF4, to achieve tissue specific Wnt function (Verzi et al., 2010). Thus while Cdx factors would act as an activator, the epigenetic state of the DNA, the signaling state of the cell and the availability of other transcription factors in the cell, will determine whether Cdx target genes are activated or not.

5.3 *Cdx4* dynamical expression pattern in the neural tube

Cdx factors are known to be induced in the caudal end of the embryo by FGF and Wnt factors (Bel-Vialar et al., 2002; Keenan et al., 2006; Nordstrom et al., 2006; Pilon et al., 2006). Due to the graded nature of FGF-Wnt signaling along the rostro-caudal axis (Dubrulle and Pourquie, 2004), Cdx factors have been suggested to have a caudal high to rostral-low gradient (Gaunt et al., 2005). My result showed that the *Cdx4* rostro-caudal gradient also has a dynamical dorso-ventral aspect to it (Fig 3.2), which could explain the rostro-caudal gradient initially reported. At the caudal end, where *Cdx4* is transcribed in high concentration, the transcript is present throughout the mediolateral (dorso-ventral) domain of the neural plate/tube (Fig 3.2). However, in the rostral direction, with progressive decrease in the concentration of *Cdx4* transcripts, there is also a subsequent

dorsal restriction of the expression domain. Interestingly, there is also a marked absence of *Cdx4* from the roof plate (Fig 3.2).

The dorso-ventral expression of *Cdx4* could be a result of dorso-ventral restriction of FGF-Wnt signaling. While *Wnt3a* (Alvarez-Medina et al., 2008) is restricted to the dorsal side in the closed neural tube, *Fgf8* and *Wnt8c* don't show DV dynamics (Olivera-Martinez and Storey, 2007), thus ruling out the possibility that the dynamic *Cdx4* expression is due to graded FGF-Wnt signaling. Another possible factor that is involved in *Cdx4* regulation could be BMPs, as BMP4/7 are known to have a localized dorsal signaling in the neural tube (Alvarez-Medina et al., 2008). While the role of BMPs in regulating *Cdx4* is not known in chicken, in zebrafish they are known to indirectly activate *cdx* genes during hematopoiesis (Lengerke et al., 2008). An alternative explanation is that *Cdx4*, directly or indirectly, is under SHH signaling control. Indeed ventral clearing of *Cdx4* is concomitant with the onset of ventral expression of *Nkx6.1* (Fig 3.3), a direct downstream target of SHH (Briscoe et al., 2000). While Cdx4 could be under SHH regulation, it is not under Nkx6.1 control because, as *Cdx4* continues its dorsal-ward restriction in the rostral direction, *Nkx6.1*'s expression is restricted only to the ventral part of the neural tube (Fig 3.3). This would suggest that a combination of DV patterning factors are involved in regulating DV restriction of *Cdx4* expression.

Initial evaluation of Cdx4 function in the spinal cord D/V patterning did not reveal any novel functions besides what I have already described for *Pax6*. Over-expression of *Cdx4* didn't change the overall DV patterning of the neural tube (Fig 3.4). In these experiments, over-expression of *Cdx4* did not alter the DV domain of *Pax7* and *Nkx6*.1, only that of *Pax6*. However, Cdx4's regulation of *Pax6* could provide indirect regulation

of DV patterning factors that are inhibited or activated by Pax6. One factor that is inhibited by Pax6 is *Nkx2.2* , which is involved in floor plate specification (Briscoe et al., 2000). Importantly, *Sax1* is also shown to be involved in floor plate competence by inhibiting *Pax6* expression in the floor plate (Sasai et al., 2014). As seen in my experiments, Cdx4 activates *Pax6* and inhibits *Sax1*. Thus ventrally, these observations raise the interesting possibility of Cdx4 contributing to the early specification of the floor plate.

In contrast, in the dorsal side, *Cdx4* overlaps with *Pax3*. Recent studies in mice have shown a direct role of Cdx2 in regulating *Pax3* in neural crest precursors (Sanchez-Ferras et al., 2012). Based on the functional redundancy of Cdx factors, Cdx4 would also be a possible regulator of *Pax3*. However, in my experiments, *Cdx4* over-expression didn't change *Pax3* DV domain (not shown). Three possibilities could explain the discrepancy between my results and those described in mice (Sanchez-Ferras et al., 2012). First, it's possible that *Pax3* regulation is restricted to neural crest cells, a cell population I did not examine, as opposed to dorsal neural tube. Second, only Cdx2 and not Cdx4 can regulate *Pax3*. Finally, the regulation of *Pax3* by Cdx factors is species specific. In my analysis *Cdx4* was observed to be absent in roof plate that contains neural crest precursors. While Cdx2 has shown to promote neural crest specification in mouse, the absence of *Cdx4* in roof plate suggests that Cdx4 does not have the same function in chicken.

5.4 Future work

Apart from the role of Cdx in spinal cord and mesoderm formation, Cdx factors are involved in regulating differentiation in trophectoderm, intestinal stem cells and

hematopoiesis. While Cdx factors do not regulate similar set of transcription factors in these tissues, they are involved in promoting differentiation and inhibiting pluripotency as seen in intestinal stem cell differentiation (Hryniuk et al., 2012; Saad et al., 2011) and hematopoiesis (McKinney-Freeman et al., 2008; Wang et al., 2008). My discovery that Cdx promotes spinal cord neurogenesis provides additional evidence that a general function of Cdx factors during development is in making cell fate decisions. Future studies can focus on the conserved and divergent mechanisms by which Cdx factors achieve differentiation in various tissues. One possible mechanism is the regulation of chromatin modification. Cdx factors are known to regulate chromatin opening during *Hox* gene activation in mice during spinal cord patterning (Mazzoni et al., 2013). A similar regulatory mechanism, where Cdx factors dictate the accessibility of gene locus to activators via modulating chromatin modification could be a common mechanism for making cell fate decisions.

Importantly, during spinal cord development and mesoderm formation, Cdx factors coordinate upstream signaling information and convey it downstream to a transcription network. A number of *Hox* and non-*Hox* genes are regulated by Cdx during axial elongation processes (Savory et al., 2009; Shimizu et al., 2006; van Rooijen et al., 2012), suggesting that Cdx regulation is not restricted to *Hox* genes modulation. Having a common regulator that coordinates patterning and differentiation events would be important for proper specification of tissue identity. My work expands the role of Cdx in spinal cord development, but further research is needed to properly understand the regulation of downstream target genes. The current study also lacks a proper loss of *Cdx4* analysis due the unavailability of genetic techniques in chicken to knock down gene

expression and function. In the future, Cdx factors can be studied in mouse where more efficient genetic strategies could be used to properly remove Cdx factors.

Importantly, cross regulation and feedback among downstream targets of Cdx should also be investigated to understand the built-in robustness in the system that regulates proper development in the presence of extrinsic and intrinsic noise. As suggested by my experiments, Cdx4 represses the expression of *Sax1* and *Ngn2* via indirect mechanism. Finding this missing mechanism would shed further light on the role of Cdx in regulating spinal cord development.

In conclusion, Cdx factors are at the core of gene regulatory network that regulate patterning and differentiation across tissue during vertebrate embryonic development. Importantly, the role of Cdx factors as a coordinator of upstream signaling make them indispensable for proper embryonic development.

APPENDIX

A) SGNDYN.m: MATLAB code of simulating signaling dynamics.

```
function []= SGNDYN()

% Modeling the signaling switch.
% Basic skeleton: FGF activates Wnt and inhibit RA, Wnt activates
% retinoic acid (RA) and Retinoic acid inhibits FGF.
%
% Model simulate signaling dynamics in a static spatial domain over time to
% evaluate steady state profile of signaling factors. The spatial domain is
% static with respect to the caudal end that is travels caudaly as the
% embryonic axis extends.
%
% Intially, in the undifferentiated region (neural plate) Fgf8 mRNA is
% present. The Fgf8 mRNA drives production of FGF8 protein. FGF8
% protein regulates transcription of Wnt8c mRNA. Wnt8c mRNA drives
% production of Wnt8c protein. Wnt8c activates and FGF8 inhibits Raldh2
% mRNA transcription. Raldh2 is also regulated by retinoic acid (RA), a
% product of enzyme synthesized by Raldh2. Retinoic acid represses Fgf8
% transcription. Retinoic acid is also degraded by FGF8 dependent
% mechanism.
%
% All the signaling molecules, FGF8, Wnt8c and retinoic acid are
% diffusible. Hence I am using the pdepe solver to model the signaling
% dynamics.
% For more description of the solver:
% http://www.mathworks.com/help/matlab/ref/pdepe.html
%

% 1D space. Unit: micrometer. The spatial domain is intended to represent
% neural region from caudal end to the portion surrounded by last 4-5
% somites.
x=linspace(0,2500,1000);

% Time span. Unit: mintue.
tspan=linspace(0,10000,5000);

% Symmetry
m=0;

% Calling pdepe sovler
sol=pdepe(m,@eqs,@initial,@bc,x,tspan);
```

```
% Storing values of FGF, Wnt and RA mrna and protein in separate matrices.

FGFO=sol(:,:,1);
FGFM=sol(:,:,2);
FGFP=sol(:,:,3);
WNTM=sol(:,:,4);
WNTP=sol(:,:,5);
RAM=sol(:,:,6);
RAP=sol(:,:,7);

% Generating figures
%
% 3D
%
% figure
% h=surf(x,tspan,FGFM);
% set(h,'LineStyle','none')
% xlabel('X'),ylabel('Time'),zlabel('Fgf8');
%
% figure
% h=surf(x,tspan,FGFP);
% set(h,'LineStyle','none')
% xlabel('X'),ylabel('Time'),zlabel('FGF8');
%
% figure
% h=surf(x,tspan,WNTM);
% set(h,'LineStyle','none')
% xlabel('X'),ylabel('Time'),zlabel('Wnt8c');
%
% figure
% h=surf(x,tspan,WNTP);
% set(h,'LineStyle','none')
% xlabel('X'),ylabel('Time'),zlabel('WNT8C');
%
% figure
% h=surf(x,tspan,RAM);
% set(h,'LineStyle','none')
% xlabel('X'),ylabel('Time'),zlabel('Raldh2');
%
figure
h=surf(x,tspan,RAP);
set(h,'LineStyle','none')
xlabel('X'),ylabel('Time'),zlabel('RA');


%
```

```
% 2D
% Plotting mRNA data overspace and time.
% Size of the time, space and entity vectors in the final matrix.
% [i,j,k]=size(sol);
% Diving the time into equally spaced smaller vector.
% o=1:50:i;

% 'For loop' for plotting mRNA concentrations in the static space after
% certain duration to show the change in mRNA landscape as the
% differentiation proceeds.
% figure
%for p=1:1:length(o)
  % subplot(length(o),1,p);
  % plot(x,FGFM(o(p),:),x,WNTM(o(p),:),x,RAM(o(p),:));
  % axis([0 500 0 35])
%end
%legend('Fgf8','Wnt8c','Raldh2');

% 'For loop' for plotting protein concentrations in the static space after
% certain duration to show the change in protein landscape as the
% differentiation proceeds.
%
% figure
% for p=1:1:length(o)
%
%   %subplot(length(o),1,p);
%   plot(x,FGFP(o(p),:),x,WNTP(o(p),:),x,RAP(o(p),:));
%   %axis([0 500 0 70])
%   title(['Time=' num2str(o(p))])
%
% end
% legend('FGF8','WNT8C','RA');
%
% Plotting mRNA profile at the beginning of simulation.
% figure
% plot(x,FGFM(1,:),x,WNTM(1,:),x,RAM(1,:));
% legend('Fgf8','Wnt8C','Raldh2');
%
% % Plotting protein profile at the beginning of simulation.
% figure
% plot(x,FGFP(1,:),x,WNTP(1,:),x,RAP(1,:));
% legend('FGF8','WNT8C','RA');

% Plotting mRNA profile at the end of simulation.
figure
plot(x,FGFM(5000,:),x,WNTM(5000,:),x,RAM(5000,:),'LineWidth',2);
```

```
axis([0 2500 0 40]);
legend('Fgf8','Wnt8C','Raldh2');

% Plotting protein profile at the end of simulation.
figure
plot(x,FGFP(5000,:),x,WNTP(5000,:),x,RAP(5000,:),'LineWidth',2);
axis([0 2500 0 500]);
legend('FGF8','WNT8C','RA');


%Functions
% Defined as per the example on the MATLAB website.

    function [c,b,s]=eqs(x,tspan,u,dudx)
    % Equations detialing regulatory relationships between FGF8, WNT8C and
    % RA mRNA and protein synthesis and degradation, as described above.
    %
    % Transcripton rate constants alpha(a)for mRNAs (min-1):
    aFm=1; aWm=0.1;aRm=1;
    % Translation rate constants alpha(a)for proteins (min-1):
    aFp=.3;aWp=.3;aRp=.3;

    % Degradation rate constants beta(b)for mRNAs and proteins (min-1):
    bFm=0.006;bFp=0.005;bWm=0.03;bWp=0.01;bRm=0.03;bRp=0.025;


    % Hill constants.
    % FGF8 on Wnt8c mRNA synthesis
    Fw=10;
    % FGF8 on Raldh2 mRNA synthesis
    Fr=1;
    % FGF8 on RA degradation synthesis
    Fr2=2;

    % WNT8C on Raldh2 mRNA synthesis
    Wr=1;

    % RA on Raldh2 mRNA synthesis
    Rr=50;%determines the height of RA protein
    % RA on Fgf8 mRNA synthesis
    Rf=1;

    % Hill coefficients
    a=2;
    r=2;
```

```
% Descrbing FGF8, WNT8C and RA mRNA and protien rate of change based on
% interactions.
% u(1)= Constant input, u(2)= Fgf8 mRNA, u(3)= FGF8 protein,
% u(4)= Wnt8c mRNA, u(5)= WNT8C protein, u(6)= Raldh2 mRNA,
% u(7)= Retinoic acid

% Input
dF0=0;                                          %1

% Fgf8 mRNA synthesis is inhibited by action of RA
dFm=aFm*u(1)*(1/(1+(u(7)/Rf)^r))-bFm*u(2);              %2
% FGF8 protein synthesis
dFp=aFp*u(2)-bFp*u(3);                          %3

% Wnt8c synthesis dependent on FGF8 activation
dWm=aWm*((u(3)/Fw)^a/(1+(u(3)/Fw)^a))-bWm*u(4);         %4
% WNT8C protein synthesis
dWp=aWp*u(4)-bWp*u(5);                          %5

% Raldh2 synthesis positively regulated by WNT8C and RA, and negatively
% by FGF8
dRm=aRm*(((u(5)/Wr)^a+(u(7)/Rr)^a)/(1+(u(5)/Wr)^a+(u(7)/Rr)^a))*...
   (1/(1+(u(3)/Fr)^r))-bRm*u(6);

% RA degradation is positively regulated FGF8 which via producing
% CYP26a creates a sink for RA signaling at the posterior end of the
% neural tube.
dRp=aRp*u(6)-bRp*u(7)*(1+6*((u(3)/Fr2)^a/(1+(u(3)/Fr2)^a)));    %7


% Inserting relations defined in appropriate format to be solved by
% pdepe solver
c=[1;1;1;1;1;1;1];
% Diffusion coefficients (um^2/min) for all mRNAs is zero.
% For FGF8=120, WNT8C= 10, RA= 1200.
b=[0;0;120;0;10;0;1200].*dudx;
s=[dF0;dFm;dFp;dWm;dWp;dRm;dRp];

end


function [pl,ql,pr,qr]=bc(xl,ul,xr,ur,tspan)
% Boundary conditons for mRNAs and protiens.
%
% All mRNAs and proteins have zero flux conditions on both left and
% right boundries.
```

```
    % LHS
    pl=[0;0;0;0;0;0;0];
    ql=[1;1;1;1;1;1;1];
    % RHS
    pr=[0;0;0;0;0;0;0];
    qr=[1;1;1;1;1;1;1];

    end


    function v= initial(x)
    % Initial mRNA and protein distrubitions in space.
    %
    % Initial FGF mRNA defined by spatial exponential decay equation:
    % Fm0=10*exp(-0.002*x) proptional to the constant input
    % F0= .06*exp(-0.002*x)
    % Initial value of other entities is set to zero.

    v=[.06*exp(-0.002*x);10*exp(-0.002*x);0;0;0;0;0];

    end


end
```

B) TRNSDYN.m: MATLAB code for simulating transcriptional factor dynamics for a given signaling input

```
function []= TRNSDYN()

% Modeling the transcriptional switch.
% Model simulates the transcription factor dynamics overtime.
% DESCRIPTION:
% At T=0, in the undifferentiated region (neural plate) T(Bra), Sax1 and
% Cdx4 mRNAs and proteins are present as defined by the levels of FGF8 and
% WNT8C protein value.
% As time proceeds, the overlying signaling factor information changes, as
% obtained from SGNDYN, activates the transcription network that drives
% transcription factor dynamics.
%
% For transcription factor dynamics I am using the ode45 solver as there
% are no diffusable entities in the model. For more description of the
% solver:
% http://www.mathworks.com/help/matlab/ref/ode45.html?searchHighlight=ode45
%
% Time duration. This duration is equal to the temporal duration of
% simulation in SGNDYN.
tspan1=[0 1000];
tspan2=[0 900];

%--
%Model parameters.

%Max rate of transcription: 1/min.(Kiparissides et al 2011)
aTm=1;aSm=1;aCm=1;aXm=1;aPm=1;aYm=1;aNm=1;

%Translation rate(min-1).
aTp=1;aSp=1;aCp=1;
aXp=1;aPp=1;aYp=1;

%Degradation constants 'beta'(min-1).
bTm=0.03;bTp=0.2;bSm=0.03;bSp=0.2;bCm=0.03;bCp=0.05;
bXm=0.03;bXp=0.2;bPm=0.03;bPp=0.2;bYm=0.03;bYp=0.2;bNm=0.03;

%Hill constants
%FGF interactions
% Positive
Ft=1000;
Fc=1;
```

```
%Negative
Fx=1;
Fy=1;

%WNT
%Positive
Ws=50;Wc=50;

%Sax1
%Positive
%Ss=20;
%Negative
Sp=20;Ss=100;

%Cdx4
%Positive
Cp=10;Cx=20;
%Negative

%X
%negative
Xs=1;Xn=1;
%Pax6
%Positive
Py=5;Pn=20;
%Y
%Ngetaive
Yc=5;
%RA
%Positive
Rp=10;

% Ft=20;
% Fc=20;
% %Negative
% Fx=20;Fy=20;
%
% %WNT
% %Positive
% Ws=20;Wc=20;
%
% %Sax1
% %Positive
% %Ss=20;
% %Negative
% Sp=20;Ss=20;
```

```
%
% %Cdx4
% %Positive
% Cp=20;Cx=20;
% %Negative
%
% %X
% %negative
% Xs=20;Xn=20;
% %Pax6
% %Positive
% Py=20;Pn=20;
% %Y
% %Ngetaive
% Yc=20;
% %RA
% %Positive
% Rp=20;


%Hill coefficients
a=2;
r=2;
% End of parameters
%----

% Running the model to find steady state values of transcription factors in
% the stem cell on the left.
iv1=[476.5542278;99.279997334;0;0;0;0;0;0;0;0;0;0;0;0;0;0];

%Calling the ODE solver
[t,X]=ode45(@TSDS,tspan1,iv1);
% Plotting steady state data.
% figure
% plot(t,X(:,1),t,X(:,2),t,X(:,3))
% legend('FGF8','WNT8C','RA')
% figure
% plot(t,X(:,4),t,X(:,6),t,X(:,8),t,X(:,10),t,X(:,12),t,X(:,16))
% legend('Bra','Sax1','Cdx4','X','Pax6','Ngn2')
% figure
%
% Running the model to with the steady state values of transcription factors.
iv2=[476.5542278;99.279997334;0.00000189;X(end,4);X(end,5);X(end,6);X(end,7);...

X(end,8);X(end,9);X(end,10);X(end,11);X(end,12);X(end,13);X(end,14);X(end,15);X(en
d,16)];
```

```
%
% Calling the ODE solver
[t,Y]=ode45(@TSD,tspan2,iv2);

O=3.*t; %Converting time into spatial domain. Speed= 3 um/min
%Plotting the overlying signaling factor profile
figure
plot(O,Y(:,1),O,Y(:,2),O,Y(:,3),'LineWidth',2)
legend('FGF8','WNT8C','RA')
axis([0 2700 0 500])

%Plotting the trasncription factor mRNA dynamics
figure
plot(O,Y(:,4),O,Y(:,6),O,Y(:,8),O,Y(:,10),O,Y(:,12),O,Y(:,14),O,Y(:,16),'LineWidth',2)
legend('Bra','Sax1','Cdx4','X','Pax6','Y','Ngn2')
axis([0 2700 0 100])

%ODE function
%For finding steady state transcription factor values.
function res= TSDS(t,V)

%Descrbing FGF, WNT and RA gradient in the stem cell.
dF=0; %1
dW=0; %2
dR=0; %3

%Transcription factor dynamics in the stem cell.

% T(Bra) is activated by FGF8.
dTm=aTm*((V(1)/Ft)^a/(1+(V(1)/Ft)^a))-bTm*V(4); %4
dTp=aTp*V(4)-bTp*V(5); %5

%Sax1 is activated by WNT8C and inhibited by X and Sax1.
% dSm=0; %6 Loss of Sax1
dSm=aSm*((V(2)/Ws)^a/(1+(V(2)/Ws)^a+(V(7)/Ss)^r+(V(11)/Xs)^r))-bSm*V(6);  %6
dSp=aSp*V(6)-bSp*V(7); %7

%Cdx4 is activated by FGF8 and WNT8C and inhibited by Y.
% dCm=0;  %8 Loss of Cdx4
dCm=aCm*(((V(1)/Fc)^a+(V(2)/Wc)^a)/(1+(V(1)/Fc)^a+(V(2)/Wc)^a+(V(15)/Yc)^r))-
bCm*V(8);  %8
dCp=aCp*V(8)-bCp*V(9); %9

%X is activated by Cdx4 and inhbited by FGF8.
dXm=aXm*((V(9)/Cx)^a/(1+(V(9)/Cx)^a+(V(1)/Fx)^r))-bXm*V(10); %10
```

```
dXp=aXp*V(10)-bXp*V(11); %11

%Pax6 is activated by Cdx4 in presence of RA and maintained by RA. It is
%inhibited by Sax1.
dPm=aPm*(((V(9)/Cp)^a/(1+(V(9)/Cp)^a+(V(7)/Sp)^r))+1)*((V(3)/Rp)^a/...
      (1+(V(3)/Rp)^a))-bPm*V(12); %12
dPp=aPp*V(12)-bPp*V(13); %13

%Factor Y is activated by Pax6 and inhibited by FGF8.
dYm=aYm*((V(13)/Py)^a/(1+(V(13)/Py)^a+(V(1)/Fy)^a))-bYm*V(14); %14
dYp=aYp*V(14)-bYp*V(15); %15

%Ngn2 is activated by Pax6 and inhibited by X.
dNm=aNm*((V(13)/Pn)^a/(1+(V(13)/Pn)^a+(V(11)/Xn)^r))-bNm*V(16); %16


res=[dF;dW;dR;dTm;dTp;dSm;dSp;dCm;dCp;dXm;dXp;dPm;dPp;dYm;dYp;dNm];
end

% For findign transcription factor dynamics with steady state starting
% values.

function res= TSD(t,V)


%No noise
dF=-0.0000147643*(630.1-V(1))*V(1);%1
dW=-0.000320910556*(99.28-V(2))*V(2); %2
dR=0.00008619678335*(317.1-V(3))*V(3); %3

%Periodic Noise 1
% if t>333 && t<700
% dF=-0.0000147643*(630.1-V(1))*V(1)*(1+15*sin(.6*t));%1
% dW=-0.000320910556*(99.28-V(2))*V(2)*(1+15*sin(0.6*t)); %2
% dR=0.00008619678335*(317.1-V(3))*V(3)*(1+15*sin(0.6*t)); %3
% else
% dF=-0.0000147643*(630.1-V(1))*V(1);%1
% dW=-0.000320910556*(99.28-V(2))*V(2); %2
% dR=0.00008619678335*(317.1-V(3))*V(3); %3
% end

%Random Noise 2
% if t>333 && t<700
% RAN=(1+1).*rand(1)-1;
% dF=-0.0000147643*(630.1-V(1))*V(1)*(1+100*sin(RAN*t));%1
% dW=-0.000320910556*(99.28-V(2))*V(2)*(1+50*sin(RAN*t)); %2
```

```
% dR=0.00008619678335*(317.1-V(3))*V(3)*(1+30*sin(RAN*t)); %3
% else
% dF=-0.0000147643*(630.1-V(1))*V(1);%1
% dW=-0.000320910556*(99.28-V(2))*V(2); %2
% dR=0.00008619678335*(317.1-V(3))*V(3); %3
% end


% Step Signals
%     dF=0;%1
%     dW=0; %2
%     dR=0; %3
%
%
% if t>500 && (t<=667)
%     dR=0.667*V(1)-V(3);%3
% elseif t>667
%     dF=-V(1);%1
%     dW=-V(2); %2
% end

%Linear gradient
% if t<500
%     dF=-.71364318;%1
%     dW=-.1488456; %2
%     dR=0; %3
%
% elseif (t>500) && (t<=667)
%     dF=-.71364318;%1
%     dW=-.1488456; %2
%     dR=0.79; %3
% else
%     dF=0;%1
%     dW=0; %2
%     dR=0.79; %3
% end

% %Transcription factor dynamics

% T(Bra) is activated by FGF8.
dTm=aTm*((V(1)/Ft)^a/(1+(V(1)/Ft)^a))-bTm*V(4); %4
dTp=aTp*V(4)-bTp*V(5); %5

%Sax1 is activated by WNT8C and inhibited by X and Sax1.
% dSm=0; %6 Loss of Sax1
dSm=aSm*((V(2)/Ws)^a/(1+(V(2)/Ws)^a+(V(7)/Ss)^r+(V(11)/Xs)^r))-bSm*V(6);  %6
```

```
dSp=aSp*V(6)-bSp*V(7); %7

%Cdx4 is activated by FGF8 and WNT8C and inhibited by Y.
% dCm=0;  %8 Loss of Cdx4
dCm=aCm*(((V(1)/Fc)^a+(V(2)/Wc)^a)/(1+(V(1)/Fc)^a+(V(2)/Wc)^a+(V(15)/Yc)^r))-
bCm*V(8);  %8
dCp=aCp*V(8)-bCp*V(9); %9

%Cdx4 intrinsic noise
% RAN=(1+1).*rand(1)-1;
%
dCm=aCm*(((V(1)/Fc)^a+(V(2)/Wc)^a)/(1+(V(1)/Fc)^a+(V(2)/Wc)^a+(V(15)/Yc)^r))...
%     *(1+100*sin(RAN*t))-bCm*V(8);;%8


%X is activated by Cdx4 and inhbited by FGF8.
dXm=aXm*((V(9)/Cx)^a/(1+(V(9)/Cx)^a+(V(1)/Fx)^r))-bXm*V(10); %10
dXp=aXp*V(10)-bXp*V(11); %11

%Pax6 is activated by Cdx4 in presence of RA and maintained by RA. It is
%inhibited by Sax1.
dPm=aPm*(((V(9)/Cp)^a/(1+(V(9)/Cp)^a+(V(7)/Sp)^r))+1)*((V(3)/Rp)^a/...
       (1+(V(3)/Rp)^a))-bPm*V(12); %12
dPp=aPp*V(12)-bPp*V(13); %13

%Factor Y is activated by Pax6 and inhibited by FGF8.
dYm=aYm*((V(13)/Py)^a/(1+(V(13)/Py)^a+(V(1)/Fy)^a))-bYm*V(14); %14
dYp=aYp*V(14)-bYp*V(15); %15

%Ngn2 is activated by Pax6 and inhibited by X.
dNm=aNm*((V(13)/Pn)^a/(1+(V(13)/Pn)^a+(V(11)/Xn)^r))-bNm*V(16); %16


res=[dF;dW;dR;dTm;dTp;dSm;dSp;dCm;dCp;dXm;dXp;dPm;dPp;dYm;dYp;dNm];
end
end
```

REFERENCES

1. Adler, R., 2005. Challenges in the study of neuronal differentiation: a view from the embryonic eye. Developmental dynamics : an official publication of the American Association of Anatomists 234, 454-463.

2. Akai, J., Halley, P.A., Storey, K.G., 2005. FGF-dependent Notch signaling maintains the spinal cord stem zone. Genes & development 19, 2877-2887.

3. Alon, U., 2007. Network motifs: theory and experimental approaches. Nature reviews. Genetics 8, 450-461.

4. Alvarez-Medina, R., Cayuso, J., Okubo, T., Takada, S., Marti, E., 2008. Wnt canonical pathway restricts graded Shh/Gli patterning activity through the regulation of Gli3 expression. Development (Cambridge, England) 135, 237-247.

5. Andersson, E.R., Sandberg, R., Lendahl, U., 2011. Notch signaling: simplicity in design, versatility in function. Development (Cambridge, England) 138, 3593-3612.

6. Arce, L., Yokoyama, N.N., Waterman, M.L., 2006. Diversity of LEF/TCF action in development and disease. Oncogene 25, 7492-7504.

7. Aulehla, A., Wehrle, C., Brand-Saberi, B., Kemler, R., Gossler, A., Kanzler, B., Herrmann, B.G., 2003. Wnt3a plays a major role in the segmentation clock controlling somitogenesis. Developmental cell 4, 395-406.

8. Aw Yeang, H.X., Hamdam, J.M., Al-Huseini, L.M., Sethu, S., Djouhri, L., Walsh, J., Kitteringham, N., Park, B.K., Goldring, C.E., Sathish, J.G., 2012. Loss of transcription factor nuclear factor-erythroid 2 (NF-E2) p45-related factor-2 (Nrf2) leads to dysregulation of immune functions, redox homeostasis, and intracellular signaling in dendritic cells. The Journal of biological chemistry 287, 10556-10564.

9. Balasubramanian, R., Zhang, X., 2015. Mechanisms of FGF gradient formation during embryogenesis. Seminars in cell & developmental biology.

10. Becker, C.G., Diez Del Corral, R., 2015. Neural development and regeneration: it's all in your spinal cord. Development (Cambridge, England) 142, 811-816.

11. Bel-Vialar, S., Itasaki, N., Krumlauf, R., 2002. Initiating Hox gene expression: in the early chick neural tube differential sensitivity to FGF and RA signaling subdivides the HoxB genes in two distinct groups. Development (Cambridge, England) 129, 5103-5115.

12. Bel-Vialar, S., Medevielle, F., Pituello, F., 2007. The on/off of Pax6 controls the tempo of neuronal differentiation in the developing spinal cord. Developmental biology 305, 659-673.

13. Bertrand, N., Medevielle, F., Pituello, F., 2000. FGF signalling controls the timing of Pax6 activation in the neural tube. Development (Cambridge, England) 127, 4837-4843.

14. Bertrand, V., Hobert, O., 2010. Lineage programming: navigating through transient regulatory states via binary decisions. Current opinion in genetics & development 20, 362-368.

15. Boettger, T., Wittler, L., Kessel, M., 1999. FGF8 functions in the specification of the right body side of the chick. Current biology : CB 9, 277-280.

16. Boulet, A.M., Capecchi, M.R., 2012. Signaling by FGF4 and FGF8 is required for axial elongation of the mouse embryo. Developmental biology 371, 235-245.

17. Briata, P., Ilengo, C., Bobola, N., Corte, G., 1999. Binding properties of the human homeodomain protein OTX2 to a DNA target sequence. FEBS letters 445, 160-164.

18. Briscoe, J., Pierani, A., Jessell, T.M., Ericson, J., 2000. A homeodomain protein code specifies progenitor cell identity and neuronal fate in the ventral neural tube. Cell 101, 435-445.

19. Brown, J.M., Storey, K.G., 2000. A region of the vertebrate neural plate in which neighbouring cells can adopt neural or epidermal fates. Current biology : CB 10, 869-872.

20. Butler, S.J., Bronner, M.E., 2015. From classical to current: analyzing peripheral nervous system and spinal cord lineage and fate. Developmental biology 398, 135-146.

21. Calo, E., Wysocka, J., 2013. Modification of enhancer chromatin: what, how, and why? Molecular cell 49, 825-837.

22. Cambray, N., Wilson, V., 2002. Axial progenitors with extensive potency are localised to the mouse chordoneural hinge. Development (Cambridge, England) 129, 4855-4866.

23. Cambray, N., Wilson, V., 2007. Two distinct sources for a population of maturing axial progenitors. Development (Cambridge, England) 134, 2829-2840.

24. Chalamalasetty, R.B., Garriock, R.J., Dunty, W.C., Jr., Kennedy, M.W., Jailwala, P., Si, H., Yamaguchi, T.P., 2014. Mesogenin 1 is a master regulator of paraxial presomitic mesoderm differentiation. Development (Cambridge, England) 141, 4285-4297.

25. Chambers, D., Mason, I., 2000. Expression of sprouty2 during early development of the chick embryo is coincident with known sites of FGF signalling. Mechanisms of development 91, 361-364.

26. Charite, J., de Graaff, W., Consten, D., Reijnen, M.J., Korving, J., Deschamps, J., 1998. Transducing positional information to the Hox genes: critical interaction of cdx gene products with position-sensitive regulatory elements. Development (Cambridge, England) 125, 4349-4358.

27. Charrier, J.B., Lapointe, F., Le Douarin, N.M., Teillet, M.A., 2002. Dual origin of the floor plate in the avian embryo. Development (Cambridge, England) 129, 4785-4796.

28. Chawengsaksophak, K., de Graaff, W., Rossant, J., Deschamps, J., Beck, F., 2004. Cdx2 is essential for axial elongation in mouse development. Proceedings of the National Academy of Sciences of the United States of America 101, 7641-7645.

29. Cheng, P.Y., Lin, C.C., Wu, C.S., Lu, Y.F., Lin, C.Y., Chung, C.C., Chu, C.Y., Huang, C.J., Tsai, C.Y., Korzh, S., Wu, J.L., Hwang, S.P., 2008. Zebrafish cdx1b regulates expression of downstream factors of Nodal signaling during early endoderm formation. Development (Cambridge, England) 135, 941-952.

30. Cooper, D.N., Krawczak, M., Polychronakos, C., Tyler-Smith, C., Kehrer-Sawatzki, H., 2013. Where genotype is not predictive of phenotype: towards an understanding of the molecular basis of reduced penetrance in human inherited disease. Human Genetics 132, 1077-1130.

31. Cooper, G.M., 2000. Signaling in Development and Differentiation., The Cell: A Molecular Approach., 2nd ed. Sinauer Associates, Sunderland (MA).

32. Crossley, P.H., Martin, G.R., 1995. The mouse Fgf8 gene encodes a family of polypeptides and is expressed in regions that direct outgrowth and patterning in the developing embryo. Development (Cambridge, England) 121, 439-451.

33. Cunningham, T.J., Colas, A., Duester, G., 2016. Early molecular events during retinoic acid induced differentiation of neuromesodermal progenitors. Biology open 5, 1821-1833.

34. Davidson, A.J., Ernst, P., Wang, Y., Dekens, M.P., Kingsley, P.D., Palis, J., Korsmeyer, S.J., Daley, G.Q., Zon, L.I., 2003a. cdx4 mutants fail to specify blood progenitors and can be rescued by multiple hox genes. Nature 425, 300-306.

35. Davidson, A.J., Zon, L.I., 2006. The caudal-related homeobox genes cdx1a and cdx4 act redundantly to regulate hox gene expression and the formation of putative hematopoietic stem cells during zebrafish embryogenesis. Developmental biology 292, 506-518.

36. Davidson, E.H., 2010. Emerging properties of animal gene regulatory networks. Nature 468, 911-920.

37. Davidson, E.H., McClay, D.R., Hood, L., 2003b. Regulatory gene networks and the properties of the developmental process. Proceedings of the National Academy of Sciences of the United States of America 100, 1475-1480.

38. De Luca, A., Cerrato, V., Fuca, E., Parmigiani, E., Buffo, A., Leto, K., 2015. Sonic hedgehog patterning during cerebellar development. Cellular and molecular life sciences : CMLS.

39. Delfino-Machin, M., Lunn, J.S., Breitkreuz, D.N., Akai, J., Storey, K.G., 2005. Specification and maintenance of the spinal cord stem zone. Development (Cambridge, England) 132, 4273-4283.

40. Denans, N., Iimura, T., Pourquie, O., 2015. Hox genes control vertebrate body elongation by collinear Wnt repression. eLife 4.

41. Deschamps, J., van Nes, J., 2005. Developmental regulation of the Hox genes during axial morphogenesis in the mouse. Development (Cambridge, England) 132, 2931-2942.

42. Diez del Corral, R., Breitkreuz, D.N., Storey, K.G., 2002. Onset of neuronal differentiation is regulated by paraxial mesoderm and requires attenuation of FGF signalling. Development (Cambridge, England) 129, 1681-1691.

43. Diez del Corral, R., Olivera-Martinez, I., Goriely, A., Gale, E., Maden, M., Storey, K., 2003. Opposing FGF and retinoid pathways control ventral neural pattern, neuronal differentiation, and segmentation during body axis extension. Neuron 40, 65-79.

44. Diez del Corral, R., Storey, K.G., 2004. Opposing FGF and retinoid pathways: a signalling switch that controls differentiation and patterning onset in the extending vertebrate body axis. BioEssays : news and reviews in molecular, cellular and developmental biology 26, 857-869.

45. Doyle, B., Fudenberg, G., Imakaev, M., Mirny, L.A., 2014. Chromatin loops as allosteric modulators of enhancer-promoter interactions. PLoS computational biology 10, e1003867.

46. Dubrulle, J., Pourquie, O., 2004. fgf8 mRNA decay establishes a gradient that couples axial elongation to patterning in the vertebrate embryo. Nature 427, 419-422.

47. Egli, D., Birkhoff, G., Eggan, K., 2008. Mediators of reprogramming: transcription factors and transitions through mitosis. Nature reviews. Molecular cell biology 9, 505-516.

48. Engelkamp, D., van Heyningen, V., 1996. Transcription factors in disease. Current opinion in genetics & development 6, 334-342.

49. Ericson, J., Rashbass, P., Schedl, A., Brenner-Morton, S., Kawakami, A., van Heyningen, V., Jessell, T.M., Briscoe, J., 1997. Pax6 controls progenitor cell identity and neuronal fate in response to graded Shh signaling. Cell 90, 169-180.

50. Eroshkin, F.M., Nesterenko, A.M., Borodulin, A.V., Martynova, N.Y., Ermakova, G.V., Gyoeva, F.K., Orlov, E.E., Belogurov, A.A., Lukyanov, K.A., Bayramov, A.V., Zaraisky, A.G., 2016. Noggin4 is a long-range inhibitor of Wnt8 signalling that regulates head development in Xenopus laevis. Scientific reports 6, 23049.

51. Erwin, D.H., Davidson, E.H., 2009. The evolution of hierarchical gene regulatory networks. Nature reviews. Genetics 10, 141-148.

52. Evans, D.J., 2003. Contribution of somitic cells to the avian ribs. Developmental biology 256, 114-126.

53. Faas, L., Isaacs, H.V., 2009. Overlapping functions of Cdx1, Cdx2, and Cdx4 in the development of the amphibian Xenopus tropicalis. Developmental dynamics : an official publication of the American Association of Anatomists 238, 835-852.

54. Ferrell, J.E., Jr., 2002. Self-perpetuating states in signal transduction: positive feedback, double-negative feedback and bistability. Current opinion in cell biology 14, 140-148.

55. Frelinger, J.A., 2015. Big Data, Big Opportunities, and Big Challenges. The journal of investigative dermatology. Symposium proceedings 17, 33-35.

56. Frumkin, A., Rangini, Z., Ben-Yehuda, A., Gruenbaum, Y., Fainsod, A., 1991. A chicken caudal homologue, CHox-cad, is expressed in the epiblast with posterior localization and in the early endodermal lineage. Development (Cambridge, England) 112, 207-219.

57. Fry, C.J., Farnham, P.J., 1999. Context-dependent transcriptional regulation. The Journal of biological chemistry 274, 29583-29586.

58. Garriock, R.J., Chalamalasetty, R.B., Kennedy, M.W., Canizales, L.C., Lewandoski, M., Yamaguchi, T.P., 2015. Lineage tracing of neuromesodermal progenitors reveals novel Wnt-dependent roles in trunk progenitor cell maintenance and differentiation. Development (Cambridge, England) 142, 1628-1638.

59. Gaunt, S.J., Drage, D., Trubshaw, R.C., 2005. cdx4/lacZ and cdx2/lacZ protein gradients formed by decay during gastrulation in the mouse. The International journal of developmental biology 49, 901-908.

60. Gilbert, S.F., 2000. Formation of the Neural Tube., Developmental biology, 6th ed. Sinauer Associates, Sunderland (MA).

61. Goldbeter, A., Gonze, D., Pourquie, O., 2007. Sharp developmental thresholds defined through bistability by antagonistic gradients of retinoic acid and FGF signaling. Developmental dynamics : an official publication of the American Association of Anatomists 236, 1495-1508.

62. Gouti, M., Metzis, V., Briscoe, J., 2015. The route to spinal cord cell types: a tale of signals and switches. Trends in genetics : TIG 31, 282-289.

63. Gouti, M., Tsakiridis, A., Wymeersch, F.J., Huang, Y., Kleinjung, J., Wilson, V., Briscoe, J., 2014. In vitro generation of neuromesodermal progenitors reveals distinct roles for wnt signalling in the specification of spinal cord and paraxial mesoderm identity. PLoS biology 12, e1001937.

64. Green, D., Whitener, A.E., Mohanty, S., Lekven, A.C., 2015. Vertebrate nervous system posteriorization: Grading the function of Wnt signaling. Developmental dynamics : an official publication of the American Association of Anatomists 244, 507-512.

65. Gregory, P.A., Gardner-Stephen, D.A., Rogers, A., Michael, M.Z., Mackenzie, P.I., 2006. The caudal-related homeodomain protein Cdx2 and hepatocyte nuclear factor 1alpha cooperatively regulate the UDP-glucuronosyltransferase 2B7 gene promoter. Pharmacogenetics and genomics 16, 527-536.

66. Hamburger, V., Hamilton, H.L., 1951. A series of normal stages in the development of the chick embryo. Journal of morphology 88, 49-92.

67. Han, K., Manley, J.L., 1993. Functional domains of the Drosophila Engrailed protein. The EMBO journal 12, 2723-2733.

68. Hardy, K.M., Garriock, R.J., Yatskievych, T.A., D'Agostino, S.L., Antin, P.B., Krieg, P.A., 2008. Non-canonical Wnt signaling through Wnt5a/b and a novel Wnt11 gene, Wnt11b, regulates cell migration during avian gastrulation. Developmental biology 320, 391-401.

69. Harradine, K.A., Akhurst, R.J., 2006. Mutations of TGFbeta signaling molecules in human disease. Annals of medicine 38, 403-414.

70. Harvey Lodish, A.B., S Lawrence Zipursky, Paul Matsudaira, David Baltimore, and James Darnell., 2000. Overview of Extracellular Signaling., Molecular Cell Biology 4th ed. W. H. Freeman, New York.

71. Hayward, A.G., 2nd, Joshi, P., Skromne, I., 2015. Spatiotemporal analysis of zebrafish hox gene regulation by Cdx4. Developmental dynamics : an official publication of the American Association of Anatomists 244, 1564-1573.

72. Henrique, D., Abranches, E., Verrier, L., Storey, K.G., 2015. Neuromesodermal progenitors and the making of the spinal cord. Development (Cambridge, England) 142, 2864-2875.

73. Hinman, V.F., Davidson, E.H., 2007. Evolutionary plasticity of developmental gene regulatory network architecture. Proceedings of the National Academy of Sciences of the United States of America 104, 19404-19409.

74. Holmberg, J., Perlmann, T., 2012. Maintaining differentiated cellular identity. Nature reviews. Genetics 13, 429-439.

75. Hryniuk, A., Grainger, S., Savory, J.G., Lohnes, D., 2012. Cdx function is required for maintenance of intestinal identity in the adult. Developmental biology 363, 426-437.

76. Isaacs, H.V., Pownall, M.E., Slack, J.M., 1998. Regulation of Hox gene expression and posterior development by the Xenopus caudal homologue Xcad3. The EMBO journal 17, 3413-3427.

77. Itasaki, N., Bel-Vialar, S., Krumlauf, R., 1999. 'Shocking' developments in chick embryology: electroporation and in ovo gene expression. Nature cell biology 1, E203-207.

78. Iwafuchi-Doi, M., Yoshida, Y., Onichtchouk, D., Leichsenring, M., Driever, W., Takemoto, T., Uchikawa, M., Kamachi, Y., Kondoh, H., 2011. The Pou5f1/Pou3f-dependent but SoxB-independent regulation of conserved enhancer N2 initiates Sox2 expression during epiblast to neural plate stages in vertebrates. Developmental biology 352, 354-366.

79. Karabagli, H., Karabagli, P., Ladher, R.K., Schoenwolf, G.C., 2002. Comparison of the expression patterns of several fibroblast growth factors during chick gastrulation and neurulation. Anatomy and embryology 205, 365-370.

80. Karlebach, G., Shamir, R., 2008. Modelling and analysis of gene regulatory networks. Nature reviews. Molecular cell biology 9, 770-780.

81. Keenan, I.D., Sharrard, R.M., Isaacs, H.V., 2006. FGF signal transduction and the regulation of Cdx gene expression. Developmental biology 299, 478-488.

82. Kim, M.Y., Mauro, S., Gevry, N., Lis, J.T., Kraus, W.L., 2004. NAD+-dependent modulation of chromatin structure and transcription by nucleosome binding properties of PARP-1. Cell 119, 803-814.

83. Kiparissides, A., Koutinas, M., Moss, T., Newman, J., Pistikopoulos, E.N., Mantalaris, A., 2011. Modelling the Delta1/Notch1 pathway: in search of the mediator(s) of neural stem cell differentiation. PloS one 6, e14668.

84. Kumar, S., Duester, G., 2014. Retinoic acid controls body axis extension by directly repressing Fgf8 transcription. Development (Cambridge, England) 141, 2972-2977.

85. Lacomme, M., Liaubet, L., Pituello, F., Bel-Vialar, S., 2012. NEUROG2 drives cell cycle exit of neuronal precursors by specifically repressing a subset of cyclins acting at the G1 and S phases of the cell cycle. Molecular and cellular biology 32, 2596-2607.

86. Lassar, A.B., Paterson, B.M., Weintraub, H., 1986. Transfection of a DNA locus that mediates the conversion of 10T1/2 fibroblasts to myoblasts. Cell 47, 649-656.

87. Le Dreau, G., Marti, E., 2012. Dorsal-ventral patterning of the neural tube: a tale of three signals. Developmental neurobiology 72, 1471-1481.

88. Lee, K., Skromne, I., 2014. Retinoic acid regulates size, pattern and alignment of tissues at the head-trunk transition. Development (Cambridge, England) 141, 4375-4384.

89. Lengerke, C., Schmitt, S., Bowman, T.V., Jang, I.H., Maouche-Chretien, L., McKinney-Freeman, S., Davidson, A.J., Hammerschmidt, M., Rentzsch, F., Green, J.B., Zon, L.I., Daley, G.Q., 2008. BMP and Wnt specify hematopoietic fate by activation of the Cdx-Hox pathway. Cell stem cell 2, 72-82.

90. Lewis, K.E., Eisen, J.S., 2003. From cells to circuits: development of the zebrafish spinal cord. Progress in neurobiology 69, 419-449.

91. Lewis, M.H., 2004. Environmental complexity and central nervous system development and function. Mental retardation and developmental disabilities research reviews 10, 91-95.

92. Liu, C., Nakamura, E., Knezevic, V., Hunter, S., Thompson, K., Mackem, S., 2003. A role for the mesenchymal T-box gene Brachyury in AER formation during limb development. Development (Cambridge, England) 130, 1327-1337.

93. Liu, J.P., Laufer, E., Jessell, T.M., 2001. Assigning the positional identity of spinal motor neurons: rostrocaudal patterning of Hox-c expression by FGFs, Gdf11, and retinoids. Neuron 32, 997-1012.

94. Lock, R., Cichowski, K., 2015. Loss of negative regulators amplifies RAS signaling. Nature genetics 47, 426-427.

95. Lohnes, D., 2003. The Cdx1 homeodomain protein: an integrator of posterior signaling in the mouse. BioEssays : news and reviews in molecular, cellular and developmental biology 25, 971-980.

96. Lunn, J.S., Fishwick, K.J., Halley, P.A., Storey, K.G., 2007. A spatial and temporal map of FGF/Erk1/2 activity and response repertoires in the early chick embryo. Developmental biology 302, 536-552.

97. Maden, M., 2006. Retinoids and spinal cord development. Journal of neurobiology 66, 726-738.

98. Mahmood, R., Kiefer, P., Guthrie, S., Dickson, C., Mason, I., 1995. Multiple roles for FGF-3 during cranial neural development in the chicken. Development (Cambridge, England) 121, 1399-1410.

99. Marletaz, F., Maeso, I., Faas, L., Isaacs, H.V., Holland, P.W., 2015. Cdx ParaHox genes acquired distinct developmental roles after gene duplication in vertebrate evolution. BMC biology 13, 56.

100. Marom, K., Shapira, E., Fainsod, A., 1997. The chicken caudal genes establish an anterior-posterior gradient by partially overlapping temporal and spatial patterns of expression. Mechanisms of development 64, 41-52.

101. Martin, B.L., Kimelman, D., 2008. Regulation of canonical Wnt signaling by Brachyury is essential for posterior mesoderm formation. Developmental cell 15, 121-133.

102. Martin, B.L., Kimelman, D., 2012. Canonical Wnt signaling dynamically controls multiple stem cell fate decisions during vertebrate body formation. Developmental cell 22, 223-232.

103. Martinez-Morales, P.L., Diez del Corral, R., Olivera-Martinez, I., Quiroga, A.C., Das, R.M., Barbas, J.A., Storey, K.G., Morales, A.V., 2011. FGF and retinoic acid activity gradients control the timing of neural crest cell emigration in the trunk. The Journal of cell biology 194, 489-503.

104. Mathis, L., Kulesa, P.M., Fraser, S.E., 2001. FGF receptor signalling is required to maintain neural progenitors during Hensen's node progression. Nature cell biology 3, 559-566.

105. Matsuda, T., Cepko, C.L., 2004. Electroporation and RNA interference in the rodent retina in vivo and in vitro. Proceedings of the National Academy of Sciences of the United States of America 101, 16-22.

106. Mazzoni, E.O., Mahony, S., Peljto, M., Patel, T., Thornton, S.R., McCuine, S., Reeder, C., Boyer, L.A., Young, R.A., Gifford, D.K., Wichterle, H., 2013. Saltatory remodeling of Hox chromatin in response to rostrocaudal patterning signals. Nature neuroscience 16, 1191-1198.

107. McClellan, M.J., Wood, C.D., Ojeniyi, O., Cooper, T.J., Kanhere, A., Arvey, A., Webb, H.M., Palermo, R.D., Harth-Hertle, M.L., Kempkes, B., Jenner, R.G., West, M.J., 2013. Modulation of enhancer looping and differential gene targeting by Epstein-Barr virus transcription factors directs cellular reprogramming. PLoS pathogens 9, e1003636.

108. McGrew, M.J., Sherman, A., Lillico, S.G., Ellard, F.M., Radcliffe, P.A., Gilhooley, H.J., Mitrophanous, K.A., Cambray, N., Wilson, V., Sang, H., 2008. Localised axial progenitor cell populations in the avian tail bud are not committed to a posterior Hox identity. Development (Cambridge, England) 135, 2289-2299.

109. McKinney-Freeman, S.L., Lengerke, C., Jang, I.H., Schmitt, S., Wang, Y., Philitas, M., Shea, J., Daley, G.Q., 2008. Modulation of murine embryonic stem cell-derived CD41+c-kit+ hematopoietic progenitors by ectopic expression of Cdx genes. Blood 111, 4944-4953.

110. Megason, S.G., McMahon, A.P., 2002. A mitogen gradient of dorsal midline Wnts organizes growth in the CNS. Development (Cambridge, England) 129, 2087-2098.

111. Meijer, D., Graus, A., Kraay, R., Langeveld, A., Mulder, M.P., Grosveld, G., 1990. The octamer binding factor Oct6: cDNA cloning and expression in early embryonic cells. Nucleic acids research 18, 7357-7365.

112. Merino, F., Bouvier, B., Cojocaru, V., 2015. Cooperative DNA Recognition Modulated by an Interplay between Protein-Protein Interactions and DNA-Mediated Allostery. PLoS computational biology 11, e1004287.

113. Mills, L.D., Zhang, Y., Marler, R.J., Herreros-Villanueva, M., Zhang, L., Almada, L.L., Couch, F., Wetmore, C., Pasca di Magliano, M., Fernandez-Zapico, M.E., 2013. Loss of the transcription factor GLI1 identifies a signaling network in the tumor microenvironment mediating KRAS oncogene-induced transformation. The Journal of biological chemistry 288, 11786-11794.

114. Miyagi, S., Nishimoto, M., Saito, T., Ninomiya, M., Sawamoto, K., Okano, H., Muramatsu, M., Oguro, H., Iwama, A., Okuda, A., 2006. The Sox2 regulatory region 2 functions as a neural stem cell-specific enhancer in the telencephalon. The Journal of biological chemistry 281, 13374-13381.

115. Molotkova, N., Molotkov, A., Sirbu, I.O., Duester, G., 2005. Requirement of mesodermal retinoic acid generated by Raldh2 for posterior neural transformation. Mechanisms of development 122, 145-155.

116. Morales, A.V., de la Rosa, E.J., de Pablo, F., 1996. Expression of the cCdx-B homeobox gene in chick embryo suggests its participation in rostrocaudal axial patterning. Developmental dynamics : an official publication of the American Association of Anatomists 206, 343-353.

117. Moreno, T.A., Kintner, C., 2004. Regulation of segmental patterning by retinoic acid signaling during Xenopus somitogenesis. Developmental cell 6, 205-218.

118. Moss Bendtsen, K., Jensen, M.H., Krishna, S., Semsey, S., 2015. The role of mRNA and protein stability in the function of coupled positive and negative feedback systems in eukaryotic cells. Scientific reports 5, 13910.

119. Muller, P., Rogers, K.W., Yu, S.R., Brand, M., Schier, A.F., 2013. Morphogen transport. Development (Cambridge, England) 140, 1621-1638.

120. Muller, P., Schier, A.F., 2011. Extracellular movement of signaling molecules. Developmental cell 21, 145-158.

121. Mullor, J.L., Sanchez, P., Ruiz i Altaba, A., 2002. Pathways and consequences: Hedgehog signaling in human disease. Trends in cell biology 12, 562-569.

122. Naiche, L.A., Holder, N., Lewandoski, M., 2011. FGF4 and FGF8 comprise the wavefront activity that controls somitogenesis. Proceedings of the National Academy of Sciences of the United States of America 108, 4018-4023.

123. Nakamura, H., Funahashi, J., 2001. Introduction of DNA into chick embryos by in ovo electroporation. Methods (San Diego, Calif.) 24, 43-48.

124. Nakamura, Y., Sakakibara, S., Miyata, T., Ogawa, M., Shimazaki, T., Weiss, S., Kageyama, R., Okano, H., 2000. The bHLH gene hes1 as a repressor of the neuronal commitment of CNS stem cells. The Journal of neuroscience : the official journal of the Society for Neuroscience 20, 283-293.

125. Nordstrom, U., Maier, E., Jessell, T.M., Edlund, T., 2006. An early role for WNT signaling in specifying neural patterns of Cdx and Hox gene expression and motor neuron subtype identity. PLoS biology 4, e252.

126. Novak, B., Tyson, J.J., 2008. Design principles of biochemical oscillators. Nature reviews. Molecular cell biology 9, 981-991.

127. Novitch, B.G., Chen, A.I., Jessell, T.M., 2001. Coordinate regulation of motor neuron subtype identity and pan-neuronal properties by the bHLH repressor Olig2. Neuron 31, 773-789.

128. Novitch, B.G., Wichterle, H., Jessell, T.M., Sockanathan, S., 2003. A requirement for retinoic acid-mediated transcriptional activation in ventral neural patterning and motor neuron specification. Neuron 40, 81-95.

129. Nusse, R., 2005. Wnt signaling in disease and in development. Cell research 15, 28-32.

130. Nutt, S.L., Heavey, B., Rolink, A.G., Busslinger, M., 1999. Commitment to the B-lymphoid lineage depends on the transcription factor Pax5. Nature 401, 556-562.

131. Ohuchi, H., Kimura, S., Watamoto, M., Itoh, N., 2000. Involvement of fibroblast growth factor (FGF)18-FGF8 signaling in specification of left-right asymmetry and brain and limb development of the chick embryo. Mechanisms of development 95, 55-66.

132. Olivera-Martinez, I., Harada, H., Halley, P.A., Storey, K.G., 2012. Loss of FGF-dependent mesoderm identity and rise of endogenous retinoid signalling determine cessation of body axis elongation. PLoS biology 10, e1001415.

133. Olivera-Martinez, I., Schurch, N., Li, R.A., Song, J., Halley, P.A., Das, R.M., Burt, D.W., Barton, G.J., Storey, K.G., 2014. Major transcriptome re-organisation and abrupt changes in signalling, cell cycle and chromatin regulation at neural differentiation in vivo. Development (Cambridge, England) 141, 3266-3276.

134. Olivera-Martinez, I., Storey, K.G., 2007. Wnt signals provide a timing mechanism for the FGF-retinoid differentiation switch during vertebrate body axis extension. Development (Cambridge, England) 134, 2125-2135.

135. Oliveri, P., Tu, Q., Davidson, E.H., 2008. Global regulatory logic for specification of an embryonic cell lineage. Proceedings of the National Academy of Sciences of the United States of America 105, 5955-5962.

136. Packham, E.A., Brook, J.D., 2003. T-box genes in human disorders. Human molecular genetics 12 Spec No 1, R37-44.

137. Papadopoulos, D.K., Skouloudaki, K., Adachi, Y., Samakovlis, C., Gehring, W.J., 2012. Dimer formation via the homeodomain is required for function and specificity of Sex combs reduced in Drosophila. Developmental biology 367, 78-89.

138. Parmar, K., Blyuss, K.B., Kyrychko, Y.N., Hogan, S.J., 2015. Time-Delayed Models of Gene Regulatory Networks. Computational and mathematical methods in medicine 2015, 347273.

139. Parras, C.M., Schuurmans, C., Scardigli, R., Kim, J., Anderson, D.J., Guillemot, F., 2002. Divergent functions of the proneural genes Mash1 and Ngn2 in the specification of neuronal subtype identity. Genes & development 16, 324-338.

140. Patel, N.S., Rhinn, M., Semprich, C.I., Halley, P.A., Dolle, P., Bickmore, W.A., Storey, K.G., 2013. FGF signalling regulates chromatin organisation during neural differentiation via mechanisms that can be uncoupled from transcription. PLoS genetics 9, e1003614.

141. Pera, E.M., Acosta, H., Gouignard, N., Climent, M., Arregi, I., 2014. Active signals, gradient formation and regional specificity in neural induction. Experimental cell research 321, 25-31.

142. Pigolotti, S., Krishna, S., Jensen, M.H., 2007. Oscillation patterns in negative feedback loops. Proceedings of the National Academy of Sciences of the United States of America 104, 6533-6537.

143. Pilon, N., Oh, K., Sylvestre, J.R., Bouchard, N., Savory, J., Lohnes, D., 2006. Cdx4 is a direct target of the canonical Wnt pathway. Developmental biology 289, 55-63.

144. Pituello, F., Medevielle, F., Foulquier, F., Duprat, A.M., 1999. Activation of Pax6 depends on somitogenesis in the chick embryo cervical spinal cord. Development (Cambridge, England) 126, 587-596.

145. Plachetka, A., Chayka, O., Wilczek, C., Melnik, S., Bonifer, C., Klempnauer, K.H., 2008. C/EBPbeta induces chromatin opening at a cell-type-specific enhancer. Molecular and cellular biology 28, 2102-2112.

146. Polynikis, A., Hogan, S.J., di Bernardo, M., 2009. Comparing different ODE modelling approaches for gene regulatory networks. Journal of theoretical biology 261, 511-530.

147. Reece-Hoyes, J.S., Keenan, I.D., Isaacs, H.V., 2002. Cloning and expression of the Cdx family from the frog Xenopus tropicalis. Developmental dynamics : an official publication of the American Association of Anatomists 223, 134-140.

148. Ribes, V., Le Roux, I., Rhinn, M., Schuhbaur, B., Dolle, P., 2009. Early mouse caudal development relies on crosstalk between retinoic acid, Shh and Fgf signalling pathways. Development (Cambridge, England) 136, 665-676.

149. Riese, J., Zeller, R., Dono, R., 1995. Nucleo-cytoplasmic translocation and secretion of fibroblast growth factor-2 during avian gastrulation. Mechanisms of development 49, 13-22.

150. Rivera-Perez, J.A., Magnuson, T., 2005. Primitive streak formation in mice is preceded by localized activation of Brachyury and Wnt3. Developmental biology 288, 363-371.

151. Rothenberg, E.V., 2010. Lineage determination in the immune system. Immunological reviews 238, 5-11.

152. Ruiz-Villalba, A., Hoppler, S., van den Hoff, M.J., 2015. Wnt signaling in the heart fields: Variations on a common theme. Developmental dynamics : an official publication of the American Association of Anatomists.

153. Saad, R.S., Ghorab, Z., Khalifa, M.A., Xu, M., 2011. CDX2 as a marker for intestinal differentiation: Its utility and limitations. World journal of gastrointestinal surgery 3, 159-166.

154. Sadowski, I., Ma, J., Triezenberg, S., Ptashne, M., 1988. GAL4-VP16 is an unusually potent transcriptional activator. Nature 335, 563-564.

155. Sakai, Y., Meno, C., Fujii, H., Nishino, J., Shiratori, H., Saijoh, Y., Rossant, J., Hamada, H., 2001. The retinoic acid-inactivating enzyme CYP26 is essential for establishing an uneven distribution of retinoic acid along the anterio-posterior axis within the mouse embryo. Genes & development 15, 213-225.

156. Sanchez-Ferras, O., Bernas, G., Farnos, O., Toure, A.M., Souchkova, O., Pilon, N., 2016. A direct role for murine Cdx proteins in the trunk neural crest gene regulatory network. Development (Cambridge, England) 143, 1363-1374.

157. Sanchez-Ferras, O., Coutaud, B., Djavanbakht Samani, T., Tremblay, I., Souchkova, O., Pilon, N., 2012. Caudal-related homeobox (Cdx) protein-dependent integration of canonical Wnt signaling on paired-box 3 (Pax3) neural crest enhancer. The Journal of biological chemistry 287, 16623-16635.

158. Sandmann, T., Girardot, C., Brehme, M., Tongprasit, W., Stolc, V., Furlong, E.E., 2007. A core transcriptional network for early mesoderm development in Drosophila melanogaster. Genes & development 21, 436-449.

159. Santillan, M., 2008. On the use of the hill functions in mathematical models of gene regulatory networks. Mathematical modelling of natural phenomena 3, 85-97.

160. Sasai, N., Kutejova, E., Briscoe, J., 2014. Integration of signals along orthogonal axes of the vertebrate neural tube controls progenitor competence and increases cell diversity. PLoS biology 12, e1001907.

161. Saunders, L.R., McClay, D.R., 2014. Sub-circuits of a gene regulatory network control a developmental epithelial-mesenchymal transition. Development (Cambridge, England) 141, 1503-1513.

162. Savory, J.G., Bouchard, N., Pierre, V., Rijli, F.M., De Repentigny, Y., Kothary, R., Lohnes, D., 2009. Cdx2 regulation of posterior development through non-Hox targets. Development (Cambridge, England) 136, 4099-4110.

163. Scardigli, R., Baumer, N., Gruss, P., Guillemot, F., Le Roux, I., 2003. Direct and concentration-dependent regulation of the proneural gene Neurogenin2 by Pax6. Development (Cambridge, England) 130, 3269-3281.

164. Scardigli, R., Schuurmans, C., Gradwohl, G., Guillemot, F., 2001. Crossregulation between Neurogenin2 and pathways specifying neuronal identity in the spinal cord. Neuron 31, 203-217.

165. Schneider, C.A., Rasband, W.S., Eliceiri, K.W., 2012. NIH Image to ImageJ: 25 years of image analysis. Nature methods 9, 671-675.

166. Scholl, C., Bansal, D., Dohner, K., Eiwen, K., Huntly, B.J., Lee, B.H., Rucker, F.G., Schlenk, R.F., Bullinger, L., Dohner, H., Gilliland, D.G., Frohling, S., 2007. The homeobox gene CDX2 is aberrantly expressed in most cases of acute myeloid leukemia and promotes leukemogenesis. The Journal of clinical investigation 117, 1037-1048.

167. Selleck, M.A., Stern, C.D., 1991. Fate mapping and cell lineage analysis of Hensen's node in the chick embryo. Development (Cambridge, England) 112, 615-626.

168. Shamim, H., Mason, I., 1999. Expression of Fgf4 during early development of the chick embryo. Mechanisms of development 85, 189-192.

169. Sherman, M.S., Cohen, B.A., 2012. Thermodynamic state ensemble models of cis-regulation. PLoS computational biology 8, e1002407.

170. Shi, W., Ma, W., Xiong, L., Zhang, M., Tang, C., 2017. Adaptation with transcriptional regulation. Scientific reports 7, 42648.

171. Shimizu, T., Bae, Y.K., Hibi, M., 2006. Cdx-Hox code controls competence for responding to Fgfs and retinoic acid in zebrafish neural tissue. Development (Cambridge, England) 133, 4709-4719.

172. Shu, J., Fu, H., Qiu, G., Kaye, P., Ilyas, M., 2013. Segmenting overlapping cell nuclei in digital histopathology images. Conference proceedings : ... Annual International Conference of the IEEE Engineering in Medicine and Biology Society. IEEE Engineering in Medicine and Biology Society. Annual Conference 2013, 5445-5448.

173. Simmons, A.D., Horton, S., Abney, A.L., Johnson, J.E., 2001. Neurogenin2 expression in ventral and dorsal spinal neural tube progenitor cells is regulated by distinct enhancers. Developmental biology 229, 327-339.

174. Simoes-Costa, M., Bronner, M.E., 2015. Establishing neural crest identity: a gene regulatory recipe. Development (Cambridge, England) 142, 242-257.

175. Singh, S., Stellrecht, C.M., Tang, H.K., Saunders, G.F., 2000. Modulation of PAX6 homeodomain function by the paired domain. The Journal of biological chemistry 275, 17306-17313.

176. Skaggs, K., Martin, D.M., Novitch, B.G., 2011. Regulation of spinal interneuron development by the Olig-related protein Bhlhb5 and Notch signaling. Development (Cambridge, England) 138, 3199-3211.

177. Skromne, I., Thorsen, D., Hale, M., Prince, V.E., Ho, R.K., 2007. Repression of the hindbrain developmental program by Cdx factors is required for the specification of the vertebrate spinal cord. Development (Cambridge, England) 134, 2147-2158.

178. Song, H., Zhang, B., Watson, M.A., Humphrey, P.A., Lim, H., Milbrandt, J., 2009. Loss of Nkx3.1 leads to the activation of discrete downstream target genes during prostate tumorigenesis. Oncogene 28, 3307-3319.

179. Stavridis, M.P., Collins, B.J., Storey, K.G., 2010. Retinoic acid orchestrates fibroblast growth factor signalling to drive embryonic stem cell differentiation. Development (Cambridge, England) 137, 881-890.

180. Stonestrom, A.J., Hsu, S.C., Jahn, K.S., Huang, P., Keller, C.A., Giardine, B.M., Kadauke, S., Campbell, A.E., Evans, P., Hardison, R.C., Blobel, G.A., 2015. Functions of BET proteins in erythroid gene expression. Blood 125, 2825-2834.

181. Strumpf, D., Mao, C.A., Yamanaka, Y., Ralston, A., Chawengsaksophak, K., Beck, F., Rossant, J., 2005. Cdx2 is required for correct cell fate specification and differentiation of trophectoderm in the mouse blastocyst. Development (Cambridge, England) 132, 2093-2102.

182. Takada, S., Stark, K.L., Shea, M.J., Vassileva, G., McMahon, J.A., McMahon, A.P., 1994. Wnt-3a regulates somite and tailbud formation in the mouse embryo. Genes & development 8, 174-189.

183. Takemoto, T., Uchikawa, M., Kamachi, Y., Kondoh, H., 2006. Convergence of Wnt and FGF signals in the genesis of posterior neural plate through activation of the Sox2 enhancer N-1. Development (Cambridge, England) 133, 297-306.

184. Tamashiro, D.A., Alarcon, V.B., Marikawa, Y., 2012. Nkx1-2 is a transcriptional repressor and is essential for the activation of Brachyury in P19 mouse embryonal carcinoma cell. Differentiation; research in biological diversity 83, 282-292.

185. Tiedemann, H.B., Schneltzer, E., Zeiser, S., Hoesel, B., Beckers, J., Przemeck, G.K., de Angelis, M.H., 2012. From dynamic expression patterns to boundary formation in the presomitic mesoderm. PLoS computational biology 8, e1002586.

186. Trapnell, C., 2015. Defining cell types and states with single-cell genomics. Genome research 25, 1491-1498.

187. Turner, D.A., Hayward, P.C., Baillie-Johnson, P., Rue, P., Broome, R., Faunes, F., Martinez Arias, A., 2014. Wnt/beta-catenin and FGF signalling direct the specification and maintenance of a neuromesodermal axial progenitor in ensembles of mouse embryonic stem cells. Development (Cambridge, England) 141, 4243-4253.

188. Turner, N., Grose, R., 2010. Fibroblast growth factor signalling: from development to cancer. Nature reviews. Cancer 10, 116-129.

189. Tzouanacou, E., Wegener, A., Wymeersch, F.J., Wilson, V., Nicolas, J.F., 2009. Redefining the progression of lineage segregations during mammalian embryogenesis by clonal analysis. Developmental cell 17, 365-376.

190. van den Akker, E., Forlani, S., Chawengsaksophak, K., de Graaff, W., Beck, F., Meyer, B.I., Deschamps, J., 2002. Cdx1 and Cdx2 have overlapping functions in anteroposterior patterning and posterior axis elongation. Development (Cambridge, England) 129, 2181-2193.

191. van Dijk, A.D., van Mourik, S., van Ham, R.C., 2012. Mutational robustness of gene regulatory networks. PloS one 7, e30591.

192. van Nes, J., de Graaff, W., Lebrin, F., Gerhard, M., Beck, F., Deschamps, J., 2006. The Cdx4 mutation affects axial development and reveals an essential role of Cdx genes in the ontogenesis of the placental labyrinth in mice. Development (Cambridge, England) 133, 419-428.

193. van Rooijen, C., Simmini, S., Bialecka, M., Neijts, R., van de Ven, C., Beck, F., Deschamps, J., 2012. Evolutionarily conserved requirement of Cdx for post-occipital tissue emergence. Development (Cambridge, England) 139, 2576-2583.

194. Verzi, M.P., Hatzis, P., Sulahian, R., Philips, J., Schuijers, J., Shin, H., Freed, E., Lynch, J.P., Dang, D.T., Brown, M., Clevers, H., Liu, X.S., Shivdasani, R.A., 2010. TCF4 and CDX2, major transcription factors for intestinal function, converge on the same cis-regulatory regions. Proceedings of the National Academy of Sciences of the United States of America 107, 15157-15162.

195. Voss, T.C., Hager, G.L., 2014. Dynamic regulation of transcriptional states by chromatin and transcription factors. Nature reviews. Genetics 15, 69-81.

196. Wang, Y., Yabuuchi, A., McKinney-Freeman, S., Ducharme, D.M., Ray, M.K., Chawengsaksophak, K., Archer, T.K., Daley, G.Q., 2008. Cdx gene deficiency compromises embryonic hematopoiesis in the mouse. Proceedings of the National Academy of Sciences of the United States of America 105, 7756-7761.

197. White, R.J., Nie, Q., Lander, A.D., Schilling, T.F., 2007. Complex regulation of cyp26a1 creates a robust retinoic acid gradient in the zebrafish embryo. PLoS biology 5, e304.

198. Wilkinson, D.G., Nieto, M.A., 1993. Detection of messenger RNA by in situ hybridization to tissue sections and whole mounts. Methods in enzymology 225, 361-373.

199. Wilson, L., Gale, E., Chambers, D., Maden, M., 2004. Retinoic acid and the control of dorsoventral patterning in the avian spinal cord. Developmental biology 269, 433-446.

200. Wilson, V., Olivera-Martinez, I., Storey, K.G., 2009. Stem cells, signals and vertebrate body axis extension. Development (Cambridge, England) 136, 1591-1604.

201. Wolfe, P.J., 2013. Making sense of big data. Proceedings of the National Academy of Sciences 110, 18031-18032.

202. Woodcock, D.J., Vance, K.W., Komorowski, M., Koentges, G., Finkenstadt, B., Rand, D.A., 2013. A hierarchical model of transcriptional dynamics allows robust estimation of transcription rates in populations of single cells with variable gene copy number. Bioinformatics (Oxford, England) 29, 1519-1525.

203. Wu, G., Gentile, L., Fuchikami, T., Sutter, J., Psathaki, K., Esteves, T.C., Arauzo-Bravo, M.J., Ortmeier, C., Verberk, G., Abe, K., Scholer, H.R., 2010. Initiation of trophectoderm lineage specification in mouse embryos is independent of Cdx2. Development (Cambridge, England) 137, 4159-4169.

204. Wu, W., Cheng, Y., Keller, C.A., Ernst, J., Kumar, S.A., Mishra, T., Morrissey, C., Dorman, C.M., Chen, K.B., Drautz, D., Giardine, B., Shibata, Y., Song, L., Pimkin, M., Crawford, G.E., Furey, T.S., Kellis, M., Miller, W., Taylor, J., Schuster, S.C., Zhang, Y., Chiaromonte, F., Blobel, G.A., Weiss, M.J., Hardison, R.C., 2011. Dynamics of the epigenetic landscape during erythroid differentiation after GATA1 restoration. Genome research 21, 1659-1671.

205. Yamaguchi, T.P., Takada, S., Yoshikawa, Y., Wu, N., McMahon, A.P., 1999. T (Brachyury) is a direct target of Wnt3a during paraxial mesoderm specification. Genes & development 13, 3185-3190.

206. Yamamoto, H., Miyamoto, K., Li, B., Taketani, Y., Kitano, M., Inoue, Y., Morita, K., Pike, J.W., Takeda, E., 1999. The caudal-related homeodomain protein Cdx-2 regulates vitamin D receptor gene expression in the small intestine. Journal of bone and mineral research : the official journal of the American Society for Bone and Mineral Research 14, 240-247.

207. Yang, Z., Ding, K., Pan, L., Deng, M., Gan, L., 2003. Math5 determines the competence state of retinal ganglion cell progenitors. Developmental biology 264, 240-254.

208. Yoshida, M., Uchikawa, M., Rizzoti, K., Lovell-Badge, R., Takemoto, T., Kondoh, H., 2014. Regulation of mesodermal precursor production by low-level expression of B1 Sox genes in the caudal lateral epiblast. Mechanisms of development 132, 59-68.

209. Yoshikawa, Y., Fujimori, T., McMahon, A.P., Takada, S., 1997. Evidence that absence of Wnt-3a signaling promotes neuralization instead of paraxial mesoderm development in the mouse. Developmental biology 183, 234-242.

210. Young, T., Rowland, J.E., van de Ven, C., Bialecka, M., Novoa, A., Carapuco, M., van Nes, J., de Graaff, W., Duluc, I., Freund, J.N., Beck, F., Mallo, M., Deschamps, J., 2009. Cdx and Hox genes differentially regulate posterior axial growth in mammalian embryos. Developmental cell 17, 516-526.

211. Yu, S.R., Burkhardt, M., Nowak, M., Ries, J., Petrasek, Z., Scholpp, S., Schwille, P., Brand, M., 2009. Fgf8 morphogen gradient forms by a source-sink mechanism with freely diffusing molecules. Nature 461, 533-536.

212. Zhang, Q., Ramlee, M.K., Brunmeir, R., Villanueva, C.J., Halperin, D., Xu, F., 2012. Dynamic and distinct histone modifications modulate the expression of key adipogenesis regulatory genes. Cell cycle (Georgetown, Tex.) 11, 4310-4322.